# THE COUNTERFLOW COOLING OF FEED PELLETS

By

Dirk E. Maier

A THESIS

Submitted to
Michigan State University
in partial fulfillment of the requirements
for the degree of

MASTER OF SCIENCE

in

Agricultural Engineering

Department of Agricultural Engineering

1988

# ABSTRACT

## THE COUNTERFLOW COOLING OF FEED PELLETS

By

Dirk E. Maier

Counterflow pellet coolers have only recently become commercially available in the feed industry. Their design has been by trial and error mainly . This study presents the first experimental and analytical investigation of counterflow pellet cooling.

A laboratory-size counterflow cooler was modified and used to measure the influence of various design parameters, such as bed depth, pellet conditions, and air conditions, on the cooling rate and the moisture loss of feed pellets.

A simulation model was developed based on four differential equations constituting a two-point boundary value problem which was solved in a two-step procedure. The experimental data was used to validate the simulation model.

A thorough analysis was made of the pellet cooling process based on the experimental and simulated data. It was established that the most important operating and design parameters for a counterflow pellet cooler with respect to the cooling rate, moisture loss and internal moisture gradient are the bed depth and the residence time.

Approved _____
Major Professor
11/9/88

Approved _____
Department Chairman
11/10/88

## ACKNOWLEDGMENTS

The author wishes to express his deepest gratitude to the continued encouragement, guidance and support of Dr. F. W. Bakker-Arkema. His trust and confidence as a mentor and friend is greatly appreciated.

Appreciation is expressed to Dr. R. C. Brook, Dr. K. A. Berglund, and Dr. I. P. Schisler for serving on the committee.

The financial support of the California Pellet Mill Company (CPM) was greatly appreciated. Special thanks goes to Mr. Henry Pierik, CPM Manager of Quality Assurance, for his advice and confidence.

Also acknowledged is the willingness of Purina Mills of Millet, MI, specifically Mr. Jim Wilson, Plant Manager, to provide us with the freshly extruded feed pellets without which this research would not have been possible.

Thank you to Dr. Joao D. Biagi for assisting in the experimental tests; to Dr. Irwin P. Schisler for helping in the development of the computer simulation; to my friends in the Post Harvest Technology Group: Rosana Moreira, Abbas Eltigani, John Anderson, Joao Biagi, Suhargo, Damiano Chiuswa, Sergio Perez, Dan Tyrrell, and Brad Marks for their friendship and fellowship throughout the past two-and-a-half years; to our favorite secretary Marti Meggitt who always knows how to cheer up the day; and to a special friend, Todd Forbush, who has been a constant source of intellectual challenge and encouragement ever since I set foot in this department.

Special thanks goes to my family in Germany, specifically my parents, Dieter and Ursel Maier, my brother, Lars, and my sister, Wenke; and my family in the United States, specifically my god parents, Rudolph and Maude Steeby, my in-laws, Bill and Toby Hanson, and my foster parents, Art and Connie Hooker, for their special support and encouragement.

Deepest gratitude is expressed to my wife, Heidi S. Maier, for her love, her patience, her support and her understanding. You make my life meaningful!

Praise be to My Lord, who leadeth my every step and has given me eternal salvation. 'Whosoever therefore shall confess me before men, him will I confess also before my Father which is in heaven.' (Matthew 10:32)

TABLE OF CONTENTS

LIST OF TABLES

LIST OF FIGURES

## LIST OF SYMBOLS

| | |
|---|---|
| D | diffusion coefficient, [$m^2/h$] |
| G | flow rate, [kg dry product/h/$m^2$] |
| H | depth of the cooling bed, [m] |
| M | average moisture content, dry basis [decimal] |
| M' | local moisture content, dry basis [decimal] |
| Q | volumetric airflow, [$m^3/m^2/s$] |
| RH | relative humidity, [decimal] |
| SP | static pressure, [Pa/m] |
| T | air temperature, [°C] |
| W | absolute humidity, [kg/kg] |
| WF | weighting factor, [decimal] |
| a | specific surface area, [$m^{-1}$] |
| $c_a$ | specific heat of dry air, [kJ/kg/°C] |
| $c_p$ | specific heat of dry pellets, [kJ/kg/°C] |
| $c_v$ | specific heat of water vapor, [kJ/kg/°C] |
| $c_w$ | specific heat of liquid water, [kJ/kg/°C] |
| d | pellet diameter, [m] |
| h | convective heat transfer coefficient, [kJ/h/$m^2$/°C] |
| $h_D$ | convective mass transfer coefficient, [kg/h/$m^2$] |
| $h_{fg}$ | heat of vaporization, [kJ/kg] |
| $\ell$ | pellet length, [m] |
| r | radial particle coordinate, [m] |
| $r_o$ | initial pellet radius, [m] |
| $r_1$ | Ricatti equation function |

$r_2$ Ricatti equation function

t time, [s]

u dependent invariant imbedding variable

v dependent invariant imbedding variable

x bed depth coordinate, [m]

z independent invariant imbedding variable

$\Delta$ change over time

$\alpha$ invariant imbedding boundary condition

$\beta$ invariant imbedding boundary condition

$\epsilon$ void ratio, [decimal]

$\theta$ pellet temperature, [°C]

$\mu$ dynamic viscosity, [kg/m/s]

<u>subscripts</u>

a air

abs absolute

eq equilibrium

exp experimental

in inlet

p product

s pellet surface

sim simulated

w wet basis

weq wet basis equilibrium

win wet basis inlet

**coordinates**

| | |
|---|---|
| L | pellet outlet of cooler bed |
| 0 | pellet inlet to cooler bed |
| 1 | first internal moisture subregion |
| 2 | second internal subregion |
| 3 | third internal subregion |

# INTRODUCTION

Feed processing refers to any treatment that a feedstuff or part of a feedstuff undergoes prior to the consumption by animals. The processing may consist of one step or a series of steps, including cooking, extraction, dehydration, grinding, and pelleting.

In the United States approximately 60% of the non-forage feeds are processed in feed mills (Perry, 1984). The commercial feed industry ranks among the top 25 industries in the country. In 1984, 119.6 Million metric tons (MMT) of feed were produced in the United States (Lin and Ash, 1988).

In the European Community 97 MMT of mixed feeds were produced in 1986 (Koch, 1987). The Netherlands leads Europe with 16.5 MMT, followed by West Germany with 16.4 MMT. In Europe over 33 MMT were produced as dairy and calf feeds, followed by hog feed with 32.6 MMT and poultry feed with 26.3 MMT.

The mixed feed industry has been growing steadily during recent years (Föller-Friedrich, 1984). This is primarily due to the improvements and developments in the fields of animal breeding, nutritional physiology, and feed compound technology. Research in feed compound technology has brought about significant developments in technological manufacturing which has lead to an overall improvement in feed mill operations throughout the world.

The central process in the feed mill is the pelleting

operation. After the feed pellets leave the pellet press, immediate cooling is required to maintain the pellet quality. Four pellet cooler types are presently available on the market: (1) the vertical cooler, (2) the horizontal (belt) cooler, (3) the rotary (carousel) cooler, and (4) the counterflow (tank) cooler. The counterflow design has only recently been applied to the cooling of feed pellets. The first company to successfully market this cooler type was Geleen Techniek, B.V., Geleen, The Netherlands.

The counterflow cooler claims the following advantages over conventional pellet coolers (Kraftfutter, 1985): (1) lower energy use, (2) smaller dimensions, (3) lower maintenance, and (4) less moisture loss by the pellets.

In the counterflow pellet cooler, the pellets and the cooling air flow in opposite directions through the cooler. The effects of various design parameters, such as bed depth, airflow rate, pellet flowrate, pellet-to-airflow ratio, initial pellet temperature and moisture content, inlet air temperature and relative humidity, pellet type and diameter on the pellet cooling rate and the moisture loss are unknown. No experimental data on counterflow pellet cooling is available in the technical literature, or the trade press.

This study presents experimental data on the cooling of feed pellets in a laboratory-size counterflow cooler. The data are used to develop a simulation model of the counterflow cooling of feed pellets. The results are used to determine the influence of various parameters on the design of a counterflow cooler.

## 2. OBJECTIVES

The objectives of this research are:

(1) To determine experimental data on the cooling behavior of feed pellets in a counterflow cooler.

(2) To develop a simulation model of the counterflow cooling of feed pellets and to validate the model with the experimental data.

(3) To determine the influence of various design parameters on the operation of a counterflow cooler.

## 3. LITERATURE REVIEW

### 3.1 FEED MANUFACTURING IN THE UNITED STATES

Feed milling in the United States has a relatively short history, beginning in 1929 with the conception and design of pelleting equipment using the die-and-roller principle. For many years, pelleting was considered an art rather than a science. Only during the past years has the feed industry become open to a more scientific approach.

In the United States, feed manufacturing is divided into two categories (McEllhiney, 1985):

(1) Primary Feed Manufacturing - The processing and mixing of separate feed ingredients, sometimes with the addition of a premix at a rate of less than 50 kg per MT of finished feed. [A premix is defined below.]

(2) Secondary Feed Manufacturing - The processing and mixing

of one or more grains and ingredients with formula feed supplements. The supplements are usually added at a rate of 150 kg or more per MT of finished feed. [A supplement is defined below.]

The American Feed Manufacturers Association distinguishes four types of feeds (McEllhiney, 1985):

(1) Complete Feeds - They contain a proper balance of nutrients and are intended to be the sole ration for non-ruminant animals. Roughage is normally excluded from this type of feed.

(2) Supplements/Concentrates - They contain the proper balance of protein, vitamins, minerals, and trace minerals. They are added with grain and/or roughage at approximately 100 kg, or more, per MT to make a balanced ration.

(3) Base Mixes/Super Concentrates - They contain only part of an animal's protein requirements. They are added with grain and other high protein ingredients at 50 kg, or more, per MT to make a balanced ration.

(4) Premixes - They are formulations of one, or more, microingedients, such as vitamins, minerals, trace minerals, or drugs, which are mixed with a carrier ingredient. A premix is usually added at less than 50 kg per MT with grain and other protein ingredients to make a balanced ration for non-ruminant animals.

By 1984, the number of feed mills in the United States was 6,720, a decrease of 1,200 mills since 1970 (Lin and Ash, 1988). On the average, a U.S. feed mill produced 17,750 MT per year in 1984, compared to 18,200 MT in 1975. The largest mills

are located in the Pacific region. They have an average production of 47,700 MT. The size of mills has expanded rapidly in the Southeast from 26,800 MT per mill per year in 1975 to 34,000 MT in 1984 - a 27% increase - primarily due to the increase of the broiler industry in that region. In the Corn Belt, Northern Plains, Appalachians, and Lake States the average yearly production of a feed mill is between 11,000 and 14,700 MT.

In the United States, 80% of the feed mills produced less than 27,500 MT per mill in 1984; they accounted for 28% of the annual production. Only 5% of the U.S. feed mills have an annual production over 75,000 MT per year; they accounted for 44% of the total mixed feed production in 1984.

In 1984, nearly 59% of U.S. feed mills were owned by corporations; they produced 71% of the total of mixed feeds. Farmer cooperatives owned 28% of the mills and produced 23% of the feeds. Partnerships and sole ownerships ran 13% of the mills; they accounted for 6% of the U.S. mixed feed production.

Poultry feed accounted for 43% of all mixed feeds produced in the United States in 1984, up from 38% in 1975. Beef cattle and sheep feed accounted for 18% of the production - a decrease of 5% since 1975. Dairy and hog feed production remained at about 31%.

## 3.2 FEED PELLETING

A typical flow diagram of the feed mill operation is shown in Figure 3.1.

No aspect of the feed manufacturing process has received

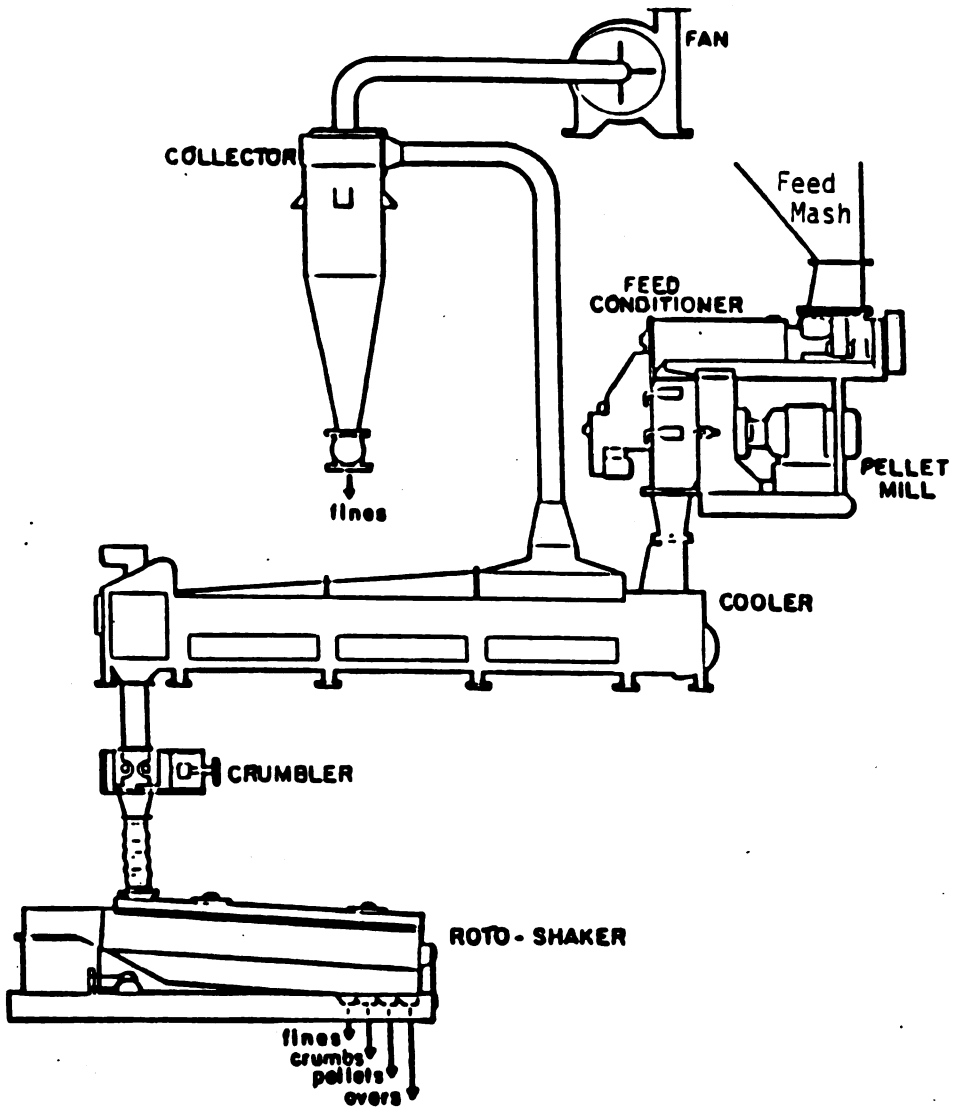


Figure 3.1 Flow diagram of the feed mill operation (Falk, 1985).

more attention in recent years than the pelleting process (McEllhiney, 1986). It is the most costly, energy-intensive, and maintenance-requiring operation in the feed mill.

The central process in the production of mixed feeds is the mechanical extrusion of the feed meal into pellets. It is defined as the agglomeration of small particulates into larger particles by means of a mechanical process combining moisture, heat and pressure treatment.

Feed meal from an overhead bin flows into the conditioner where steam and binders are added (see Figure 3.1). The conditioned meal is transferred to the pellet mill where it is extruded through the die forming the pellets. The hot pellets pass immediately to the cooler where the temperature is lowered to near-ambient. Fines that are carried with the cooling air are separated in a cyclone and returned to the feed meal for reprocessing. If desired, the cooled pellets are passed through a crumbler and over a screen within a roto-shaker to separate fines, crumbles, pellets and overs. Finally, the pellets flow into bins for final conditioning and storage, or are immediately bagged.

At the heart of the pelleting process is the pellet mill (see Figure 3.2). It consists of (a) a variable feeder unit, (b) a conditioning chamber, (c) a die-and-roller assembly, (d) a motor, and (e) a base. Pellet mills are available in a wide range of sizes and thus of capacities.

(a) Variable Feeder Unit

The feeder is generally of the screw-type and is equipped

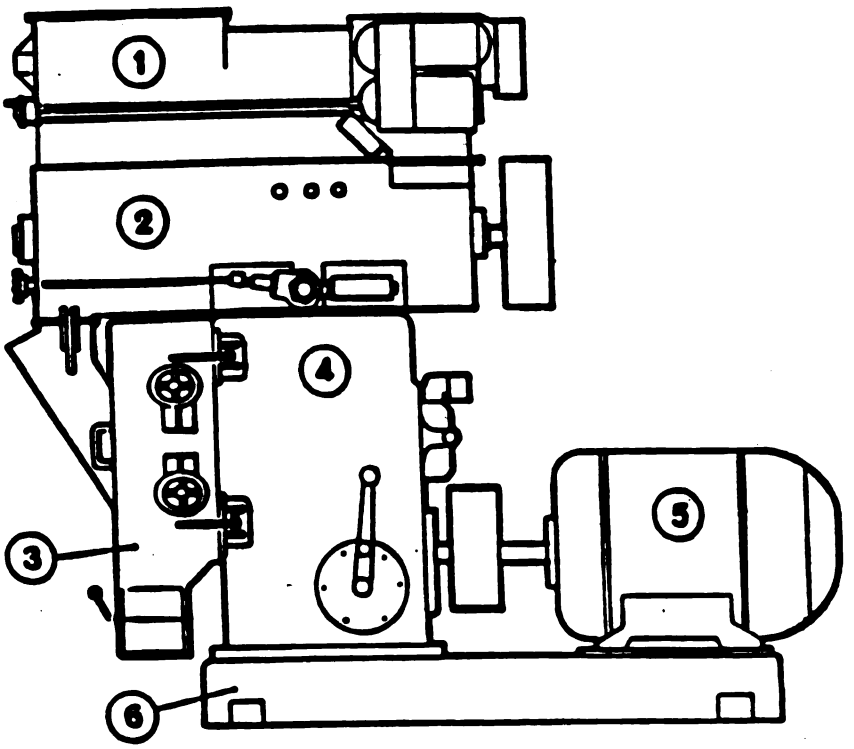


1 Variable feeder
2 Conditioning chamber
3 Die-and-roller assembly
4 Speed reduction device
5 Motor
6 Base

Figure 3.2 Components of a pellet mill (Robinson, 1981).

with a speed-control device. In normal operations, the screw-speed is above 100 rpm. The purpose of the feeder is to provide a uniform flow of feed to the pelleting operation.

(b) Conditioning Chamber

The feed value, pellet durability and power requirements of a pellet mill are improved by the conditioning process. Short-term conditioning occurs in a mixer mounted on top of the pellet press. The flow-through mixer, containing either fixed or adjustable paddles, is equipped with steam manifolds and liquid injection ports. In the chamber, steam and liquids, such as water, fats, and molasses are thoroughly mixed with the meal. The shaft speed varies from 90 to 500 rpm depending on the feed. The steam pressure ranges from 410 to 1,035 kPa (gage). The retention time in short-term conditioners is less than one minute (IFF Report, 1984).

The need to extend the conditioning times for certain feeds has long been recognized; various methods have been developed for this purpose (McEllhiney, 1986). These include: stacked horizontal conditioners, larger standard conditioners, ripeners and kettles.

The dwell-time in ripeners usually ranges from 15 to 30 minutes. Ripeners are especially effective for the pelleting of high molasses feeds. Advantages of feeds containing 7-9% molasses are: reduced energy requirements, more durable pellets, and fewer fines. Ripeners require extensive head room, high investment costs, and long change-over times between feeds.

Kettles are self-contained conditioning systems. In general,

they are not used in series with more than one standard conditioner. Each kettle has its own steam injection facilities. Kettles have lower fixed costs than ripeners, require less space, have a lower power consumption, and improve pellet quality. Disadvantages are shorter conditioning times than in ripeners, a maximum of 6% molasses in the feed, and rather high maintenance costs.

The steam conditioning of meal results in an increase in moisture content of the pellets. In the conditioner about 1% moisture is added for every 11°C increase in temperature (Atkinson, 1981). The addition of 1% molasses to dairy pellets adds 0.5% of moisture to the meal.

(c) Die-and-Roller Assembly

The actual throughput of feed in the pellet press is determined by the pellet die. The early pellet mills used horizontal flat-steel dies with four rollers running on the upper surface of the die. Today, most pellet mills employ vertical die-and-roller assemblies (see Figure 3.3). The ring-type die-and-roller pellet mills were developed in the mid 1930's and have become the most widely used system in the feed industry.

The die is fixed in the pellet mill. The rollers have a speed of about 100 to 400 rpm. The rollers compact the feed meal on the perforated die face, and force the meal to be extruded through the holes of the die. The extruded product is cut off by adjustable knives to the desired pellet length.

The inside diameter of typical dies range from 30.5 cm to 81.3 cm. The working area of dies varies from 582 $cm^2$ to 5,190

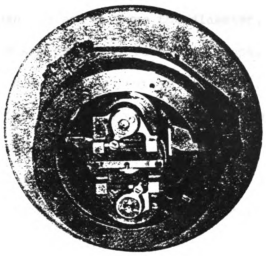

Figure 3.3a Vertical die-and-roller assembly (CPM, 1987).

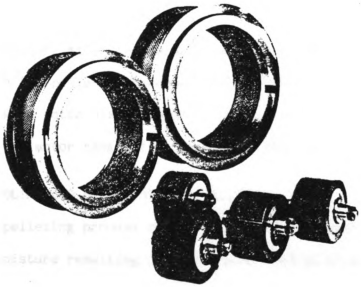

Figure 3.3b Dies and rollers separated (CPM, 1987).

$cm^2$. The hole diameter of commercially available dies is between 2.4 mm and 35 mm for cylindrical pellets. The pellet length varies between 1.5 and 3 times the diameter. Some of the larger pellets, which are primarily found in Europe, are cube- or oval-shaped. The die thickness varies between 3.2 cm and 12.7 cm. Figure 3.4 shows a range of pellet dies available for a CPM series 3000 pellet mill.

The application of fat spray at the die is relatively recent (McEllhiney, 1986). Liquid fat is sprayed on the pellets immediately after their formation. The procedure allows the addition of higher amounts of fat to the pellets than traditional fat-coating equipment since the atomized fat spray is applied when the pellets are still hot and porous. At least one U.S. manufacturer [Beta Raven] claims that absorbing the fat at the die creates a better pellet (Feed and Grain Times, 1988).

(d) Motor

The pellet mill uses as much as 66% of the total energy required in the pelleting process (Biagi, 1986). Pellet mills are available with motor sizes ranging from 14.9 kW to 522 kW. Table 3.1 shows the motor range of a CPM series 3000 pellet mill.

## 3.3 THE COOLING AND DRYING OF FEED PELLETS

The pelleting process requires a method of removing excess heat and moisture resulting from the conditioning of the meal and the frictional heating in the die. In the cooler/dryer, atmospheric air is drawn through the hot pellets, evaporating the excess moisture and at the same time reducing the temperature of

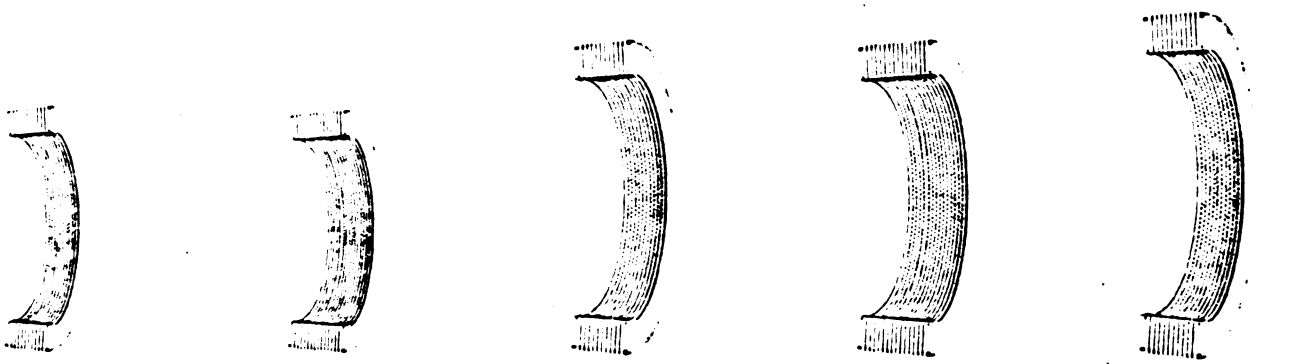

16″ ID x 3.25″ Wk. Area: 163 IN²

16″ ID x 4.56″ Wk. Area: 229 IN²

20″ ID x 4.44″ Wk. Area: 279 IN²

20″ ID x 6.12″ Wk. Area: 384 IN²

22.5″ ID x 6.12″ Wk. Area: 433 IN²

*Available *in Alloy, Mor-Ton,* and *Chrome* materials for best results.

**Figure 3.4 Range of pellet dies available for a CPM series 3000 pellet mill (CPM, 1987).**

| Die ID | | Die Width | | HP/KW | | Motor RPM | | Model | | | Wk. Area | | Die RPM | | Peripheral Speed | | |
|---|---|---|---|---|---|---|---|---|---|---|---|---|---|---|---|---|---|
| IN | MM | IN | MM | | | 60HZ | 50HZ | | IN²/HP | CM²/KW | IN² | CM² | 60HZ | 50HZ | FPM* | MPS† | |
| 16 | 406 | 3.25 | 82.6 | 150 | 110 | 1800 | 1500 | 3016-3 | 1.09 | 9.6 | 163 | 1055 | 254 | 210 | 1296 | 5.5 | 1. |
| 16 | 406 | 4.56 | 115.8 | 150 | 110 | 1800 | 1500 | 3016-4 | 1.53 | 13.4 | 229 | 1478 | 254 | 210 | 1296 | 5.5 | 1. |
| 20 | 508 | 4.44 | 112.8 | 200 | 132 | 1800 | 1500 | 3020-4 | 1.39 | 13.6 | 279 | 1800 | 254 | 210 | 1590 | 6.7 | 2. |
| 20 | 508 | 6.12 | 155.5 | 200 | 132 | 1800 | 1500 | 3020-6 | 1.92 | 18.8 | 384 | 2482 | 254 | 210 | 1590 | 6.7 | 2. |
| 22.5 | 572 | 6.12 | 155.5 | 200 | 132 | 1800 | 1500 | 3022-6 | 2.17 | 21.2 | 433 | 2792 | 254 | 210 | 1755 | 7.4 | 2. |

*FPM = Feet per minute †MPS = Meters per second 1. Peripheral speed calculated with 1-3/4″ thick die 2. Peripheral speed calculated with 2″ thick die

**Table 3.1 Technical specifications of a CPM series 3000 pellet mill (CPM, 1987).**

the pellets.

In general, the pellets leave the pellet press at a temperature of 63° to 93° C, and a moisture content of 15% to 18.5% wet basis. The final temperature of the cooled pellets should not be more than 5° to 8° C above the cooling air (IFF Report, 1984). The cooler/dryer is generally capable of removing 1% to 2% moisture from the pellets .

Improper cooling and drying of pellets can result in (Robinson, 1983): (1) poor pellet quality, (2) pellet breakdown, (3) pellet spoilage, (4) pellet heating and spontaneous combustion, (5) pellet caking in bags or bins, and (6) monetary loss from excess moisture removal.

The performance of a pellet cooler/dryer depends on the following factors: (1) cooler type, (2) air flow rate, (3) air temperature, (4) air relative humidity, (5) pellet flow rate, (6) pellet size, (7) pellet temperature, and (8) pellet moisture content.

As the cooling air moves through the pellets, its temperature increases and its relative humidity decreases. While the temperature of the pellets decreases, moisture is released by the pellets and absorbed by the air. Although the relative humidity of the air decreases as it warms up, the absolute humidity of the cooling air increases.

Various pellet cooler types are offered by equipment manufacturers. Several designs have been available since the 1950's. The cooler/dryer appears to be a weak link in the total pelleting process from the standpoint of product quality

(McEllhiney, 1986) due to the lack of control by the operator.

The pellet processing loop cannot be closed until the pellet cooler is able to communicate with the pellet mill controller. On-line moisture and durability determination of the pellets with feed back to the control device are one step. Simulation studies of pellet cooling/drying are another step in developing proper control schemes for the pellet production process.

There are four major pellet-cooler designs used in the feed processing industry: (1) vertical crossflow, (2) horizontal (belt) crossflow, (3) mixed-flow rotary, and (4) counterflow.

### 3.3.1 Vertical Crossflow Cooler

Figure 3.5 shows a schematic of a vertical cooler. The pellets flow through the vertical cooler by gravity. The cooling air is drawn through the screened vertical columns into the central plenum. The discharge control mechanism must assure an even flow of the pellets through the vertical cooling columns.

The vertical crossflow cooler has several draw-backs. It requires a high air flowrate and, therefore, has high power requirements. The vertical columns need to be full in order to operate. Since the columns are not adjustable in width, the capacity of the cooler can be regulated only through the discharge mechanism.

Commercial vertical coolers range in capacity from 4 to 24 MT/h. They are 1,400 to 1,520 mm wide, 1,980 to 5,180 mm high, and have a column width of 230 to 254 mm. A 10 to 14 MT/h capacity cooler requires approximately a 40 HP fan.

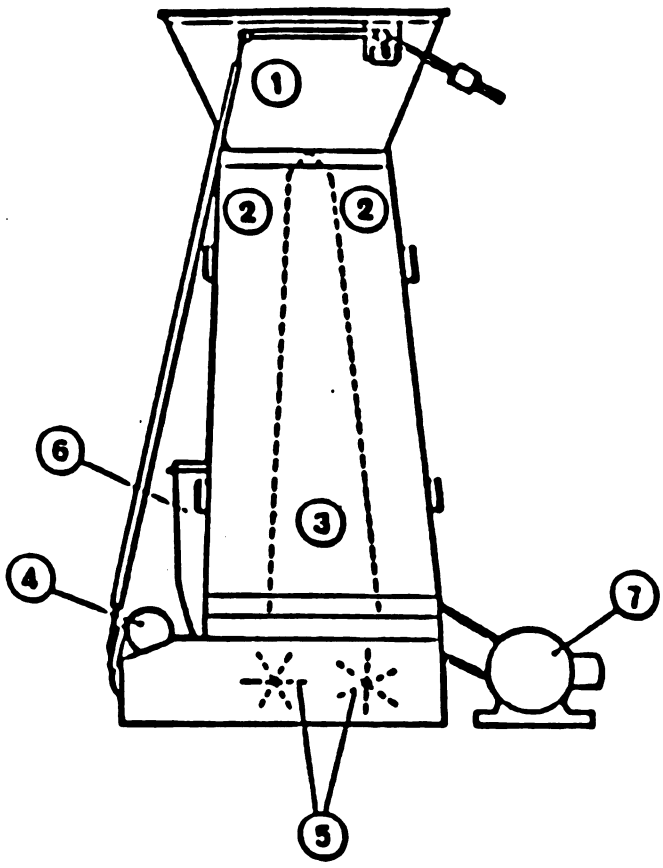


1 Hopper and level sensor
2 Cooling column
3 Plenum chamber
4 Discharge gate drive motor
5 Discharge augers
6 Centrifugal fan
7 Fan drive motor

Figure 3.5 Vertical crossflow cooler (Robinson, 1971).

### 3.3.2 Horizontal Crossflow Cooler

In horizontal crossflow coolers, the pellets are carried on a moving perforated belt; the air is drawn through the pellet layer in a crossflow pattern. The feed industry employs single-, double- and triple-belt coolers.

The capacity of a horizontal belt cooler depends on the length, width and height of the pellet layer on the belt, and the number of belts in the cooler.

The pellets are spread with an oscillating feeder onto the top belt. A constant layer-depth is maintained on the belt to assure a uniform air distribution across the bed to prevent uneven cooling of the pellets. A fan draws the air from below the bottom belt through the pellet layer(s). The cooling air is discharged through a cyclone.

The belt cooler has high maintenance requirements due to the moving belt(s). It requires excessive floor space and little headroom. The limited headroom is an advantage as many coolers are placed in the basement of feed mills.

#### 3.3.2.1 Single-Deck Horizontal Cooler

In a single-belt pellet cooler/dryer the cooling air passes through only one layer of pellets.

Figure 3.6 shows a schematic of a single-deck horizontal cooler. CPM single-belt horizontal coolers of the 5HR series range in capacity between 5 to 22 MT per hour. They are 1,829 mm wide and 4,267 to 10,363 mm long.

A recent simulation study conducted at Michigan State

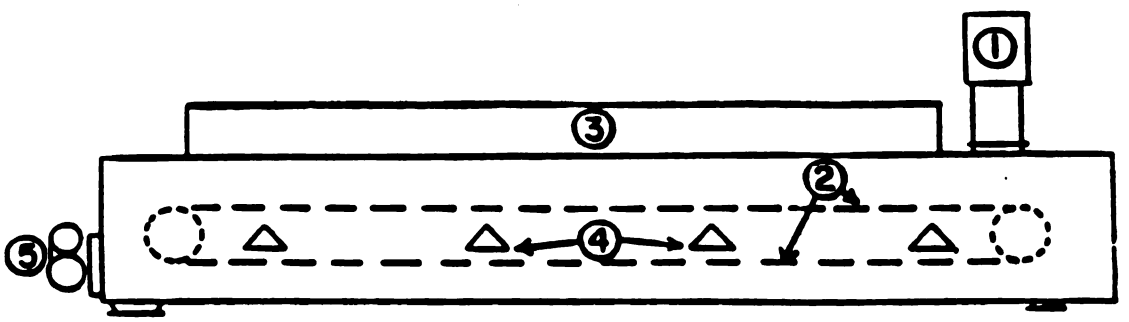


1 Oscillating feeder
2 Product carrying belt
3 Air chamber
4 Air inlet
5 Belt drive motor

Figure 3.6 Single-deck horizontal cooler (Robinson, 1970).

University considered the effects of the following parameters on the cooling and drying rate of pellets in a single-deck cooler (Bakker-Arkema et al., 1988): (1) pellet size, (2) pellet bed depth, (3) initial pellet temperature, (4) air flow rate, and (5) ambient conditions.

The results of the simulation study show that the bed depth, pellet diameter and airflow rate are important design parameters, while the initial pellet temperature and the initial moisture content have only minor influence on the cooling process. Figures 3.7 and 3.8 show the effect of the airflow rate on the average pellet temperature and average moisture content, respectively. After 10 minutes, the average pellet temperature in a cooler operating at 0.61 $m^3/m^2/s$ approaches the ambient temperature; in the cooler with 0.10 $m^3/m^2/s$ airflow rate, it is still 15°C above that level. A lower airflow leads to a lower final moisture content because the pellets remain for a longer period of time at a high temperature at which the drying rate is high. Further details of the simulation study can be found in Bakker-Arkema et al. (1988).

### 3.3.2.2 Multi-Deck Horizontal Cooler

Coolers with two, four, or more belts are considered multi-deck horizontal coolers. They are more efficient than single-deck horizontal coolers since they only require about one half, one quarter, or less of the air volume of single-deck coolers at equal capacities.

Figure 3.9 shows a CPM model 5HRS double-deck horizontal

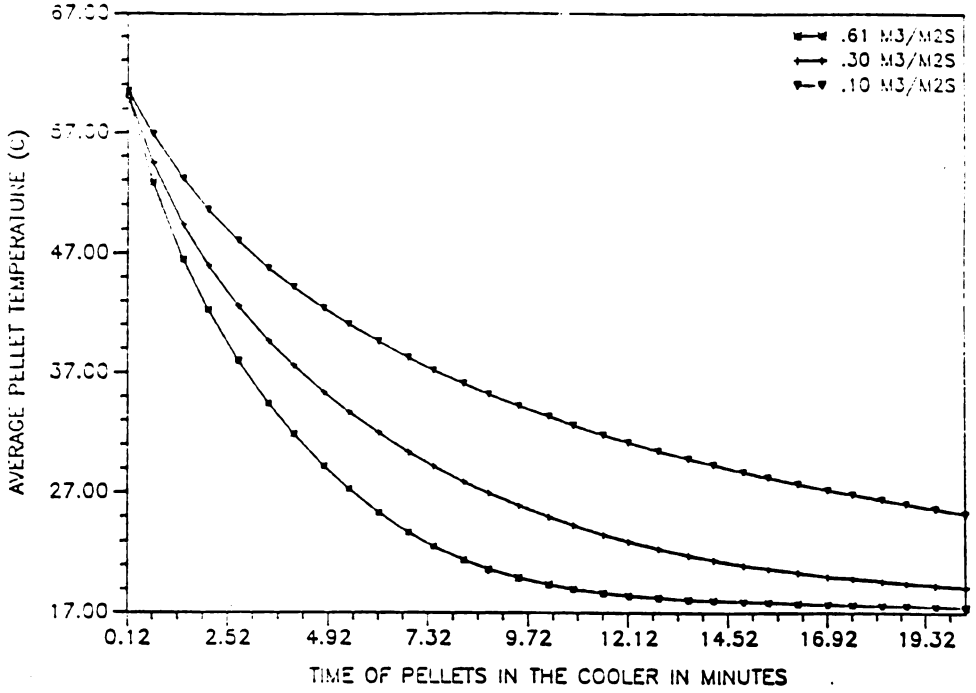


**Figure 3.7 Effect of airflow on the cooling rate in a single-deck cooler (Bakker-Arkema et al., 1988).**

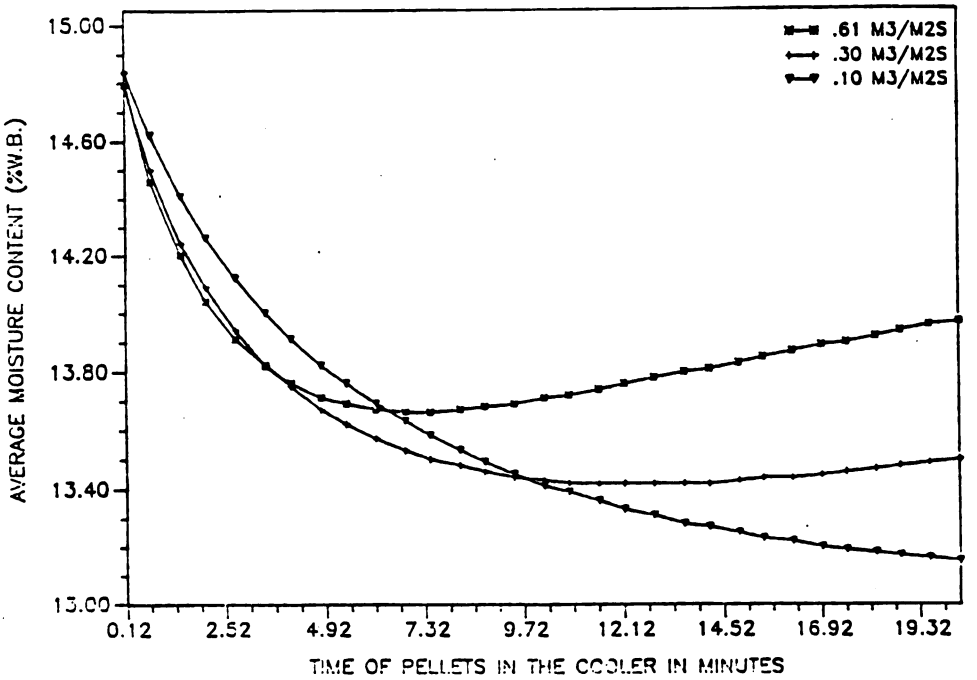


**Figure 3.8 Effect of airflow on the moisture loss in a single-deck cooler (Bakker-Arkema et al., 1988).**

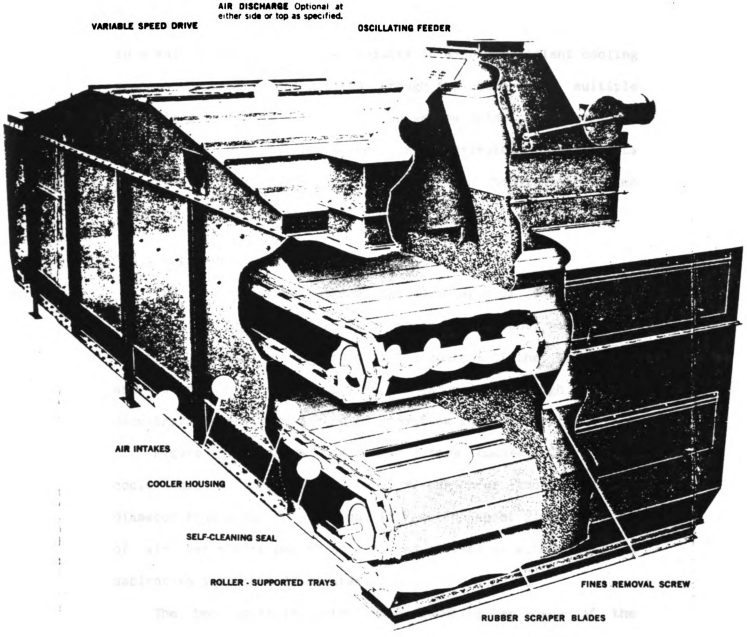


Figure 3.9 A CPM 5HRS double-deck horizontal cooler (CPM, 1987).

cooler. The cooler type has a capacity ranging from 10 to 42 MT per hour; a width of 1,829 mm, and a length ranging from 4,267 to 10,363 mm.

The increased moisture carrying capacity of the cooling air in a multi-deck pellet cooler results in a more efficient cooling process. By passing the pellets through the cooler over multiple belts in a crossflow pattern, a counterflow principle between the cooling air and the feed pellets is approximated. The pellets are cooled more uniformly in a multi-deck horizontal cooler yielding a higher final pellet quality.

### 3.3.3 Mixed-Flow Rotary Coolers

The rotary cooler combines the advantages of the vertical cooler, such as the limited floor space requirement, with those of the horizontal cooler, such as the control of the bed depth and retention time. The cooling air is drawn through several deck-trays in a mixed pattern of crossflow and counterflow.

Figure 3.10 shows a Klöckner rotary cooler. The rotary cooler has a capacity of 2 to 30 MT per hour and ranges in diameter from 2,000 to 3,000 mm. It requires about 21.7 to 25 $m^3$ of air per minute per MT to cool the pellets to within 3°C of ambient in less than 10 minutes.

The bed depth is controlled by altering the speed of the cooler. Problems occur when the pellets are not evenly distributed at the inlet (Walter, 1986). The pellets pass from deck to deck through tipping trays, which reduce the actual cooling time and disturb the airflow pattern.

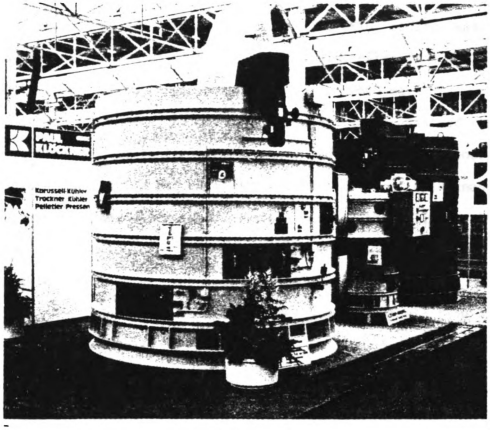


Figure 3.10 A Klöckner rotary pellet cooler (Die Mühle + Mischfuttertechnik, 1987).

### 3.3.4 Counterflow Coolers

Counterflow coolers have only recently been introduced on the market (McEllhiney, 1986). The first counterflow coolers for feed pellets were developed by Geleen Techniek of the Netherlands. Now, at least five other European manufacturers [Bühler-Miag, Klöckner, Simon-Heesen, VanAarsen, and Wijnveen] are marketing counterflow coolers. Figure 3.11 shows the Bühler-Miag model DFKG-25 counterflow cooler. The DFKG cooler has a capacity range of 7 to 17 MT per hour. Its diameter is 1,850 to 2,800 mm; its height ranges between 3,000 to 3,800 mm.

Geelen Techniek claims four primary advantages of the counterflow pellet cooler (Kraftfutter, 1985): (1) high energy savings (up to 50%), (2) small dimensions, (3) low maintenance requirements, and (4) reduced moisture loss of the pellets. The cooler is able to lower the pellet temperature to within 3°C of the ambient cooling air (Heinemans, 1986).

In the counterflow cooler, pellets and cooling air flow in opposite directions to one another. Figure 3.12 shows a comparison of the crossflow and counterflow principles. The primary advantage of the counterflow design is that the coolest pellets contact with the coldest air, and the hottest pellets contact the warmest air. This allows a gradual cooling of the pellets as they flow through the cooler and preserves pellet quality (Heinemans, 1986).

A disadvantage of the counterflow pellet cooler is the edge effects in the rectangular tanks, and a smaller capacity range

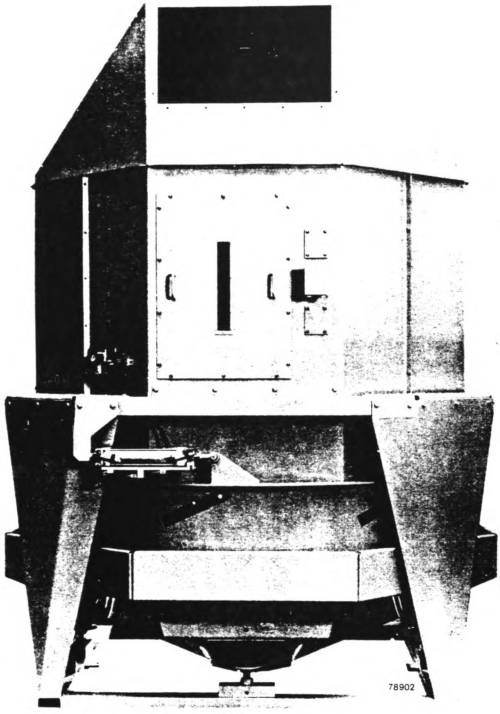


Figure 3.11 A Bühler-Miag DFKG-25 counterflow pellet cooler (Bühler-Miag, 1987).

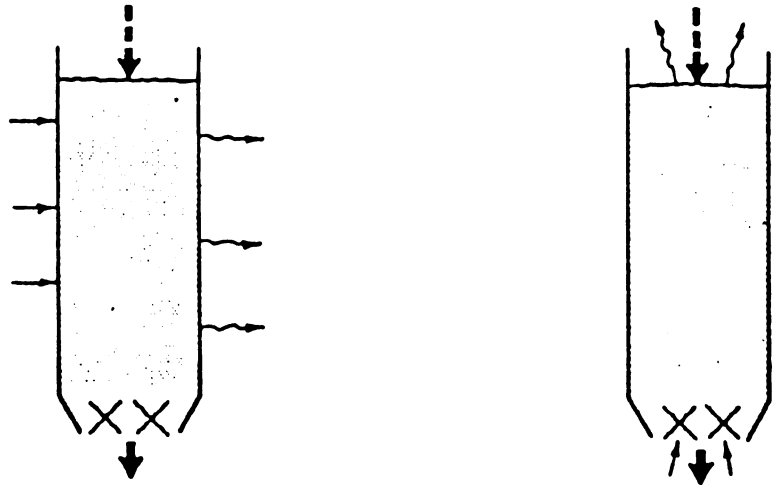

Figure 3.12 Comparison of the crossflow and counterflow cooling principles.

compared to horizontal coolers. Furthermore, the cooler is not easily adjustable for capacity.

Since counterflow coolers have only been on the market for about two years, no research studies have yet been published on the cooler performance. The only available design information is found in manufacturers' literature.

The counterflow pellet cooler constitutes a promising design. In Europe, satisfaction has been expressed with the cooler by commercial users (Apelt, 1987b).

## 3.4 PELLET PROPERTIES AND QUALITY

The quality of feed pellets depends on the physical and chemical properties (Apelt, 1987a). Chemically, it is important that the feed is easily digestible, and conducive to the animal's growth and production. Physically, it is important that the pellets yield few fines during transport, and resist crushing during handling and storage. Other important properties are the particle size distribution, the bulk density, the bulk flow characteristics, and the moisture content.

In order to define the physical quality of pellets,it is not sufficient to specify one property (Rohbohm, 1987b). Research has shown that a complete designation of pellet durability requires the measurement of the fines accumulation during mechanical and pneumatic transport, the pellet hardness, and pellet shearing resistance.

Early work in pellet quality testing was conducted at Kansas State University (KSU) (Winowiski, 1985). The KSU Pellet Tumbler

is still the standard testing device in the feed industry. The physical quality of pellets is defined as the percentage of fines generated when a sample of 500 grams of cooled and screened pellets is rotated in the tumbler at 50 rpm for 10 minutes. The tumbler gives a good estimate of the abrasion of pellets during mechanical handling in the feed mill.

Holmen Chemical and Bühler-Miag have developed on-line pneumatic pellet abrasion testers (McEllhiney, 1986). The pneumatic abrasion tester extracts a sample after the die, cures it rapidly, and tests its durability in an air-stream; this requires about two minutes per cycle (Rohbohm, 1987a). A pneumatic abrasion tester is intended to accurately simulate pneumatic handling processes in the feed mill.

Pellets are tested for hardness by measuring the horizontal force required for lengthwise crushing (Rohbohm, 1987b). Due to the variability of the crushing tests, it is recommended to break a minimum of 20 pellets per sample. The ease of shearing the pellets is determined with a flat pellet die. About 20 to 30 pellets are inserted in the holes of the die, and the force required to shear the pellets by pushing the upper half of the die across the fixed bottom half of the die is measured.

The U.S. manufacturer NORVIDAN has developed a method of determining the moisture of pellets on-line by high frequency measurement of the dielectric constant of the pellets (McEllhiney, 1986). The instrument automatically compensates for temperature and can be used to control the pellet cooler.

The control of the pelleting process depends on the ability

to monitor the various phases accurately. On-line moisture and durability testers, as described above, are essential to future successful automatic control of the pelleting operation.

The key to the accuracy of moisture, temperature, and quality sensors is how precisely the calibration curves are established; most still need to be determined for the different pellet sizes and consistencies. It will require several years before a sufficiently high level of accuracy is achieved for these instruments. The IFF is currently in the process of establishing calibration curves for this instrumentation (Rohbohm, 1987a).

# 4. DEVELOPMENT OF THE COUNTERFLOW MODEL

## 4.1 THE COUNTERFLOW DEEP-BED EQUATIONS

In the counterflow feed pellet cooler the air and the pellets flow in opposite directions. Mathematical modeling of the counterflow cooler consists of formulating energy and mass balances on an elemental volume of the system, with the pellet flow in the positive direction.

The following assumptions are made in establishing the counterflow cooling model equations:

(1) due to the small moisture loss in the pellet cooling operation, the volume shrinkage of the pellets is insignificant;

(2) the pellet-to-pellet conduction is negligible;

(3) the airflow and pellet flow in the cooling bed are plug-type;

(4) the partial derivatives of the air temperature and humidity, and of the pellet temperature with respect to time are negligible compared to the partial derivatives with respect to position;

(5) the heat capacity of the side walls of a commercial cooler is negligible compared to the pellets in the cooling bed;

(6) the heat capacities of the cooling air and the pellets are constant during short time intervals;

(7) several of the phenomenological equations are accurately described using expressions for corn, which is a major ingredient of feed pellets;

(8) the temperature gradients within the pellets are negligible;

(9) only radial moisture diffusion within the pellets is considered.

The steady-state model of the counterflow cooler/dryer consists of the following equations (Brooker et al., 1982):

$$\frac{dT}{dx} = \frac{h\,a}{G_a c_a + G_a c_v W} (T - \theta) \tag{4.1}$$

$$\frac{d\theta}{dx} = \frac{h\,a}{G_p c_p + G_p c_w M} (T - \theta) + \frac{h_{fg} + c_v (T - \theta)}{G_p c_p + G_p c_w M} G_a \frac{dW}{dx} \tag{4.2}$$

$$\frac{dW}{dx} = \frac{G_p}{G_a} \frac{dM}{dx} \tag{4.3}$$

$$\frac{dM}{dt} = \text{an appropriate drying equation} \tag{4.4}$$

The boundary and initial conditions for the counterflow system are:

$$T(L) = T_{inlet} \tag{4.5}$$

$$\theta(0) = \theta_{initial} \tag{4.6}$$

$$W(L) = W_{inlet} \tag{4.7}$$

$$M(0) = M_{initial} \tag{4.8}$$

Equations 4.1 through 4.4 yield the pellet and air temperatures, the pellet moisture contents, and the air humidities throughout the counterflow cooling bed.

The counterflow cooling model is a two-point boundary value problem. Therefore, both the air and the pellet properties are not known at any one location which results in considerable complexity in solving the model equations mathematically.

## 4.2 THE SINGLE-PELLET DRYING EQUATION

The solution of the counterflow model equations requires knowledge of the moisture loss of the feed pellets throughout the cooling/drying period. For feed pellets a single-kernel diffusion-type drying equation models the cylindrical shape and the moisture loss of the pellet best.

The cylindrical form of the diffusion equation is (Brooker et al., 1982):

$$\frac{\partial M'}{\partial t} = D \left( \frac{\partial^2 M'}{\partial r^2} + \frac{1}{r} \frac{\partial M'}{\partial r} \right) \tag{4.9}$$

The following initial and boundary conditions are assumed:

$$M'(r,0) = M_{initial} \tag{4.10}$$

$$M'(r_o,t) = M_{eq} \tag{4.11}$$

Equation 4.11 assumes that at the surface of the pellet the diffusion coefficient, D, is equal to the mass transfer coefficient, $h_D$.

Biagi (1986) proposed an Arrhenius-type relationship for the diffusion coefficient of feed pellets as a function of the pellet temperature for a range of 15.6° to 43.3°C and 40% to 70% relative humidity:

$$D = A \exp(-B/\theta_{abs}) \tag{4.12}$$

The diffusion coefficient is given in units of $m^2$ per hour. The pellet temperature, $\theta_{abs}$, is in °K.

Experimental data yielded the following equation coefficients:

$$A = 0.00001015 \ m^2/h$$
$$B = 547°K \qquad (4.12a)$$

However, the feed pellets in Biagi's thin-layer experiments did not reach equilibrium (Biagi, 1986). Therefore, the use of equation 4.12 with the coefficients of 4.12a has not been recommended (Beck, 1988).

After evaluating the experimental results, it was decided in this study to use for D the diffusion coefficient equation for corn (Chu and Hustrulid, 1968) multiplied by 3, or:

$$D = 3.0 \ A \exp(C - B/\theta_{abs}) \qquad (4.13)$$

where,

$$A = 0.0001513 \ m^2/h$$
$$B = 2513.0°K \qquad (4.13a)$$
$$C = (-5.47 + 0.045 \ \theta_{abs}) \ M$$

Originally, equation 4.13 was developed for a temperature range of 48.9° to 71.1°C, and a relative humidity range of 10% to 70%.

Solution of the diffusion equation 4.9 by finite differences establishes the moisture content distribution within the feed pellet; integration of the distribution results in the average moisture content at time, t, which is used to solve equation 4.4.

In this study the cylindrical pellet is divided internally into four subregions of equal volume; the radii of the subregions of the feed pellets used in this study are: 1.09 mm, 1.54 mm,

1.89 mm, and 2.18 mm, respectively. The four subregions yield one node at the center of the pellet, three interior nodes and one surface node. The difference between the internal moisture of the pellet and the equilibrium moisture content at the surface of the pellet provides the driving mechanism of the moisture loss of the pellet ($M > M_{eq}$), or the moisture adsorption of the pellet ($M < M_{eq}$).

## 4.3 EQUILIBRIUM MOISTURE CONTENT

A closer look at boundary condition 4.11 of the diffusion equation (eq. 4.9) shows that at time, t, the moisture content at the surface of a pellet is assumed to be in equilibrium with the cooling air. This moisture content is defined as the equilibrium moisture content (EMC).

The only available moisture sorption isotherms on feed pellets have been published by Friedrich (1980). Figure 4.1 shows the sorption isotherms of broiler, hog and dairy pellets with a diameter of 4.7 mm at 25°C. The relative humidity ranges from about 30 to 95%, the moisture content ranges from about 0.05 to 0.35 grams of water per grams of dry matter. Friedrich considered the differences of the sorption isotherms of the three pellet types negligible.

A comparison of several EMC equations (Biagi, 1986; Brook, 1981) with the graphical data of Friedrich (1980) shows that the sorption isotherm of soybeans follows the sorption isotherm of the feed pellets closely in the 30 to 80% relative humidity range (see Figure 4.2). Soybeans, similar to feed pellets, are higher

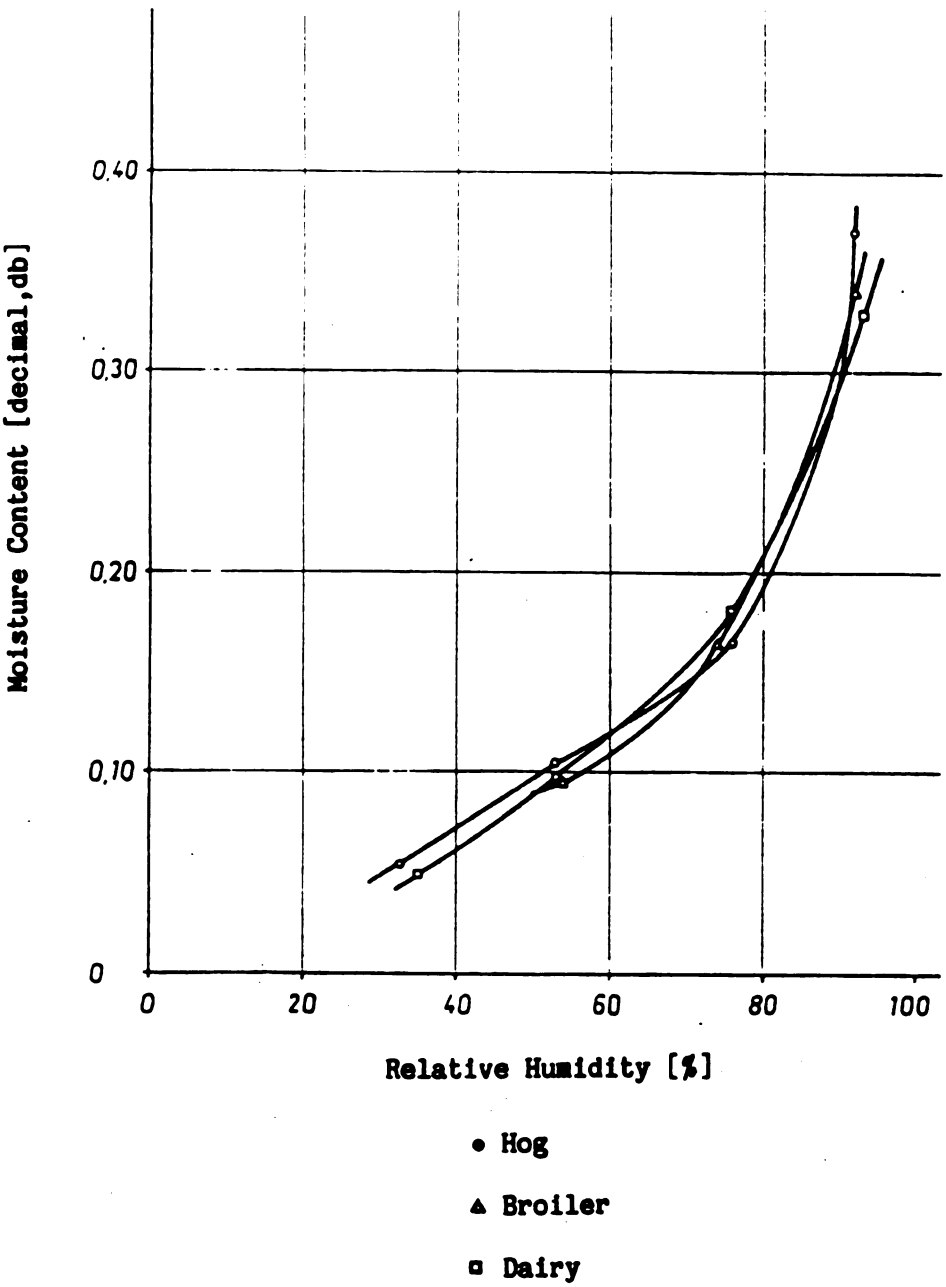


Figure 4.1 Sorption isotherm of hog, broiler and dairy pellets (Friedrich, 1980).

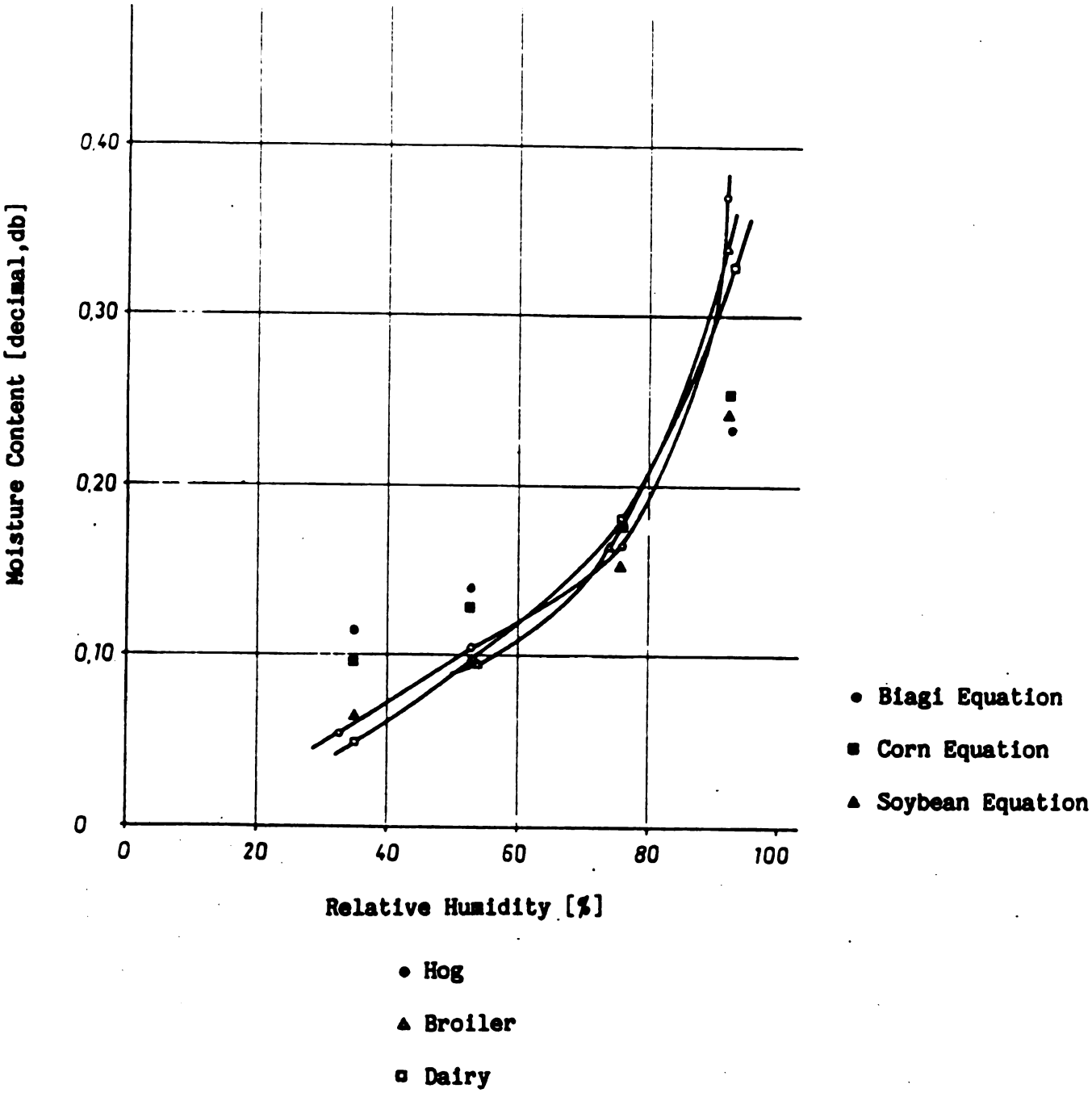


Figure 4.2 Comparison of various equilibrium moisture content equations.

in fat content than corn, thus adsorbing less moisture from the surrounding air.

It is assumed in this study that the soybean sorption isotherm, which is valid for a relative humidity range of 20% to 90%, is valid for feed pellets. Thus, the equilibrium moisture content equation for feed pellets is (Brook, 1981):

$$M_{eq} = 0.375 - 0.0668 \ln(-1.98 (T + 24.6) \ln(RH)) \qquad (4.17)$$

The equilibrium moisture content, $M_{eq}$, is in decimal dry basis; the air temperature, T, in °C; and the relative humidity in decimal.

## 4.4 SPECIFIC HEAT

An equation for the specific heat of feed pellets is not available in the literature. Table 4.1 compares the specific heat of corn, wheat, rice, soybeans (Brook, 1981) and extruded corn (Fortes and Okos, 1982) at a moisture content of 18.3% dry basis.

Table 4.1 Specific heat values for various products [kJ/kg °K].

| | |
|---|---|
| Corn | 2.117 |
| Extruded Corn | 1.859 |
| Rice | 1.929 |
| Soybeans | 1.990 |
| Wheat | 2.147 |

An equation for the specific heat, $c_p$, of grains on a dry basis and converted to SI units is (Brook, 1981):

$$c_p = A + B\,M \tag{4.18}$$

It is assumed in this study, that the specific heat of corn adequately describes the specific heat of feed pellets. The coefficients in equation 4.18 are:

$$\begin{aligned} A &= 1.465 \\ B &= 3.559 \end{aligned} \tag{4.18a}$$

when the specific heat is expressed in kJ per kg per °C, and the moisture content in decimal dry basis.

The specific heat of ambient air at 25°C is 1.0057 kJ/kg/°C (Holman, 1981). The specific heat of water vapor at 100°C is about 2.060 kJ/kg/°C. The specific heat of water is included in the specific heat equation used for the feed pellets.

## 4.5 CONVECTIVE HEAT TRANSFER COEFFICIENT

A convective heat transfer coefficient equation for feed pellets is not available in the literature. It was decided to compare the heat transfer coefficients of several grains for two equations found in the grain drying literature.

The following equation is product-specific (Brook, 1981):

$$h = A\,(G_a\,T_{abs}/B)^C \tag{4.19}$$

The second equation is size-specific (Barker, 1965):

$$h = 0.992\,c_a\,G_a\,(G_a\,d/\mu)^{-.34} \tag{4.20}$$

The heat transfer coefficient, h, in equations 4.19 and 4.20 has units of Btu/h/ft$^2$/°F, the air flow rate, $G_a$, has units of lb/h/ft$^2$, the diameter, d, has units of ft, the temperature, T, has units of °R, the specific heat of air, $c_a$, has units of Btu/lb/°F, and the dynamic viscosity, $\mu$, has units lb/h/ft.

The heat transfer coefficient equations are compared in Table 4.2 for an air flow rate of 417.67 lb/h/ft$^2$, a product specific mean diameter, and air at a temperature of 532.68°R (22.6°C) with a specific heat of 0.240 Btu/lb/°F and a dynamic viscosity of 0.044155 lb/h/ft. The mean diameters for the grains are from Brook (1981) at a moisture content of 12%. The diameter for the pellets is 11/64th inches.

Table 4.2 Comparison of the heat transfer coefficients of various products for two equations [Btu/h/ft$^2$/°F].

| | Equation 4.19 | Equation 4.20 | Diameter [ft] |
|---|---|---|---|
| Barley | --- | 18.44 | 0.0150 |
| Corn | 21.63 | 14.23 | 0.0322 |
| Navy Bean | 16.00 | 16.15 | 0.0222 |
| Wheat | --- | 18.94 | 0.0139 |
| Feed Pellet | --- | 18.74 | 0.0143 |

Although equation 4.20 neglects the effect of particle shape and surface characteristics it does consider the diameter of the product. Since the heat transfer coefficient of the feed pellet compares well with the ones of the grains, equation 4.20 is used

in this study.

In order to use equation 4.20, the air flow rate, the specific heat capacity of the cooling air at 25°C, the pellet diameter and the dynamic viscosity of the cooling air at 25°C are converted from SI units to US customary units. The resulting heat transfer coefficient is converted back from Btu/h/ft$^2$/°F to kJ/h/m$^2$/°C.

The dynamic viscosity for the cooling air at 25°C is 1.8371E-5 kg/m/s (0.044443 lb/h/ft) (Holman, 1981).

## 4.6 LATENT HEAT OF VAPORIZATION

The value of the latent heat of vaporization for the moisture in feed pellets is not available in the literature. A general latent heat equation converted to SI units for various grains is (Brook, 1981):

$$h_{fg} = (2501.11 - 2.386\ T)\ (1 + A\ \exp(B\ M)) \qquad (4.21)$$

The latent heat of vaporization, $h_{fg}$, has units of kJ/kg, the temperature, T, is in °C, and the moisture content, M, is in decimal dry basis.

The latent heats of vaporization of various grains are listed in Table 4.3 at a temperature of 25°C and a moisture content of 18.3% dry basis.

Table 4.3 The latent heats of vaporization of various grains [kJ/kg].

| | |
|---|---|
| Corn | 2583.07 |
| Rice | 2523.45 |
| Soybeans | 2536.02 |
| Wheat | 2551.89 |

It is assumed in this study that the latent heat of vaporization (eq. 4.21) for corn is valid for feed pellets. The equation coefficients for corn are (Brook, 1981):

$$A = 1.2925$$
$$B = -16.961 \qquad (4.21a)$$

## 4.7 BULK AND PELLET DENSITY

The feed pellets used for the experimental tests of this study yielded a dry bulk density of about 641 kg/m$^3$.

The single pellet density of a Milk Generator #1000 (B) pellet was determined by Biagi (1986) to be 945 kg/m$^3$. The same value is used for the pellets in this study.

## 4.8 SPECIFIC SURFACE AREA

The counterflow model equations require knowledge of the specific surface area, a, of the pellets in the cooling bed. The specific surface area is defined as the total surface area of the product per unit volume of the cooling bed. For cylindrical

pellets in a bed of 1 $m^3$ volume, the expression for the specific surface area reduces to:

$$a = (1 - \varepsilon) \frac{2 (r_o + \ell)}{r_o \ell} \qquad (4.22)$$

The specific surface area has units of $m^{-1}$. The feed pellets used in the experimental tests had a radius, $r_o$, of 0.002183 m and an average length, $\ell$, of 0.00254 m. The void ratio, $\varepsilon$, calculated from the bulk and pellet density, was 0.323. Thus, the specific surface area calculated from equation 4.22 is 673.6 $m^{-1}$.

## 4.9 STATIC PRESSURE

The static pressure equation for corn is assumed to be valid for feed pellets. The equation is (Brook, 1981):

$$SP = \frac{20{,}600\ Q^2}{\ln(1 + 30.7\ Q)} \qquad (4.23)$$

The static pressure, SP, has units of Pa/m. The airflow, Q, has units of $m^3/m^2/s$.

## 4.10 PSYCHROMETRIC PROPERTIES

The psychrometric properties of moist air are calculated using the SI-form of the equations programmed by Lerew (1972). The atmospheric pressure value used in this study is 98,599 Pa.

## 4.11 SOLUTION PROCEDURE

Evans (1970) solved the counterflow cooling equations for a grain dryer directly using the invariant imbedding method. His solution procedure is complex and requires a large execution time

on a mainframe computer.

In order to reduce the complexity of the algorithm and allow for a reasonable execution time on a micro-computer, the following two-step solution procedure for the counterflow cooling model is used in this study (Bakker-Arkema and Schisler, 1984):

(1) solve the absolute humidity (W) and moisture content (M) equations numerically using coefficients computed from stored values of the air and pellet temperatures at equally spaced positions within the cooler; and

(2) solve the air (T) and pellet ($\theta$) temperature equations directly using coefficients computed from the stored values of the moistures and humidities at equally spaced positions within the cooler.

### 4.11.1 Starting the Algorithm

The procedure is started by dividing the length of the cooling bed into a 30-node grid of equidistant points. [A choice of 30 grid points is the smallest number of points that yields a reasonably fast convergence of the algorithm on a micro-computer without a significant loss of accuracy.] Next, linear air and pellet temperature profiles are initialized based on the pellet temperature at the entrance of the cooler, $\theta(0)$, and the air temperature at the outlet of the cooler, $T(L)$. Also, the linear moisture profile is established based on the following approximation:

$$M_{weq}(0) = 0.4\ M_w(0) \qquad (4.24)$$

[Equation 4.24 is based on the observation that the equilibrium moisture content wet basis, $M_{weq}$, at the entrance of the cooler is equal to 0.1 to 0.5 times the inlet moisture content of the pellets.]

From the pellet inlet temperature and the inlet equilibrium moisture content of equation 4.24, the equilibrium moisture content equation (eq. 4.17) is solved for the relative humidity at the top of the cooler. The outlet air humidity at the entrance of the cooler is then calculated from the pellet inlet temperature and the estimated relative humidity. On the basis of equation 4.3, an approximate outlet moisture content at the bottom of the cooler is determined:

$$M(L) = M(0) - G_a/G_p \, (W(L) - W(0)) \qquad (4.25)$$

Subsequently, the initial linear moisture profile is established by linear interpolation, and the initial humidity profile is established in the cooling bed using equation 4.3.

### 4.11.2 The Moisture Subproblem

The moisture subproblem is solved numerically in the following manner.

The 30-node grid is subdivided between each pair of nodes into 10 subgrid points (see Figure 4.3). [A choice of 10 subgrid points was found to assure convergence of the algorithm at the required accuracy.] Starting at node 1 at the top of the cooler, the pointer steps to the first subgrid point (1.1) where the air temperature and humidity are calculated by linear interpolation

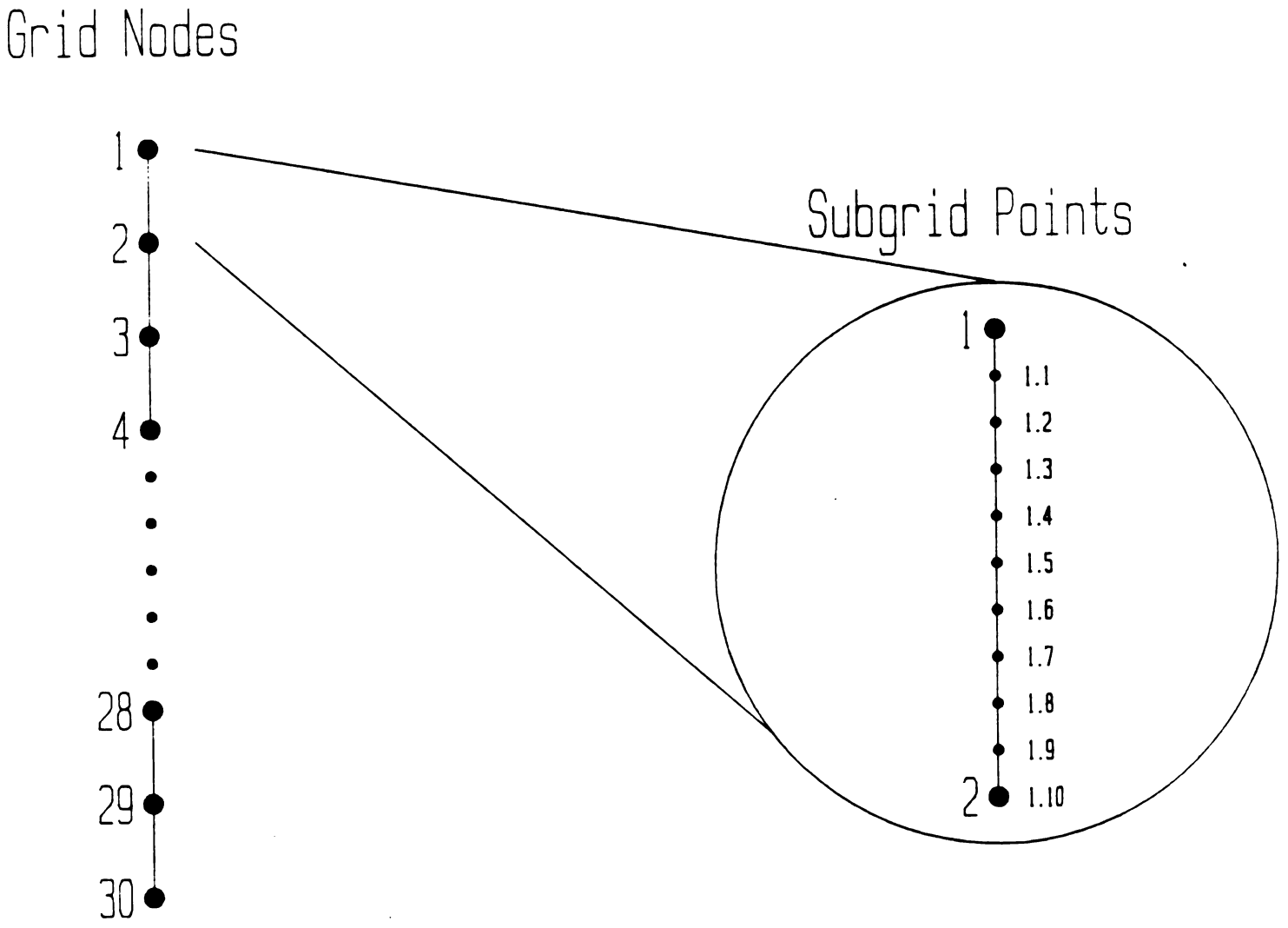


**Figure 4.3 Moisture subproblem cooling bed grid.**

from the initial profile. At this subgrid point, the air temperature and humidity are used to calculate the relative humidity and the equilibrium moisture content of the pellets. From the equilibrium moisture content, the average moisture content of the feed pellet at point 1.1 is calculated using equation 4.9.

Next, the pointer is incremented to subgrid point 1.2 and the average moisture content of the feed pellets is calculated again. When the interval of the 10 subgrid points is evaluated, the moisture content at node 2 in the cooling bed is updated and stored. The pointer then steps to node 2.1.

After all 30 nodes have been updated, a new moisture profile based on the initial pellet and air temperature profiles, and the initial humidity profile has been found. Due to the diffusion of moisture from the pellets, an internal moisture gradient in the feed pellets is established.

On the basis of this 'new' moisture profile, a 'new' humidity profile is determined using equation 4.3. The moisture loop is then repeated using the 'old' temperature profiles and the 'new' humidity profile.

Once the moisture and humidity profiles have converged, they are ready to be used in the temperature loop.

Figure 4.4 shows a flow chart of the moisture subproblem.

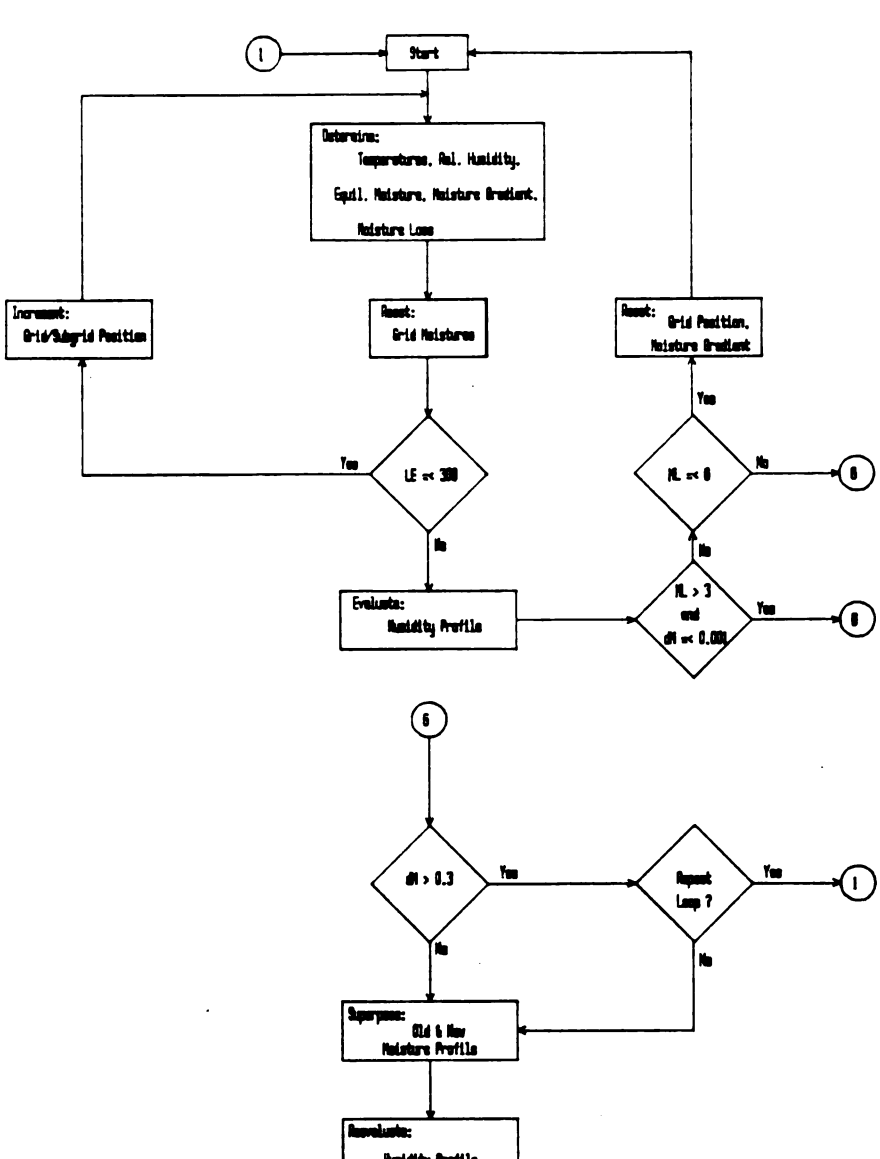


**Figure 4.4 Moisture subproblem flow chart.**

### 4.11.3 The Temperature Subproblem

The temperature subproblem is solved using a two-step method. The temperature equations are:

$$\frac{dT}{dx} = \frac{h\,a}{G_a c_a + G_a c_v W}\,(T - \theta) \tag{4.1}$$

$$\frac{d\theta}{dx} = \frac{h\,a}{G_p c_p + G_p c_w M}\,(T - \theta) + \frac{h_{fg}}{G_p c_p + G_p c_w M}\,G_a \frac{dW}{dx} \tag{4.2'}$$

subject to

$$\theta(0) = \theta_{initial} \tag{4.26}$$

$$T(L) = T_{inlet} \tag{4.27}$$

Equation 4.2' is the simplified form of equation 4.2. The size of the specific heat term, $c_v(T - \theta)$, is negligible compared to the size of the latent heat of vaporization term since in a counterflow cooler the difference between the air temperature and the pellet temperature is generally less than 5°C.

Equations 4.1 and 4.2' constitute a two-point boundary value problem, subject to equations 4.26 and 4.27. Both, the air and pellet temperatures are not known at any one location in the cooler. The invariant imbedding method allows for the direct solution of the pellet and air temperatures of equations 4.1 and 4.2' at the unknown boundaries of the cooling bed. Integration of the temperature equations 4.1 and 4.2' using the now known boundary conditions solves the cooling bed temperatures.

Invariant imbedding expresses the state variable at a given position as a function of the continuous mechanism and the boundary conditions of the system equation (Evans, 1970). The initial condition of an invariant imbedding problem is the system's response when the length of a continuous mechanism is zero. The boundary conditions of an invariant imbedding problem usually are known system responses to specific boundary conditions of the original system equation.

For the temperature subproblem of the counterflow cooler the system equations are equations 4.1 and 4.2'; the independent variable is the position within the cooling bed. The boundary conditions of the system are represented by equations 4.26 and 4.27. In the invariant imbedding formulation the state variables are T and $\theta$ which are expressed as functions of the bed depth, x, and the boundary conditions of the system equations.

The following linear boundary-value problem is used to set up the invariant imbedding method (Scott, 1973):

$$\frac{du(z)}{dz} = a(z)u(z) + b(z)v(z) + e(z) \qquad (4.28)$$

$$-\frac{dv(z)}{dz} = c(z)u(z) + d(z)v(z) + f(z) \qquad (4.29)$$

subject to

$$u(z=0) = \alpha \qquad (4.30)$$

$$v(z=L) = \beta \qquad (4.31)$$

The counterflow temperature equations 4.1 and 4.2' and the boundary conditions 4.26 and 4.28 are fitted to equations 4.28 through 4.31 by making the following substitutions:

$$\frac{du(z)}{dz} = \frac{d\theta}{dx} \tag{4.32}$$

$$a(z) = - \frac{h\ a}{G_p(c_p + c_w\ M)} \tag{4.33}$$

$$b(z) = \frac{h\ a}{G_p(c_p + c_w\ M)} \tag{4.34}$$

$$e(z) = \frac{h_{fg}}{c_p + c_w\ M} \frac{dM}{dx} \tag{4.35}$$

$$- \frac{dv(z)}{dz} = \frac{dT}{dx} \tag{4.36}$$

$$c(z) = \frac{h\ a}{G_a(c_a + c_v\ W)} \tag{4.37}$$

$$d(z) = - \frac{h\ a}{G_a(c_a + c_v\ W)} \tag{4.38}$$

$$f(z) = 0 \tag{4.39}$$

subject to

$$u(z=0) = \alpha = \theta(x=L) \tag{4.40}$$

$$v(z=L) = \beta = T(x=0) \tag{4.41}$$

The following transformation is used to express the dependent state variables u and v as a function of the independent variable z (Scott, 1973):

$$u(z) = r_1(z)v(z) + r_2(z) \tag{4.42}$$

Differentiating equation 4.42 with respect to z, yields:

$$\frac{du(z)}{dz} = \frac{dr_1(z)}{dz} v(z) + r_1(z) \frac{dv(z)}{dz} + \frac{dr_2(z)}{dz} \tag{4.43}$$

Substituting equations 4.28 and 4.29 into equation 4.43, and using equation 4.42 again, yields:

$$\frac{dr_1(z)}{dz} = b(z) + [a(z) + d(z)]\, r_1(z) + c(z)\, r_1^2(z) \tag{4.44}$$

$$\frac{dr_2(z)}{dz} = [a(z) + c(z)\, r_1(z)]\, r_2(z) + f(z)\, r_1(z) + e(z) \tag{4.45}$$

Equations 4.44 and 4.45 are known as Ricatti-type equations (Scott, 1973). A set of initial conditions for equations 4.44 and 4.45 is obtained by evaluating equation 4.42 at z = 0,

$$u(0) = \alpha = r_1(0)\, v(0) + r_2(0). \tag{4.46}$$

If it is assumed that

$$r_1(0) = 0 \tag{4.47}$$

then, $$r_2(0) = \alpha \tag{4.48}$$

The value of $r_1(0)$ can be chosen arbitrarily since v(0) is known.

The choice of $r_1 = 0$ at $z = 0$, implies that $r_2$ at the bottom of the cooler is equal to the outlet pellet temperature.

Equations 4.44 and 4.45 with boundary conditions 4.47 and 4.48 constitute an initial value problem. The equations are solved for r1(z) and r2(z) using the Adam-Moulton integration technique (Lastman, 1963).

The invariant imbedding method does not solve the interior values of u(z), since the interior values of v(z) remain unknown. Equation 4.46, however, yields the pellet temperature, u(z=0) or $\theta(x=L)$, at the air inlet, z=0 or x=L, using the air temperature, v(z=0) or T(x=L) and the boundary conditions 4.47 and 4.48.

The interior values of the counterflow cooling bed are solved using the original counterflow temperature equations (eqs. 4.1 and 4.2'). Equations 4.1 and 4.2' are integrated using the now known boundary value of u(z=0) and the initial value of v(z=0), subject to:

$$T(z=0) = T_{inlet} \tag{4.49}$$

$$\theta(z=0) = r_1(x=L)\, T_{inlet} + r_2(x=L) \tag{4.50}$$

The integration of the interior values is again performed with an Adam-Moulton routine.

The temperature loop is repeated once for the Ricatti equations (eqs. 4.44 and 4.45) and once for the counterflow system equations (eqs. 4.1 and 4.2') (see Figure 4.5). For both, the same moisture and humidity profiles, which have been calculated in the moisture loop, are used. After the temperature

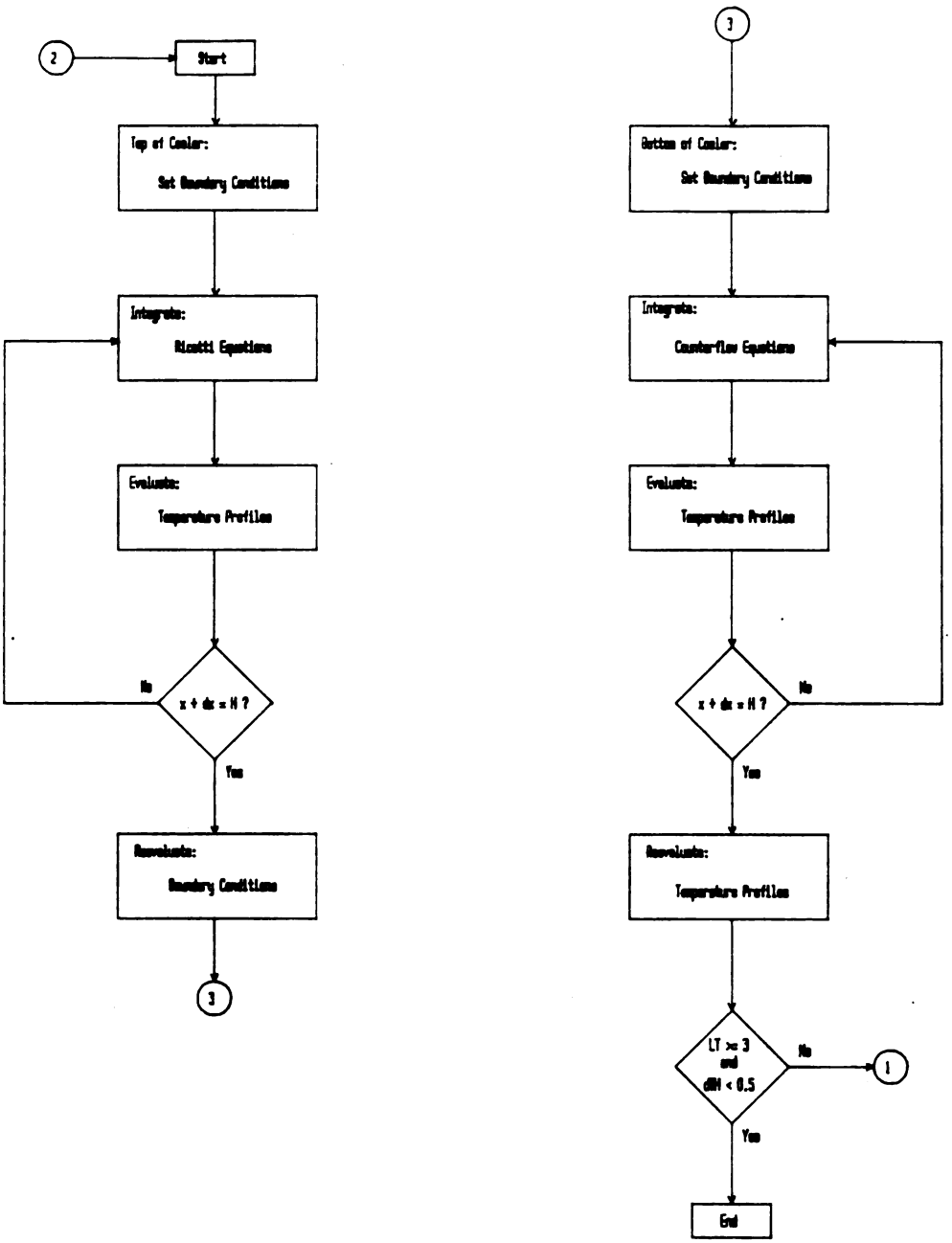


Figure 4.5 Temperature subproblem flow chart

subproblem is solved the moisture loop is repeated.

4.11.4 Convergence of the Algorithm

The moisture and temperature loops usually do not converge in one iteration. The moisture and humidity profiles are evaluated using the temperature profiles of the previous iteration (except, as mentioned, in the first iteration where the initial temperature profiles are used); the temperature profiles are evaluated using the moisture and humidity profiles of the current iteration.

The moisture loop is repeated a minimum of four times and a maximum of eight times. After the four loop repetitions, the moisture loop is terminated if the difference in the outlet moisture content between the current iteration and the previous iteration is less than 0.1% of the absolute change in moisture content. If after eight moisture loop repetitions the difference is still larger than 3%, the moisture loop is repeated one additional time.

After the moisture loop is completed, the actual moisture profile, $M_{actual}$, is determined using a weighting factor, WF:

$$M_{actual} = WF\ M_{old} + (1 - WF)\ M_{new} \qquad (4.51)$$

The weighting factor is used to insure both, convergence and stability in the counterflow model. The actual humidity profile is evaluated using $M_{actual}$ and equation 4.3. Both 'actual' profiles are passed to the temperature subproblem.

The weighting factor, WF, is also used within the moisture

loop to re-evaluate the current humidity profile. The humidity profile is calculated based on equation 4.3 and the current moisture profile. Since the rate of the diffusion of moisture from the pellets is high, the cooling air is quickly saturated. The rise in relative humidity of the air raises the equilibrium moisture content in the next moisture iteration to an extreme value; the pellets are now forced to re-adsorb most of the previously lost moisture from the air. In order to prevent the excessive moisture exchange between the air and the pellets, the rate of moisture loss is decreased by also applying the weighting factor, WF, in the determination of the current humidity profile, $W_{current}$:

$$W_{current} = WF\ W_{old} + (1 - WF)\ W_{new} \qquad (4.52)$$

$W_{old}$ represents the humidity profile of the previous moisture iteration, and $W_{new}$ represents the humidity profile based on the current moisture profile.

Convergence of the temperature and moisture/humidity coupling calculations is tested by evaluating the change in the outlet grain temperature between successive iterations. The criterion is set as ±0.5°C. A minimum of three evaluations of the temperature and moisture loops is performed before the grain temperature criterion is used. A maximum of eight evaluations is generally sufficient to allow convergence.

If eight evaluations are not sufficient, the algorithm stops. The temperature, moisture and humidity values are printed but include a message that the profiles may not have converged.

4.11.5 Stability of the Algorithm

Experience has shown that rapid moisture loss by the pellets to the air in the moisture loop may cause instability of the algorithm. As mentioned above, a weighting factor is used to decrease the rate of the moisture loss and insure stability.

It has been established by trial and error that only a varying weighting factor satisfies the convergence and stability requirements of the algorithm. In this study the following weighting factors are used:

if the coupling loop, LT = 1, then WF = 0.7 (4.53)

if the coupling loop, LT = 2, then WF = 0.5 (4.54)

if the coupling loop, LT $\geq$ 3, then WF = 0.3 (4.55)

The factors of equations 4.53, 4.54, and 4.55 are used in equations 4.49 and 4.50.

Figures 4.6 and 4.7 show convergence of the algorithm for a sample simulation run using the weighting factors of equations 4.54 through 4.56.

The input conditions are:

$T_{in}$ = 22.6°C $RH_{in}$ = 73.7%

$\theta_{in}$ = 62.6°C $M_{in}$ = 16.29%

$G_a$ = 29.26 m/min $G_p$ = 3.45 m/hr

Figures 4.6a through 4.6g show the convergence of the moisture profile for the coupled temperature-moisture loops 1 through 7. Figures 4.7a through 4.7g illustrate the convergence of the pellet temperature profile based on the moisture profiles

Figure 4.6a

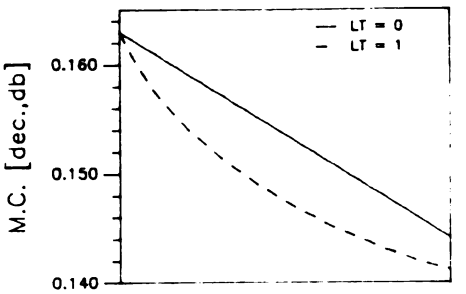


Figure 4.6b

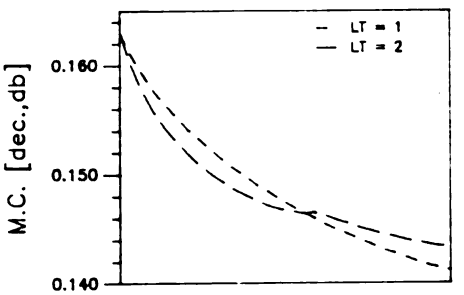


Figure 4.6c

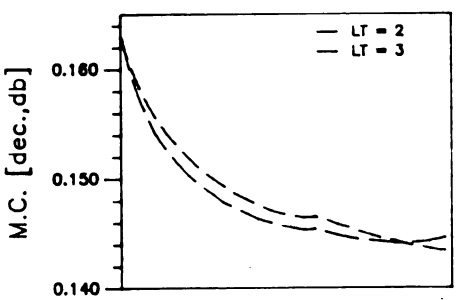


Figure 4.6d

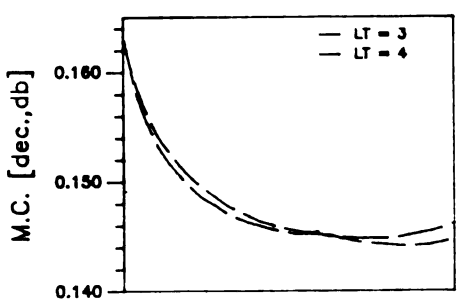


**Figure 4.6 Convergence of the pellet moisture profile.**

Figure 4.7a

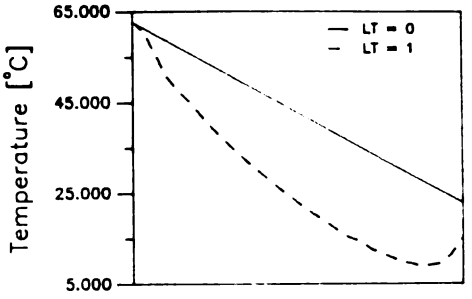


Figure 4.7b

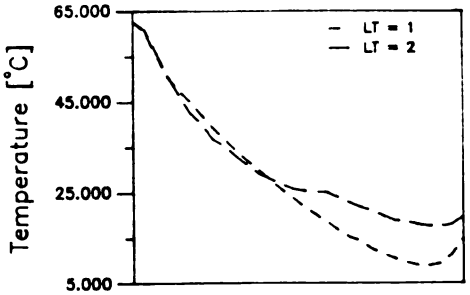


Figure 4.7c

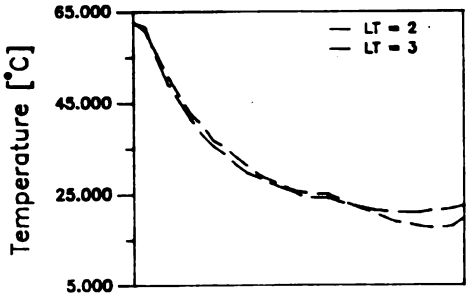


Figure 4.7d

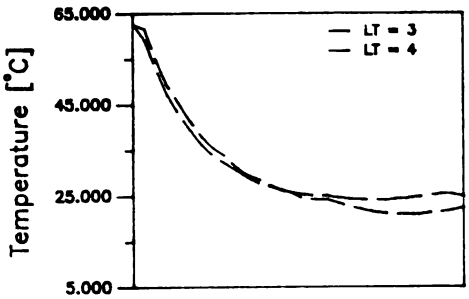


**Figure 4.7 Convergence of the pellet temperature profile.**

Figure 4.6e

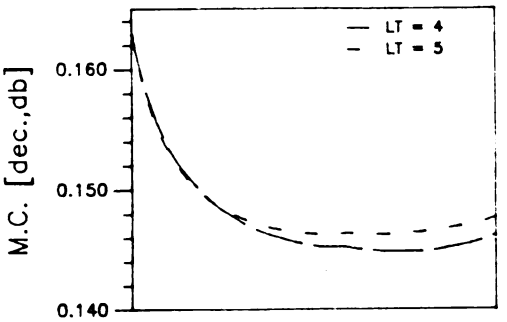


Figure 4.7e

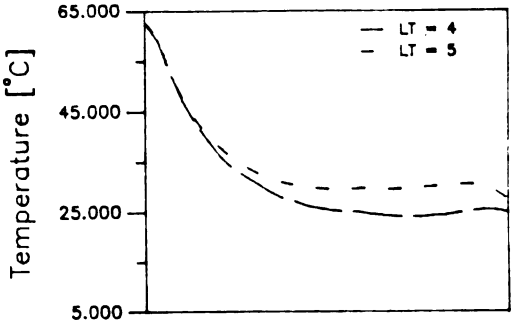


Figure 4.6f

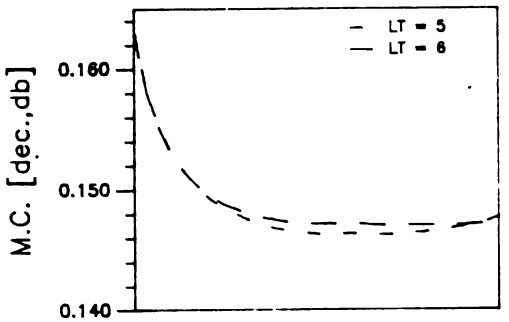


Figure 4.7f

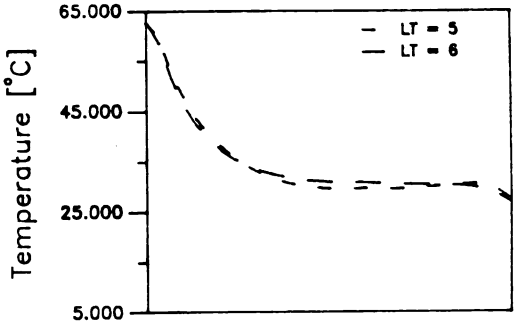


Figure 4.6g

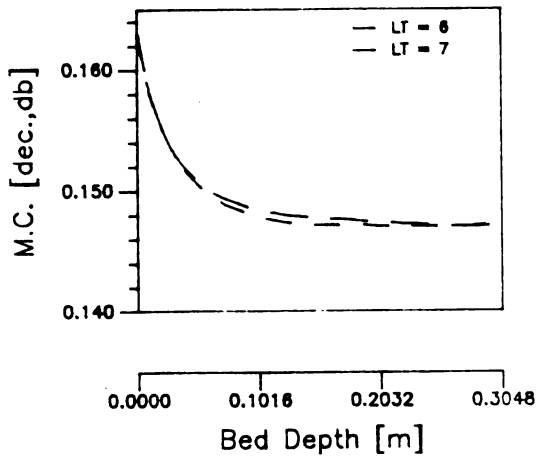


Figure 4.7g

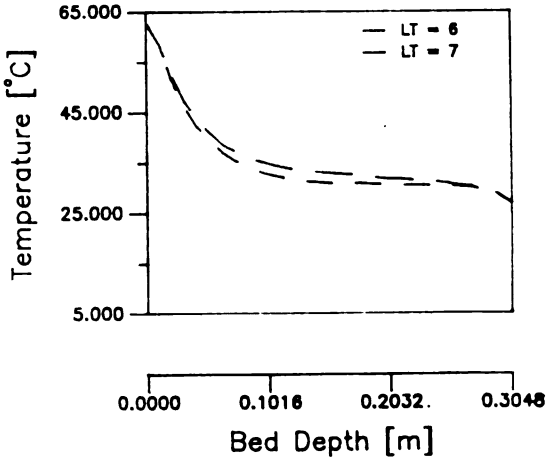


**Figure 4.6 (cont'd.)**

**Figure 4.7 (cont'd.)**

of Figure 4.6. At the end of the seventh loop, LT = 7, the algorithm has converged, as the pellet outlet temperature from loop LT = 6 to loop LT = 7 has changed by less than ±0.5°C.

# 5. EXPERIMENTAL

## 5.1 COUNTERFLOW COOLER DESIGN

Figure 5.1 is an exposed view of the dimensionalized laboratory-size counterflow cooler; Figure 5.2 is an expanded view. The model cooler was originally designed in American units, thus both metric (SI) and American engineering (USCS) units are given below.

The cooler is constructed of cylindrical 3 mm (.118 inch) thick steel sections of 0.0929 $m^2$ (1.0 $ft^2$) cross-sectional area. The height of the cooler can be increased from 0.3048 m (1 ft) by inserting 0.6096 m (2.0 ft) long sections.

Ambient cooling air is introduced at the lower section of the cooler through a wedge formed of perforated sheet metal. The wedge is bolted inside the cylindrical section. [During the analysis of the tests, the shape and placement of the wedge was found to cause slightly uneven airflows in the cooler bed.] A 5.08 cm (2 inch) long 10.2-to-12.7 cm (4 to 5 inch) transition allows a 10.2 cm (4 inch) diameter flexible hose to be installed between the cooling fan and the cooling bed. The flexible hose is divided into two 76.2 cm (30 inch) sections. The connector acts also as a shutter allowing airflow regulation.

The bottom of the counterflow section is made air-tight by a tin plate and a gasket bolted to the bottom between the base and lower counterflow section. The base is constructed of 2.54 cm (1 inch) welded square tubing.

Cooling air in tests 1 through 4 was provided by the fan of

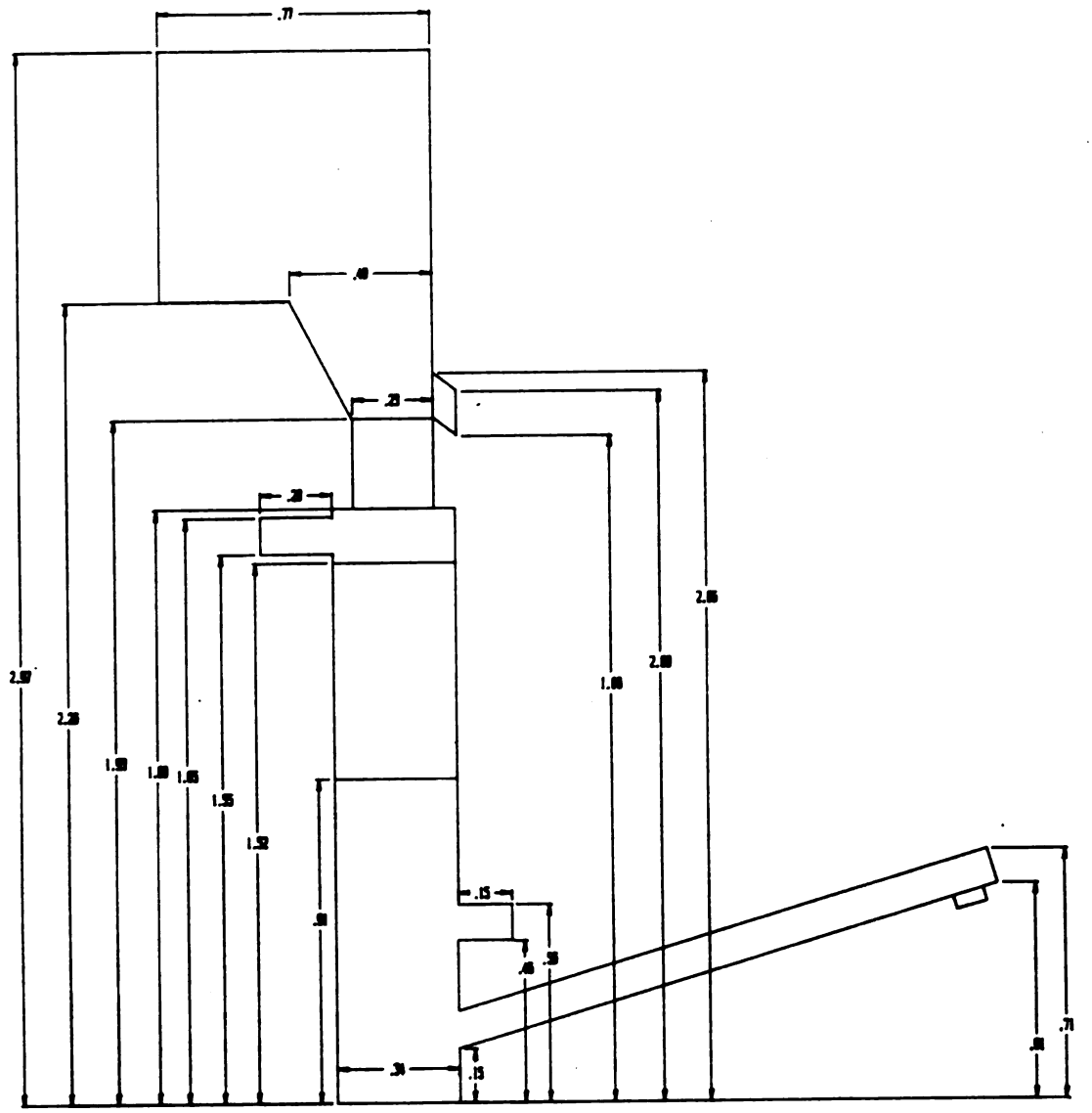


Figure 5.1 Dimensionalized experimental counterflow cooler.

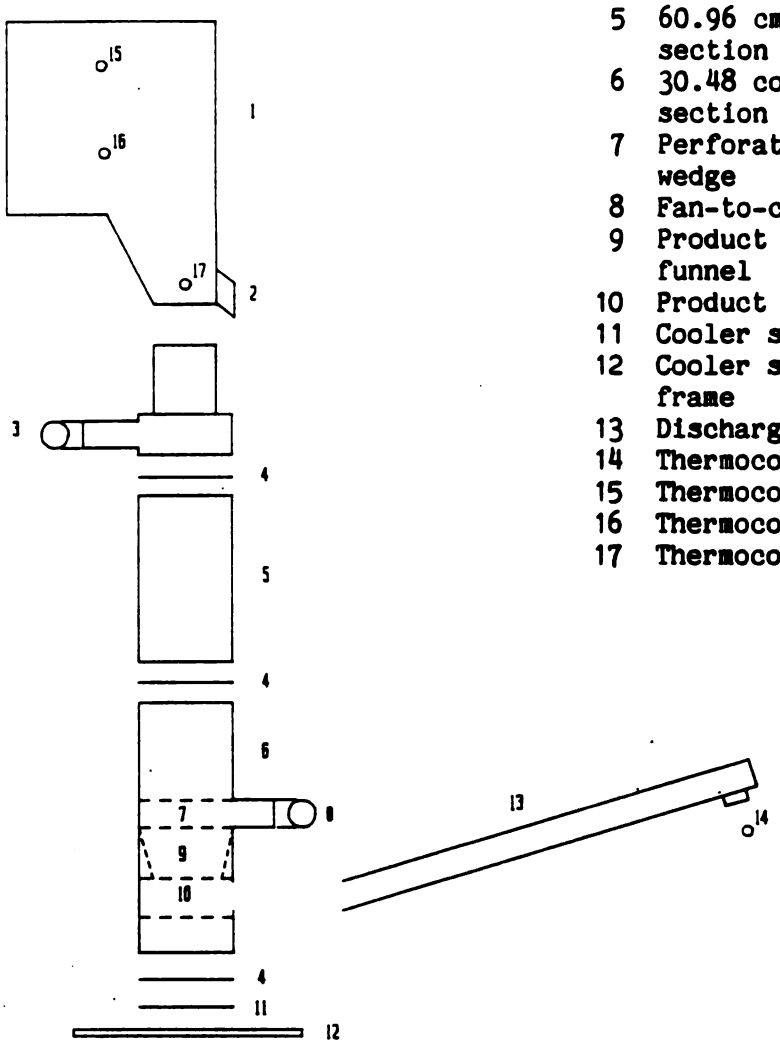


1 Feeder box
2 Moisture inlet sampling spout
3 Cooling air exhaust
4 Gasket
5 60.96 cm counterflow section
6 30.48 counterflow section
7 Perforated air inlet wedge
8 Fan-to-cooler transition
9 Product collecting funnel
10 Product collection basin
11 Cooler section end plate
12 Cooler section base frame
13 Discharge auger
14 Thermocouple 29
15 Thermocouple 31
16 Thermocouple 32
17 Thermocouple 33

Figure 5.2 Exposed view of the experimental counterflow cooler.

a 150/300 CFM Aminco-Aire air conditioning unit. Cooling air in tests 5 through 8 was provided by a 20.3 cm (8 inch) centrifugal fan powered by a 0.56 kW (3/4 horsepower) three-phase motor. The cooling airflow rate at the fan is regulated with a shutter added at the fan inlet.

The cooler unloading mechanism operates as follows. A collection funnel is held in place by sheet metal screws. The pellets are funneled via a collection basin into the discharge auger. The 10.16 cm (4 inch) auger is placed inside the lower counterflow section, and is sealed in place to prevent air leakage. A stand (not shown) is provided to support the discharge end of the 167 cm (66 inch) long auger. The pellet flowrate is controlled by changing the rpm of the discharge auger motor. The motor is a shunt-wound 0.37 kW (1/2 HP) DC motor regulated with a Dayton Vario Speed Controller.

Exhaust air exits the cooler through a 10.2 cm (4 inch) diameter, 20.32 cm (8 inch) long tube. The air outlet is located opposite and above the air inlet.

The hot pellets are stored in an insulated box which feeds the pellets by gravity into the top of the cooler. The feeder box has a volume of about 0.22 $m^3$ (7.8 $ft^3$). A stand is provided (not shown) to support the feeder box. The top of the feeder box is 145 cm (57 inches) above the top layer of the cooling bed.

## 5.2 INSTRUMENTATION AND EQUIPMENT

The instrumentation employed during the laboratory counterflow cooling tests is summarized in Table 5.1.

The pressure drop through the cooling bed is measured with a Meriam manometer with a readability of ±0.05 in. of water column. The pressure tabs are located in the cooling bed at 12.7 cm (5 inch) intervals.

The inlet air velocity is measured across the inlet pipe to the cooling bed with a hot wire anemometer. The velocity meter has a readability of 25 fps. The airflow rate is calculated from the velocity readings and the cross-sectional area of the pipe.

Table 5.1 Summary of monitoring equipment.

| Instruments | Description |
|---|---|
| 1. Manometer | Meriam, Model 40GD10WM-6 |
| 2. Airflow Meter | Weathertronics Hot Wire Anemometer, Model 2440 |
| 3. Temperature Recorder | Kaye Instrument Remote Analog Multiplexing Processor and Scanner with 64 channels and computer interface |
| 4. Data Processor | 512K Micro Buffer and Zenith Z-148PC; in-house developed and commercial software |
| 5. Drying Oven | Blue M Electric Company, Model OV510, Mercury in steel thermometer |
| 6. Scales | Mettler Laboratory Scale; Pennsylvania Scale, Model B-210 |

The temperatures are measured with copper-constantan thermocouples (type T) with an accuracy of ± 0.5%. The dry bulb inlet air temperature is measured at the transition from the flexible hose to the counterflow cooler. The air outlet temperature is measured at the cooling air exhaust. The relative humidity of the inlet air and the exhaust air from the counterflow cooler is determined using wet bulb thermocouples. The thermocouples are installed next to the dry bulb inlet and outlet thermocouples of the air. The wicks are inspected before each run. The relative humidities are calculated using equations programmed by Biagi (1986).

The temperatures in the cooling bed are measured with three thermocouples at each of four levels. Figure 5.3 shows the division of the 0.3048 m (1 ft) cooling bed into three 10.16 cm (4 inch) layers. The temperatures are measured at the top of the cooling bed, at the two quarter positions, and at the bottom, of the cooling bed. The thermocouples are fastened inside a copper tubing and spanned across the cooling bed perpendicular to the air inlet/outlet configuration.

Figure 5.4 shows the division of the 0.9144 (3 ft) cooling bed. The lower 0.3048 m (1ft) section remains the same, while the added 0.6096 m (2 ft) section is divided into five layers. The top layer is 10.16 cm (4 inch) deep, the remaining four layers are each 12.70 cm (5 inch) deep. Thus, the 0.9144 m (3 ft) bed has nine rows of thermocouples. The bottom four rows are still perpendicular to the air inlet/outlet configuration, while the top five rows are parallel to the air inlet/outlet configuration.

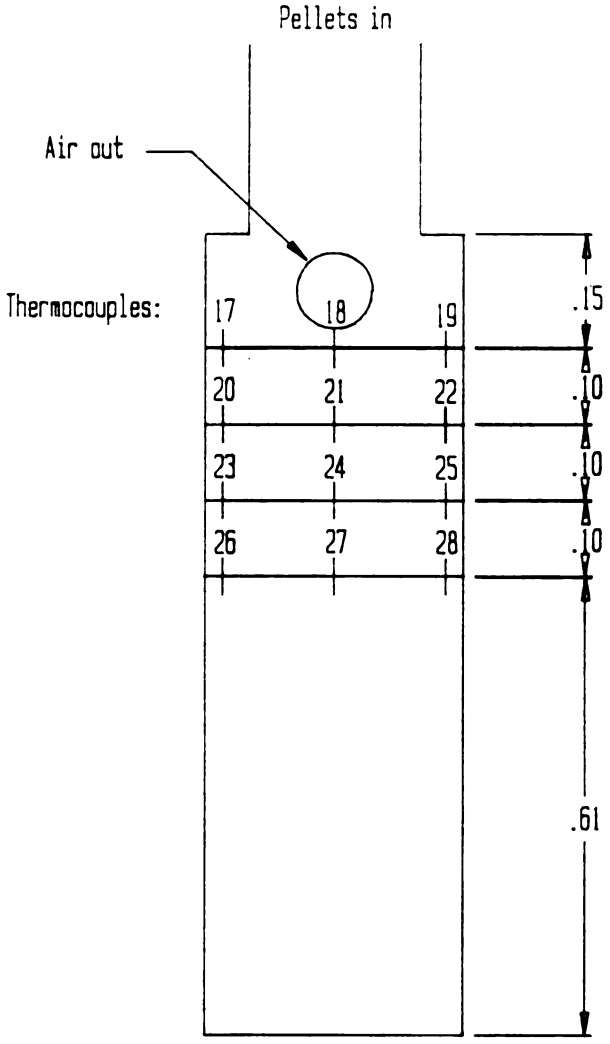


Figure 5.3 Cross-cut view of the 30.48 cm cooling bed.

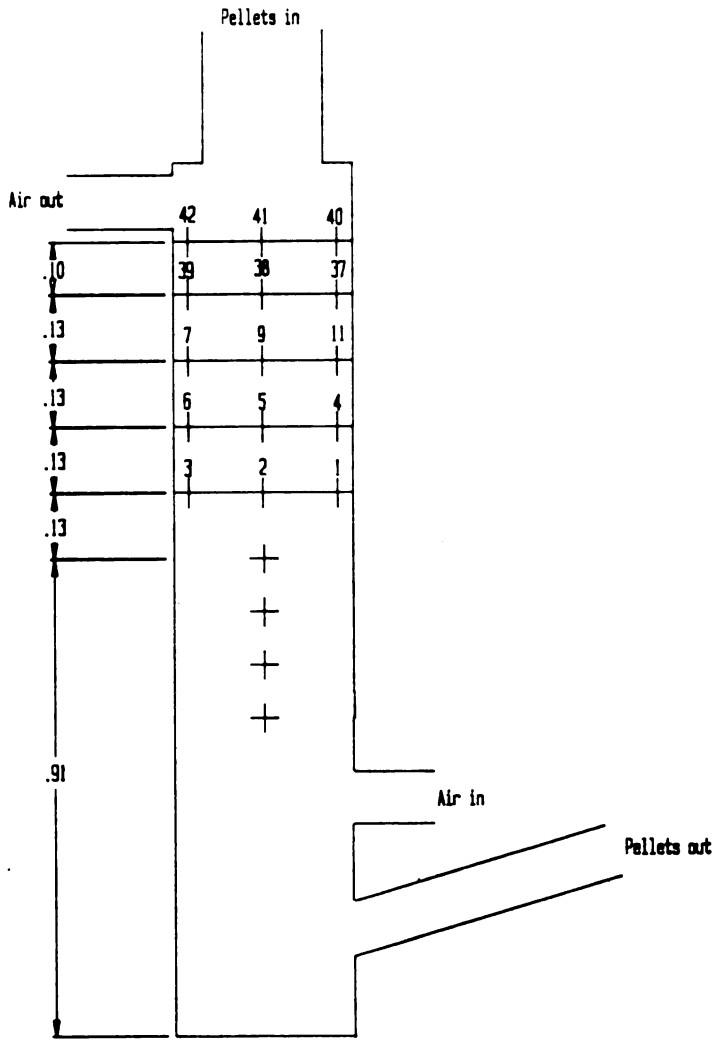


Figure 5.4 Cross-cut view of the 91.44 cm cooling bed.

Three thermocouples in the feeder box and one thermocouple in the outlet barrel are used to monitor the temperatures of the pellets at the inlet and outlet to the cooler.

A data logger is used to record the temperatures in a memory buffer from where it is down-loaded on a personal computer.

The oven-drying method is used to directly measure the moisture content of the pellets. Since there is no ASAE standard for feed pellets, several time-temperature combinations were tested. For the counterflow pellet cooling tests an oven temperature of 100° C is employed for a period of 24 hours.

The pellet samples are weighed on a Mettler laboratory scale with an accuracy of 1 mg.

The pellet flowrate is measured by taking timed samples at the auger outlet at 10 to 15 minute intervals throughout a test. The samples are weighed on a Pennsylvania Scale Model B-210 with a capacity of 10.5 kg and a readability of 5 grams.

## 5.3 PELLET PROPERTIES

The pellets used in the cooling tests were manufactured in a CPM series 7900 pellet mill located at Purina Mills in Millet, MI; the mill is located about 20 miles west of the Michigan State University Campus. The pellets were taken directly from the pellet mill, and immediately placed in 56 cm (22 inch) diameter, 71 cm (28 inch) high barrels. The pelleting temperature at the press was set between 74° to 91° C (165° to 195° F). Following the 30-minute trip to MSU, the pellets were cooled in the counterflow cooler immediately.

Three different pellet types were investigated: (1) rabbit, (2) turkey, and (3) dairy. The pellet diameter was 4.37 mm (11/64 inch); the length of the pellets varied between 12.7 to 25.7 mm (1/2 to 1 inch). The milk pellets were slightly longer (1.6 to 6.4 mm, or 1/16 to 1/4 inch) than the rabbit and turkey pellets which changed the flow behavior in the cooler with respect to the auger speed adjustment. The initial pellet moisture content was between 11.7% and 14.3% wet basis; the milk pellets were slightly higher in moisture content than the rabbit and turkey pellets. The dry bulk density of the pellets was about 641 $kg/m^3$ (40 $lb/ft^3$).

## 5.4 TEST CONDITIONS

Eight experimental tests were conducted. Two cooling bed depths were tested, of 0.3048 and 0.9144m (1.0 and 3.0 ft). The airflow rate was varied from 7.93 to 36.58 $m^3$/min per square meter (26 to 120 $cfm/ft^2$) of cooler area . The pellet flowrate through the cooler was between 1.01 to 3.51 m per hour (3.3 and 11.5 ft/h). The ambient (laboratory) conditions varied between 22.6° to 31.7° C (73° to 89° F) dry bulb temperature, and 52% to 74% relative humidity.

The duration of the tests varied from 1 to 5 hours depending upon the pellet flowrate; in each case steady-state conditions were reached.

Pellet inlet and outlet samples for moisture content determination were taken at 10 minute intervals. For each moisture determination three samples were dried in the oven. At

the beginning of each experiment three samples were also taken from the drums before they were emptied into the feeder box in order to determine the initial moisture content; the moisture content of the samples in the drums ranged from 13.5% to 14.8% wet basis.

After the drums with the hot pellets arrived at the laboratory, the temperature of the pellets was determined; the temperatures varied from 74° to 89° C. The temperature of the pellets entering the cooler ranged from 52° to 69° C (126° to 156° F).

No pellet-quality testing was performed.

## 5.5 TEMPERATURE VARIATIONS IN THE COOLING BED

Figure 5.5d shows the temperatures of the three thermocouples at the bottom layer (Bed Depth: 0.00 cm) of the 0.3048 m (1 ft) cooling bed during Test 1. The variation in the temperatures appears to be primarily due to an uneven distribution in the air flow in the cooler caused by the particular shape and positioning of the air wedge, and to a slightly non-uniform pellet flow through the cooling bed caused by the positioning of the pellet-collecting funnel and the unloading auger.

Figures 5.5a through 5.5c indicate similar temperature variations for the 10.16 cm, 20.32 cm, and 30.48 cm layers of Test 1, respectively. The temperatures varied by less than 2°C in all layers. The trend was less significant at the higher air flow rates in tests 2, 4, 5, 7, and 8; and similar in significance in

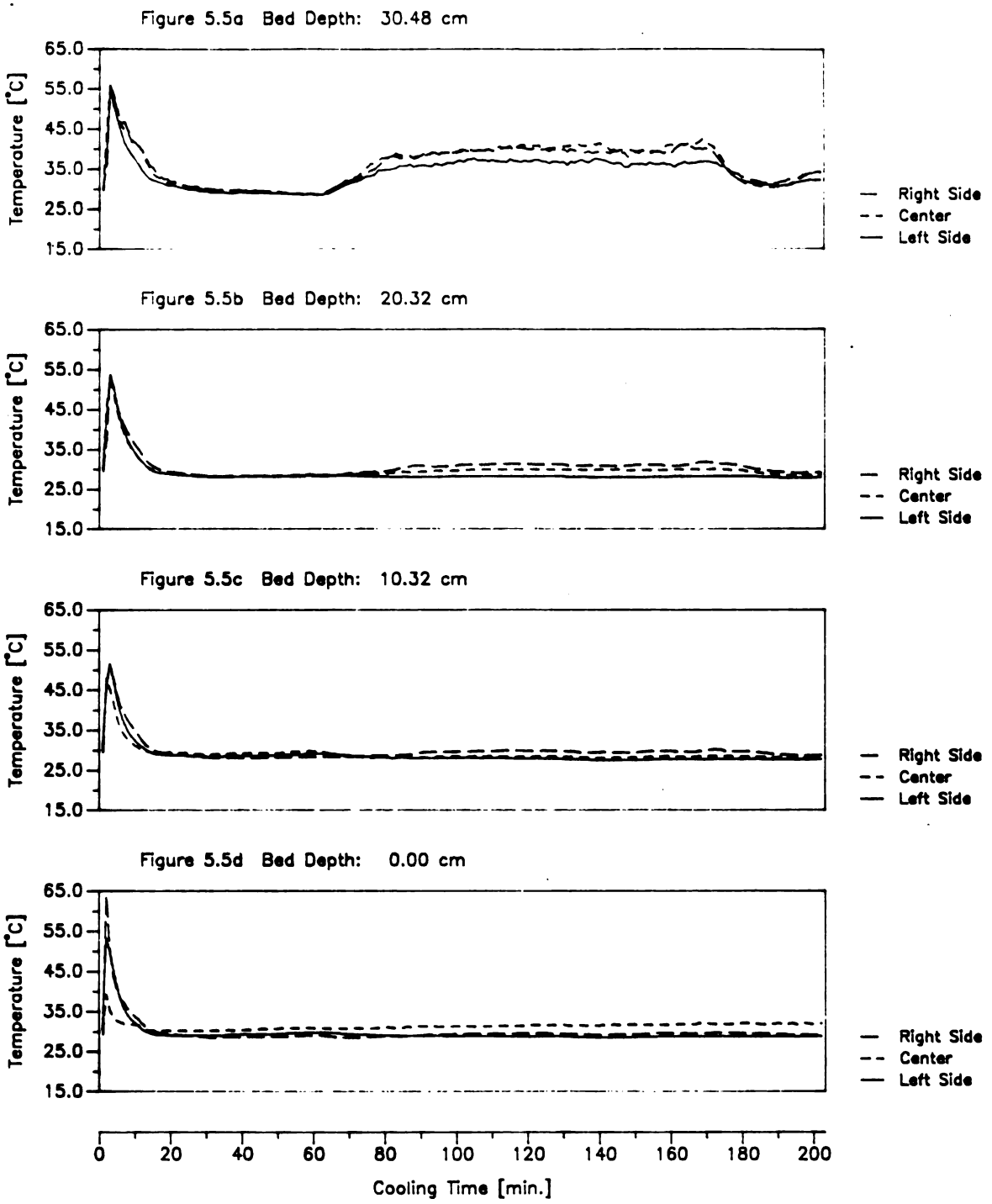


**Figure 5.5 Temperature variations in the cooling bed layers of Test 1.**

tests 3 and 6. In order to offset the non-uniformity of the air and pellet flow, it was decided to use the average of the temperatures of the three thermocouples in each layer in the remaining sections of this study.

Figure 5.6 shows the temperatures at three positions in the insulated feeder box. During the first 60 minutes of test 1 the airflow rate was very high. Since the feeder box was not sealed, the static pressure build-up in the box was not sufficient to force most of the air to exit through the cooler air outlet. Thermocouple 33 shows the influence of the higher airflow rate most significantly. The temperature at position 33 is important to the analysis of the experimental moisture loss (see section 5.6). Thermocouples 31 and 32 are positioned higher up in the feeder box, and show less effect from the higher airflow rate.

The three thermocouples show the slow decline of the pellet temperature notwithstanding the insulation of the feeder box. Since the pellets are very moist and sticky when they leave the pellet press, the pellets in the feeder box had to be stirred occasionally to counteract bridging. The opening of the feeder box and the clogging caused the sudden drops and rises in the temperatures recorded.

## 5.6 MOISTURE CONTENT SAMPLING

Due to the particular construction of the counterflow cooler, the moisture contents of the hot feed pellets were only sampled at the sample spout of the feeder box prior to the inlet to the cooler (see Figure 5.2). Thermocouple 33 was

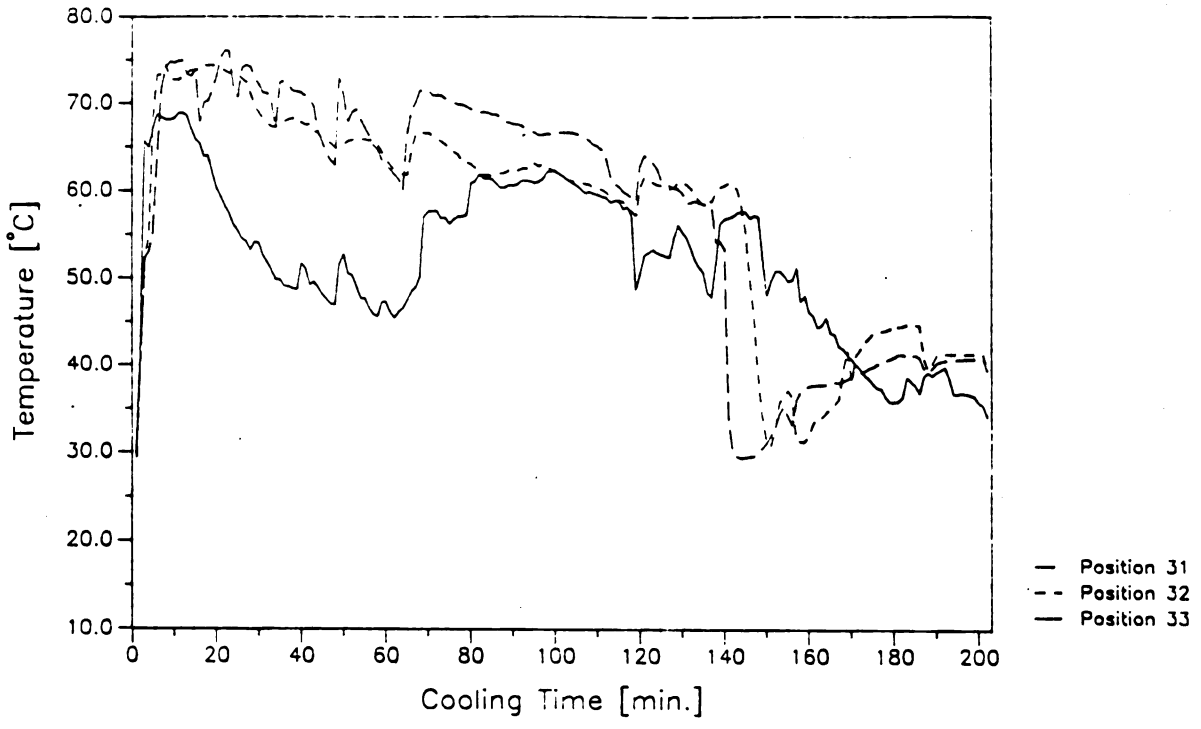


**Figure 5.6 Temperature variation in the feeder box of Test 1**

installed to monitor the temperature of the pellets at the sampling spout.

The outlet moisture contents of the feed pellets were only determined at the unloading auger outlet (see Figure 5.2). A thermocouple was installed in the barrel to monitor the temperature of the cooled pellets at this location.

In the analysis of the data, the inlet and outlet locations to and from the cooler are considered to yield the effective moisture loss of the feed pellets.

## 5.7 COOLING TESTS

As mentioned, a total of eight pellet cooling experiments were performed with the laboratory counterflow cooler. Two of the eight tests are described in detail in the following sections.

The main parameters of each of the tests are summarized in section 5.9. The temperature data curves of the remaining six experimental tests are presented in Appendix A.

### 5.7.1 TEST 2

Turkey pellets were cooled in a 0.3048 m (1 ft) cooling bed. The initial pellet temperature was 79° C; the initial average moisture content of the pellets was 14.29%.

The airflow rate was 29.26 m/min (96 ft/min). The static pressure reading for the cooler bed was 149.3 Pa at the air inlet, 161.7 Pa at the bottom layer, 124.4 Pa at the middle of the bed, 74.6 Pa at the top layer, and 24.9 Pa at the air outlet.

The pellet flowrate was measured in 10-minute intervals and ranged between 3.36 and 3.58 kg/min. Due to the high pellet

Figure 5.7a

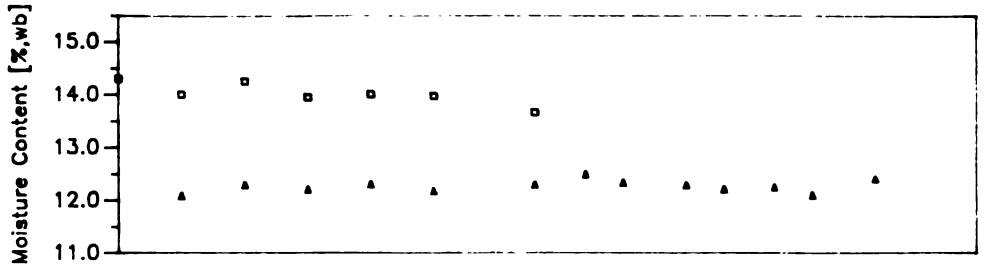


Figure 5.7b

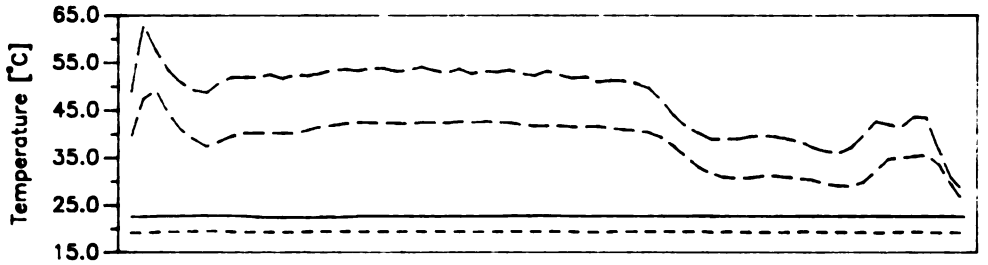


Figure 5.7c

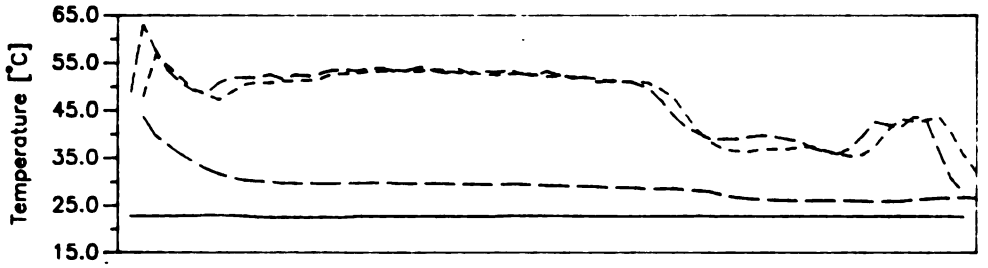


Figure 5.7d

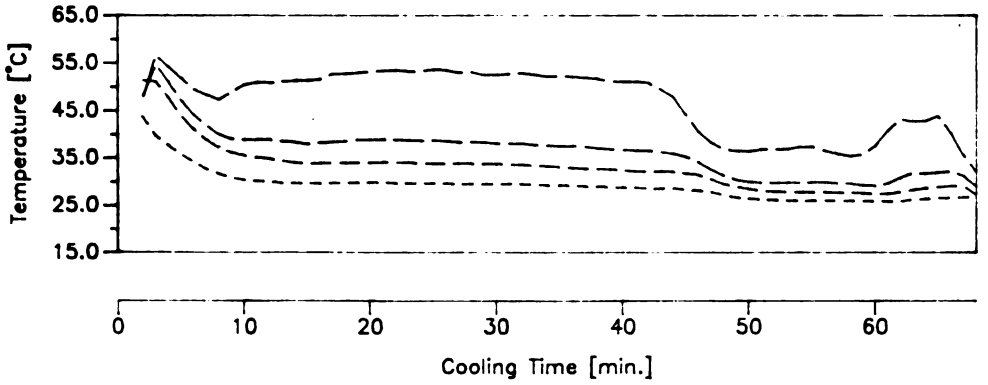


Figure 5.7 Experimental cooling results for Test 2.

flowrate the entire cooling run lasted about one hour.

Figure 5.7a shows a general decline in the average inlet moisture content of the pellets during the 30-minute sampling time. The outlet moisture content increases slightly up to about 37 minutes and then declines slowly during the next 20 minutes.

The outlet dry bulb and wet bulb air temperatures show a steady-state operation of the cooler between about 10 and 40 minutes (see Figure 5.7b). The inlet dry and wet bulb temperatures remain virtually unchanged during the experiment.

Figure 5.7c shows the temperature curves for the inlet air temperature, the pellet temperature in the top layer and the bottom layer of the cooling bed, and the outlet air temperature. The outlet air and pellet temperatures follow the same pattern, and differ only slightly. The outlet pellet temperature was about 10°C higher than the inlet air temperature.

The four cooling bed layers are compared in Figure 5.7d. The curves show the gradual decrease of the pellet temperatures from the top of the cooling bed to the bottom throughout the entire length of the cooling experiment.

### 5.7.2 TEST 8

Test 8 was performed in a 0.9144 m (3 ft) cooling bed using dairy-feed pellets. The initial pellet temperature in the drums was 84° C; the initial average moisture content was 14.83% wet basis.

The airflow was set at 29.26 m/min (96 ft/min). The static pressure was 248.8 Pa at the air inlet, 273.7 Pa at the bottom

layer, 248.8 Pa at 12.7 cm (5 inches) from the bottom, 223.9 Pa at 24.5 cm (10 inches) from the bottom, 149.3 Pa at 45.7 cm (18 inches) from the bottom, 49.8 Pa at 79.2 cm (2.6 ft) from the bottom, 24.9 Pa at the top of the cooling bed, and 0.0 Pa at the air outlet.

The pellet flowrate averaged 2.5 kg/min, with a range of 2.27 to 2.68 kg/min.

The cooler was pre-filled with cold pellets from the previous test. It required less than an hour for the cold pellets to empty from the cooler. The sampling of the inlet and outlet moisture contents was performed at 10-minute intervals.

The inlet moisture content curve showed an overall decline during the first 70 minutes of the experiment (see Figure 5.8a). A sudden rise at about 80 minutes was due to the refilling of the feeder box with wet pellets. The moisture content again shows a decline during the next 40-minute interval (see Figure 5.8a). The outlet moisture content showed overall an increase throughout the experiment. The outlet moisture contents ranged from 12.1 to 12.8 %, with an average of about 12.5% wet basis.

The inlet dry bulb and wet bulb air temperatures to the cooler increased slightly throughout the experiment (see Figure 5.8b). The outlet dry bulb and wet bulb air temperatures showed steady state operation of the cooler between 10 and 100 minutes. A maximum was reached after 65 minutes.

Figure 5.8c shows the outlet pellet temperature and inlet air temperature to be almost identical; the inlet pellet temperature and outlet air temperature follow the same pattern

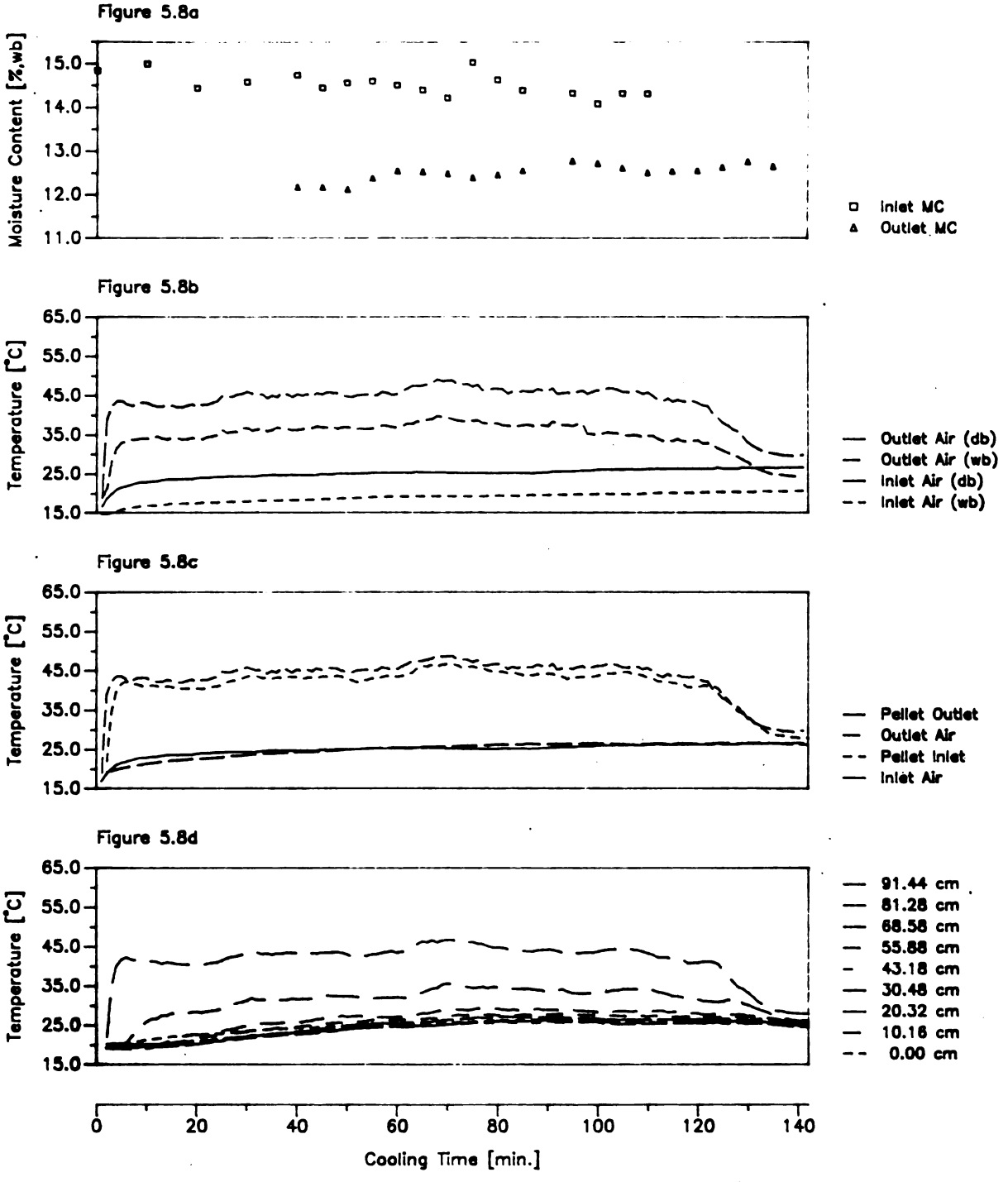


**Figure 5.8 Experimental cooling results for Test 8.**

but show a difference in temperature.

Figure 5.8d shows the average layer temperatures in the cooling bed. Most of the cooling is completed in the top of the cooler. The steady state operation of the cooler is evident. The temperatures in the bottom layers are all within a 5°C temperature band. The average temperatures of the three layers above the bottom cooling bed layer are slightly below the temperature of the bottom layer.

## 5.8 STEADY-STATE COOLING PERIOD

Tables 5.2 and 5.3 contain values of two of the eight experimental counterflow cooling tests (Tests 2 and 8) for the average temperature of the three thermocouples in each layer, and the temperatures at the inlet and outlet to the cooler.

After careful analysis of the data, a steady-state range of 40 minutes was determined for Test 2 (see Table 5.2) and of 70 minutes for Test 8 (see Table 5.3).

The steady-state temperatures of the remaining tests are listed in Appendix B.

The average air temperatures, relative humidities and specific air volumes are listed in Table 5.4 of the next section.

Table 5.2 Average pellet temperatures [°C] of Test 2.

| | Thermocouple Position/Layer | | | | | |
|---|---|---|---|---|---|---|
| Time [min] | Cooler Outlet | 0.00 cm | 10.16 cm | 20.32 cm | 30.48 cm | Cooler Inlet |
| 10 | 32.86 | 29.71 | 34.18 | 38.46 | 51.56 | 72.33 |
| 20 | 32.85 | 29.49 | 33.75 | 38.51 | 53.17 | 68.58 |
| 30 | 33.86 | 29.05 | 32.99 | 37.44 | 52.09 | 61.80 |
| 40 | 33.61 | 28.28 | 31.69 | 35.37 | 46.55 | 44.12 |
| Average | 33.28 | 29.18 | 33.23 | 37.56 | 51.07 | 62.63 |

Table 5.3 Average pellet temperatures [°C] of Test 8.

| | Thermocouple Position/Layer | | | | |
|---|---|---|---|---|---|
| Time [min] | Cooler Outlet | 0.00 cm | 10.16 cm | 20.32 cm | 30.48 cm |
| 10 | 24.37 | 25.29 | 24.59 | 24.45 | 25.34 |
| 20 | 25.14 | 25.58 | 25.00 | 24.87 | 25.88 |
| 30 | 25.75 | 26.01 | 25.69 | 25.68 | 26.81 |
| 40 | 26.32 | 26.35 | 26.19 | 26.08 | 27.15 |
| 50 | 26.86 | 26.49 | 26.20 | 25.94 | 26.88 |
| 60 | 27.09 | 26.40 | 25.78 | 25.45 | 26.44 |
| 70 | 26.41 | 26.49 | 25.84 | 25.53 | 26.41 |
| Average | 26.00 | 26.09 | 25.62 | 25.43 | 26.42 |

Table 5.3 (cont.)

| Time [min] | Thermocouple Position/Layer | | | | | |
|---|---|---|---|---|---|---|
| | 43.18 cm | 55.88 cm | 68.58 cm | 81.28 cm | 91.44 cm | Cooler Inlet |
| 10 | 24.73 | 26.16 | 27.18 | 31.99 | 42.98 | 66.85 |
| 20 | 25.04 | 26.67 | 27.94 | 33.31 | 45.28 | 69.70 |
| 30 | 25.52 | 27.58 | 29.10 | 34.90 | 45.88 | 67.70 |
| 40 | 25.72 | 27.62 | 28.99 | 34.22 | 44.20 | 66.26 |
| 50 | 25.85 | 27.70 | 28.78 | 33.42 | 43.54 | 64.64 |
| 60 | 25.80 | 27.37 | 28.48 | 33.94 | 44.20 | 63.14 |
| 70 | 25.56 | 27.19 | 28.35 | 32.70 | 41.91 | 62.72 |
| Average | 25.50 | 27.18 | 28.40 | 33.47 | 43.95 | 65.78 |

## 5.9 RESULTS AND DISCUSSION

Table 5.4 contains a summary of the results of the eight counterflow pellet cooling experiments.

### 5.9.1 Pellet Moisture Loss

As mentioned above, the moisture content samples were taken 16 inches above the top layer of the cooling bed (cooler inlet) and at the auger outlet (cooler outlet). In order to determine the actual moisture loss (calculated moisture loss) in the bed, the temperatures at the cooler inlet and outlet were monitored.

The results in Table 5.4 indicate that a correlation between the effective cooling and effective moisture loss exists; i.e. the larger the cooling effect, the larger the decrease in the moisture content of the pellets.

It is assumed that on the basis of the effective cooling and the effective moisture loss of the pellets between the inlet and

Table 5.4 Experimental results of the counterflow cooling tests.

| Test | 1 | 2 | 3 | 4 |
|---|---|---|---|---|
| Type | turkey | turkey | milk | milk |
| Diameter [mm] | 4.37 | 4.37 | 4.37 | 4.37 |
| Bed Depth [cm] | 30.48 | 30.48 | 30.48 | 30.48 |
| Temperatures [°C]: | | | | |
| Pellets: | | | | |
| Cooler Inlet | 54.4 | 62.6 | 63.8 | 52.4 |
| Cooler Outlet | 28.9 | 33.3 | 31.5 | 30.6 |
| Effective Cooling | 25.5 | 29.3 | 32.3 | 21.8 |
| Top Bed Layer | 37.9 | 51.1 | 54.8 | 40.4 |
| Bottom Bed Layer | 29.8 | 29.2 | 31.7 | 28.6 |
| Actual Bed Cooling | 8.1 | 21.9 | 23.1 | 11.8 |
| Air: | | | | |
| Dry Bulb | 31.7 | 22.6 | 25.3 | 26.1 |
| Wet Bulb | 23.7 | 19.3 | 20.5 | 20.2 |
| Bottom Layer - Dry Bulb | -1.9 | 6.6 | 6.4 | 2.5 |
| Cooler Inlet - Top Layer | 16.5 | 11.5 | 9.0 | 12.0 |
| Moistures [%,wb]: | | | | |
| Cooler Inlet | 13.35 | 14.01 | 14.19 | 14.19 |
| Cooler Outlet | 11.67 | 12.26 | 12.42 | 12.65 |
| Effective Moisture Loss | 1.68 | 1.75 | 1.77 | 1.54 |
| Top Layer* | 12.20 | 13.57 | 13.69 | 13.48 |
| Bottom Layer | 11.67 | 12.26 | 12.42 | 12.65 |
| Actual Moisture Loss* | 0.53 | 1.31 | 1.27 | 0.83 |
| Relative Humidity [%] | 51.6 | 73.7 | 64.8 | 58.8 |
| Pellet Velocity [m/h] | 1.25 | 3.51 | 1.71 | 1.71 |
| Air Velocity [m/min] | 13.72 | 29.26 | 7.92 | 29.26 |
| Pellet Flowrate [kg/h/m$^2$] | 795.84 | 2241.03 | 1083.90 | 1083.90 |
| Air Flowrate [kg/h/m$^2$] | 932.54 | 2055.50 | 551.71 | 2031.10 |
| Pellet/Air Ratio | 0.86 | 1.09 | 1.97 | 0.53 |
| Static Pressure [Pa] | 74.64 | 124.4 | 49.76 | 124.4 |
| Spec. Air Volume [m$^3$/kg] | 0.885 | 0.855 | 0.863 | 0.865 |
| Bulk Density [kg/m$^3$] | 640.74 | 640.74 | 640.74 | 640.74 |

* calculated values using equations 5.1 and 5.2

Table 5.4 (cont'd.)

| Test | 5 | 6 | 7 | 8 |
|---|---|---|---|---|
| Type | rabbit | rabbit | milk | milk |
| Diameter [mm] | 4.37 | 4.37 | 4.37 | 4.37 |
| Bed Depth [cm] | 30.48 | 91.44 | 91.44 | 91.44 |
| Temperature [°C]: | | | | |
| Pellets: | | | | |
| Cooler Inlet | 68.5 | 62.0 | 65.9 | 65.8 |
| Cooler Outlet | 32.0 | 28.7 | 21.2 | 26.0 |
| Effective Cooling | 36.5 | 33.3 | 44.7 | 39.8 |
| Top Bed Layer | 45.2 | 48.8 | 38.6 | 44.0 |
| Bottom Bed Layer | 30.6 | 29.6 | 23.1 | 26.1 |
| Actual Bed Cooling | 14.6 | 19.2 | 15.5 | 17.9 |
| Air: | | | | |
| Dry Bulb | 27.5 | 31.4 | 25.0 | 25.6 |
| Wet Bulb | 23.4 | 23.9 | 21.0 | 19.5 |
| Bottom Layer - Dry Bulb | 3.1 | -1.8 | -1.9 | 0.5 |
| Cooler Inlet - Top Layer | 23.3 | 13.2 | 27.3 | 21.8 |
| Moistures [%,wb]: | | | | |
| Cooler Inlet | 13.23 | 13.50 | 14.37 | 14.50 |
| Cooler Outlet | 11.41 | 11.77* | 12.00 | 12.49 |
| Effective Moisture Loss | 1.82 | 1.73* | 2.37 | 2.01 |
| Top Bed Layer* | 12.14 | 12.77* | 12.82 | 13.39 |
| Bottom Bed Layer | 11.41 | 11.77* | 12.00 | 12.49 |
| Actual Moisture Loss* | 0.73 | 1.00 | 0.82 | 0.90 |
| Relative Humidity [%] | 70.9 | 54.3 | 70.0 | 57.3 |
| Pellet Velocity [m/h] | 2.74 | 1.01 | 1.43 | 2.52 |
| Air Velocity [m/min] | 36.58 | 7.97 | 29.26 | 29.26 |
| Pellet Flowrate [kg/h/m$^2$] | 1757.67 | 644.48 | 917.90 | 1611.20 |
| Air Flowrate [kg/h/m$^2$] | 2509.57 | 537.07 | 2031.09 | 2035.97 |
| Pellet/Air Ratio | 0.70 | 1.20 | 0.45 | 0.79 |
| Static Pressure [Pa] | 248.8 | 24.88 | 248.8 | 248.8 |
| Spec. Air Volume [m$^3$/kg] | 0.874 | 0.884 | 0.864 | 0.862 |
| Bulk Density [kg/m$^3$] | 640.74 | 640.74 | 640.74 | 640.74 |

* calculated values using equations 5.1 and 5.2

outlet of the cooler, the actual moisture loss in the cooling bed can be calculated. Furthermore, since the pellets are not exposed to the cooling airflow after the bottom bed layer,it is assumed that the pellet moisture content does not change between the bottom layer of the cooling bed and the auger outlet. Thus, the calculated moisture loss is:

$$\Delta M_{actual} = \Delta\theta_{actual}\ \Delta M_{effective}/\Delta\theta_{effective} \qquad (5.1)$$

The calculated moisture content at the top of the cooling bed is:

$$M_{top} = M_{bottom} + \Delta M_{actual} \qquad (5.2)$$

In Test 6 all moisture samples were lost except the initial one. On the basis of the assumption that the ratio of the effective moisture loss per degree of effective cooling in Test 6 is similar to the ones in tests 7 and 8 (0.051% and 0.053% loss per °C, respectively), an effective moisture loss of 1.73% is assumed for Test 6 using equation 5.1 by multiplying an average coefficient of 0.052%/°C by 33.3°C effective cooling. With a moisture content of 11.77% wet basis in the bottom layer of the cooling bed, a moisture content of 12.77% wet basis is calculated for the top layer of the cooling bed using equation 5.2.

### 5.9.2 Initial Pellet Temperature

The effective decrease in the pellet temperature during the cooling process varied from 21.8° to 44.7° C; the actual cooling of the pellets in the cooling bed ranged from 8.1° to 23.1° C. The temperature loss of the pellets between the cooler inlet and

the top layer of the cooling bed ranged from 9.0° to 27.3° C.

The results show that the higher the initial pellet temperature at the top of the cooling bed, the higher the actual cooling rate in the cooling bed. This is indicated for both bed depths.

5.9.3 Inlet Air Temperature

The dry bulb cooling air temperature varied from 22.6° to 31.7° C.

In all but two of the tests (Tests 2 and 3) the pellets were cooled to within the industry standard of 5°C above the inlet cooling air. The difference in the pellet temperature of the bottom layer and the inlet air temperature ranged from -1.9° to +6.6° C.

The results of Table 5.4 indicate that the lower the inlet cooling air temperature, the higher the moisture loss in the 0.3048 cm (1 ft) cooling bed; and the lower the moisture loss in the 0.9144 cm (3 ft) cooling bed.

5.9.4 Initial Pellet Moisture Content

The moisture content of the feed pellets decreased between 1.54 and 2.37% wet basis. The calculated moisture loss of the pellets in the cooling bed ranged from 0.53 to 1.31% wet basis. No difference between the drying behavior of the various pellet types is evident from the data. The dairy pellets had a slightly higher initial moisture content (14.1 - 14.5% wet basis) compared to rabbit (13.2 - 13.5% wet basis) and turkey (13.3 - 14.0% wet basis) pellets.

The initial moisture content of the pellets at the top of the cooler influences the drying behavior in the following manner: the lower the initial moisture content, the lower the moisture loss in the shallow bed (except for Tests 2 and 3).

The cooling rate of the pellets in the deep bed indicate that the lower the initial moisture content, the higher the cooling rate in the bed. The cooling rate in the shallow bed shows no correlation.

### 5.9.5 Inlet Air Relative Humidity

The relative humidity of the cooling air at the inlet to the counterflow cooling bed ranged from 51.6 to 73.7%.

The following trends are indicated by the results of Table 5.4: the deeper the bed and the higher the relative humidity, the smaller the cooling rate and moisture loss in the cooling bed; the shallower the bed and the higher the relative humidity, the higher the cooling rate in the cooling bed (with the exception of Tests 2 and 3).

### 5.9.6 Airflow Rate

The airflow rate affected the performance of the cooler significantly. The higher the airflow, the higher the difference in temperature between the inlet of the cooler and the top layer of the cooling bed. Airflows ranging from 13.72 to 36.58 m/min yielded cooling rates of 11.5° to 27.3° C; while airflows below 10 m/min yielded cooling rates of 9.0° to 13.2° C.

Apparently, the feeder box was not sealed sufficiently to force the airflow out of the cooler outlet and prevent large

cooling rates to occur above the cooling air outlet.

### 5.9.7 Pellet Flowrate

The pellet flowrate affected the moisture loss and the cooling rate only slightly. The moisture loss in the cooling bed increased the cooling rate of the pellets due to evaporative cooling, thus actually 'overcooling' the pellets. This effect is obvious in tests 1, 6 and 7 with low pellet velocities of 1.25, 1.01 and 1.43 m/h, respectively. In the three tests the temperature difference between the bottom layer of the pellets and the inlet air was -1.9°, -1.8° and -1.9° C, respectively.

### 5.9.8 Pellet-to-Airflow Ratio

The pellet-to-airflow ratio shows the following general trend to exist for the 0.9144 m (3 ft) cooling bed (see Table 5.5): the lower the ratio, the lower the actual moisture loss and the lower the actual cooling of the pellets in the cooling bed.

Table 5.5 Effect of the pellet-to-airflow ratio on the 0.9144 m (3 ft) cooling bed.

| Test # | Pellet-/ Air Flow Ratio | Actual Moisture Loss [%] | Actual Cooling [°C] |
|---|---|---|---|
| 7 | 0.45 | 0.82 | 15.5 |
| 8 | 0.79 | 0.90 | 17.9 |
| 6 | 1.20 | 1.00 | 19.2 |

This correlation does not hold for the 0.3048 cm cooling bed (see Table 5.6).

Table 5.6 Effect of the pellet-to-air flow ratio on the 0.3048 m (1 ft) cooling bed.

| Test # | Pellet-/ Airflow Ratio | Actual Moisture Loss [%] | Actual Cooling [°C] |
|---|---|---|---|
| 4 | 0.53 | 0.83 | 11.8 |
| 5 | 0.70 | 0.73 | 14.6 |
| 1 | 0.86 | 0.53 | 8.1 |
| 2 | 1.09 | 1.31 | 21.9 |
| 3 | 1.97 | 1.27 | 23.1 |

Tests 1, 4, and 5 show a decrease in actual moisture loss, the higher the pellet-to-airflow ratio. The actual cooling rate shows no such correlation for the shallow bed.

In Tests 2 and 3, the pellets were not cooled adequately (6.6° and 6.4° C above the inlet air, respectively). Both tests had high pellet-to-airflow ratios (1.09 and 1.97, respectively) and yielded high moisture losses and cooling effects.

### 5.9.9 Bed Depth

As indicated in the previous sections, the bed depth has a major influence on the cooling and drying behavior of feed pellets in a counterflow cooler.

With the exception of tests 2 and 3, the bed depths show the following trends: the deeper the cooling bed, the higher the moisture loss (0.82% to 1.00% wet basis), and the larger the

cooling effect on the pellets (15.5° to 19.2° C) (see Table 5.5). The shallower bed showed a moisture loss ranging from 0.53% to 0.83% wet basis, and a cooling effect of 8.1° to 14.6° C for tests 1,4 and 5 (see Table 5.6).

5.9.10 Cooler Capacity

The highest capacity of adequate cooling was 1758 $kg/m^2/h$ at a bed depth of 30.48 cm, an air velocity of 0.61 m/s and a static pressure of 98 Pa (see Table 5.4, Test 5). In Test 8 the capacity at 1611 $kg/m^2/h$ with a bed depth of 0.9144 m (3 ft), an air velocity of 0.49 m/s, and a static pressure of 249 Pa (see Table 5.10).

5.9.11 Observed Cooling Rates

Figure 5.9 shows the steady-state temperatures at four bed locations of the 0.3048 m (1 ft) cooling bed. The graphs show that the major cooling effect of the pellets occurs in the top 10.16 cm of the bed.

Figure 5.10 shows the average steady-state temperatures at nine locations of the 0.9144 m (3 ft) cooling bed. The graph illustrates that the major portion of the cooling effect takes place in the upper 30.48 cm of the cooling bed.

The average temperature plots indicate that the pellet temperatures decrease more gradually in the deeper bed (over a 30.48 cm depth) than in the shallower cooling bed (over a 10.16 cm depth). On the other hand, both bed depth show the main cooling effect to take place in the top one-third of the cooling bed.

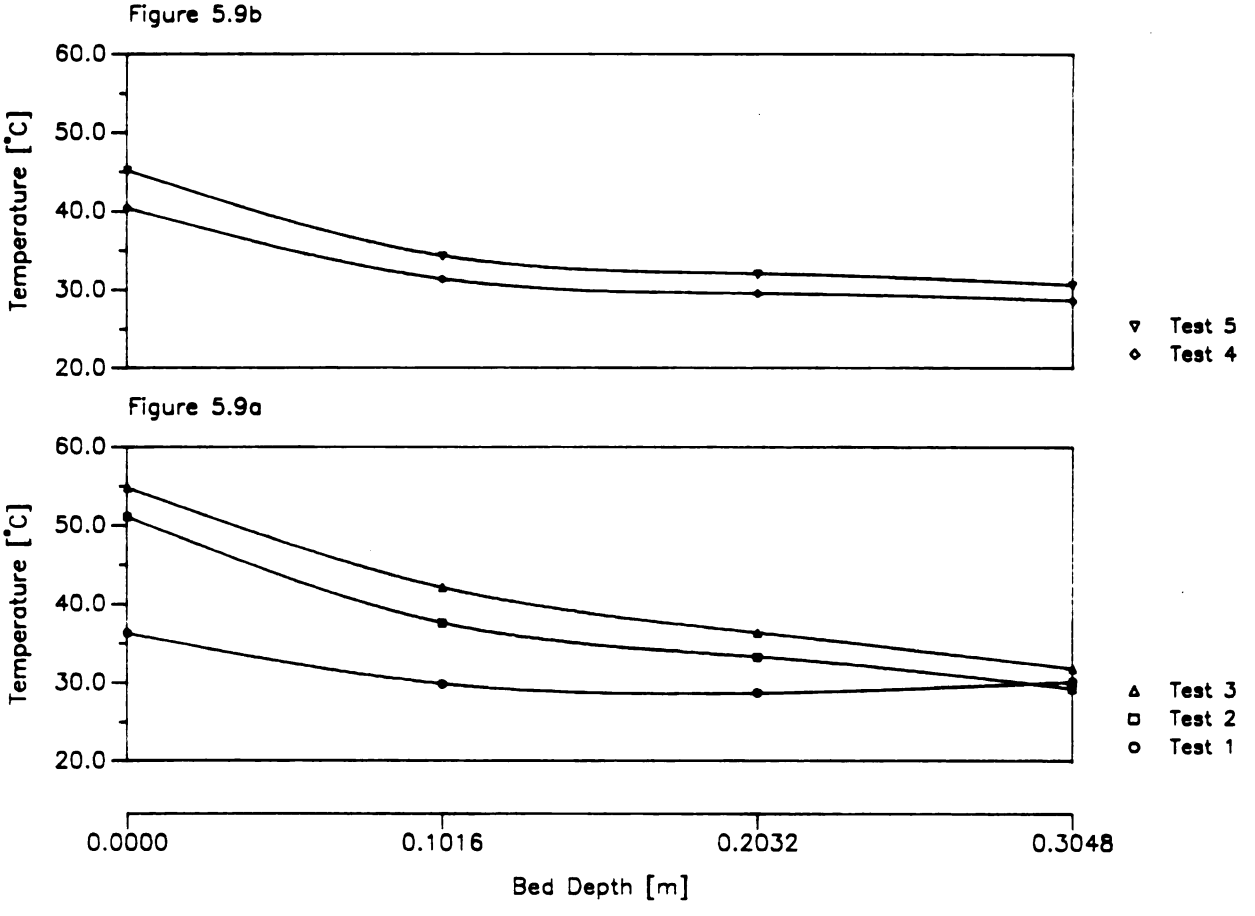


**Figure 5.9 Experimental pellet temperatures in the 30.48 cm cooling bed.**

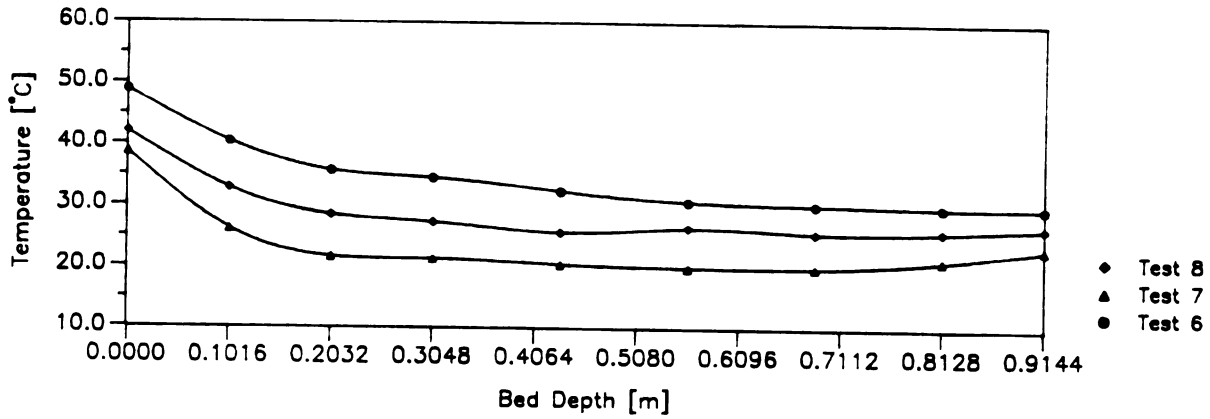


**Figure 5.10 Experimental pellet temperatures in the 91.44 cm cooling bed.**

# 6. SIMULATION

## 6.1 VERIFICATION OF THE ALGORITHM

The theoretical model of the counterflow cooling process described in Chapter 4 is verified using the experimental test results of Chapter 5.

Figure 6.1a shows the pellet temperatures in the simulated cooling bed of Test 2 versus the actual temperatures measured in the cooling bed. The temperature curves are similar in shape. In the top 10.16 cm of the cooler, the simulated temperatures are almost identical to the experimental ones, while in the bottom 20.32 cm the simulated curve deviates from the experimental data. The difference between the simulated ($\theta_{sim}$ = 24.8°C) and experimental ($\theta_{exp}$ = 29.2°C) pellet temperature at the outlet is less than 5°C.

Figure 6.1b shows the moisture loss in the simulated cooling bed to be 0.74%, while the calculated moisture loss in the bed is 1.30%. The pellets of Test 2 remained in the cooling bed for about 5.3 minutes.

Figure 6.2a shows the simulated temperatures versus the experimental temperatures of Test 3. Again, the curves are similar in shape. The simulation indicates a higher temperature drop in the cooling bed than was measured. The temperature difference at the outlet is less than 8°C with $\theta_{sim}$ = 24.3°C and $\theta_{exp}$ = 31.7°C.

Figure 6.2b is the curve of the moisture loss in the simulated bed. The simulated moisture loss of 1.31% in the

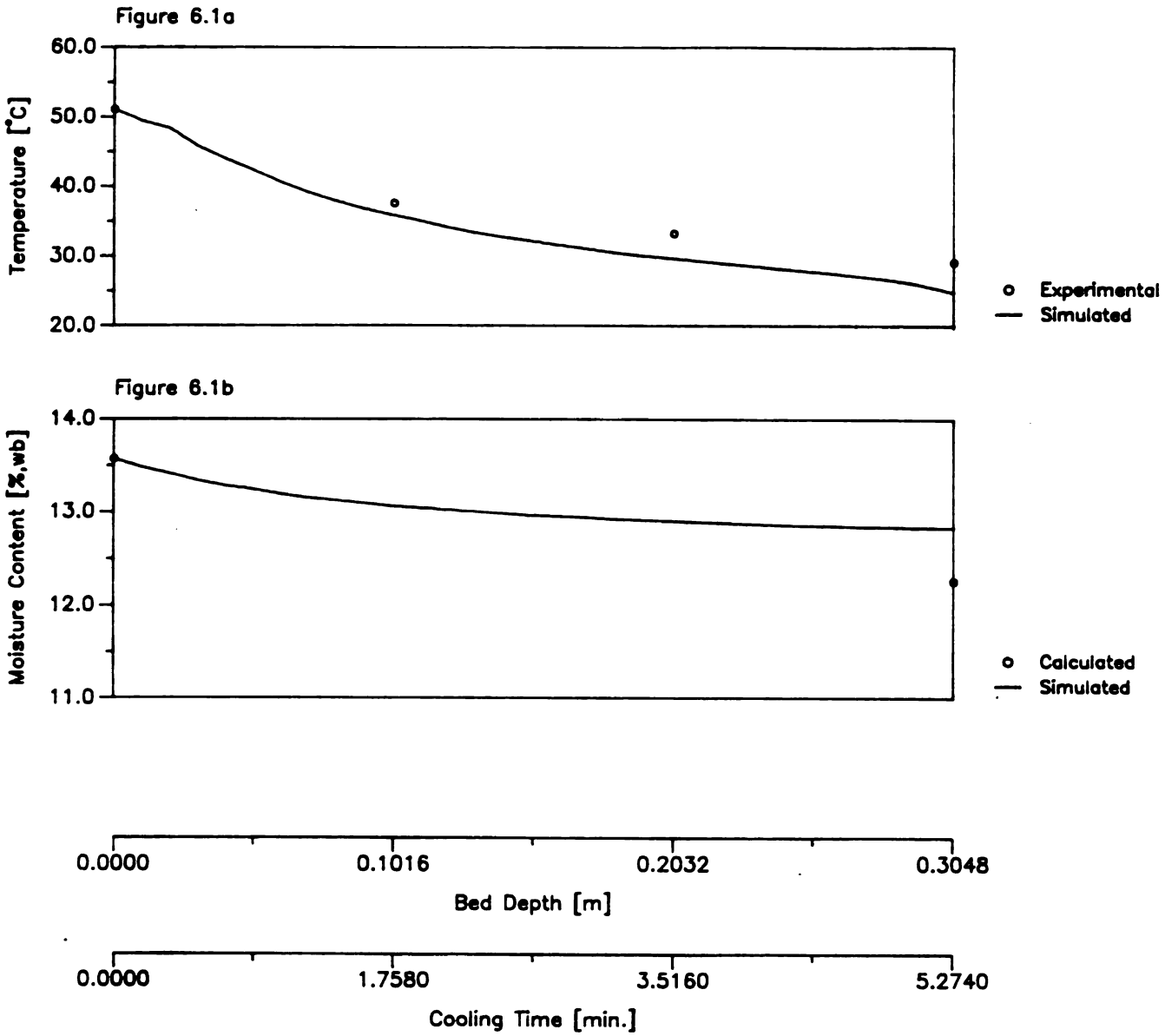


**Figure 6.1 Simulated versus experimental cooling bed temperatures and moistures for Test 2.**

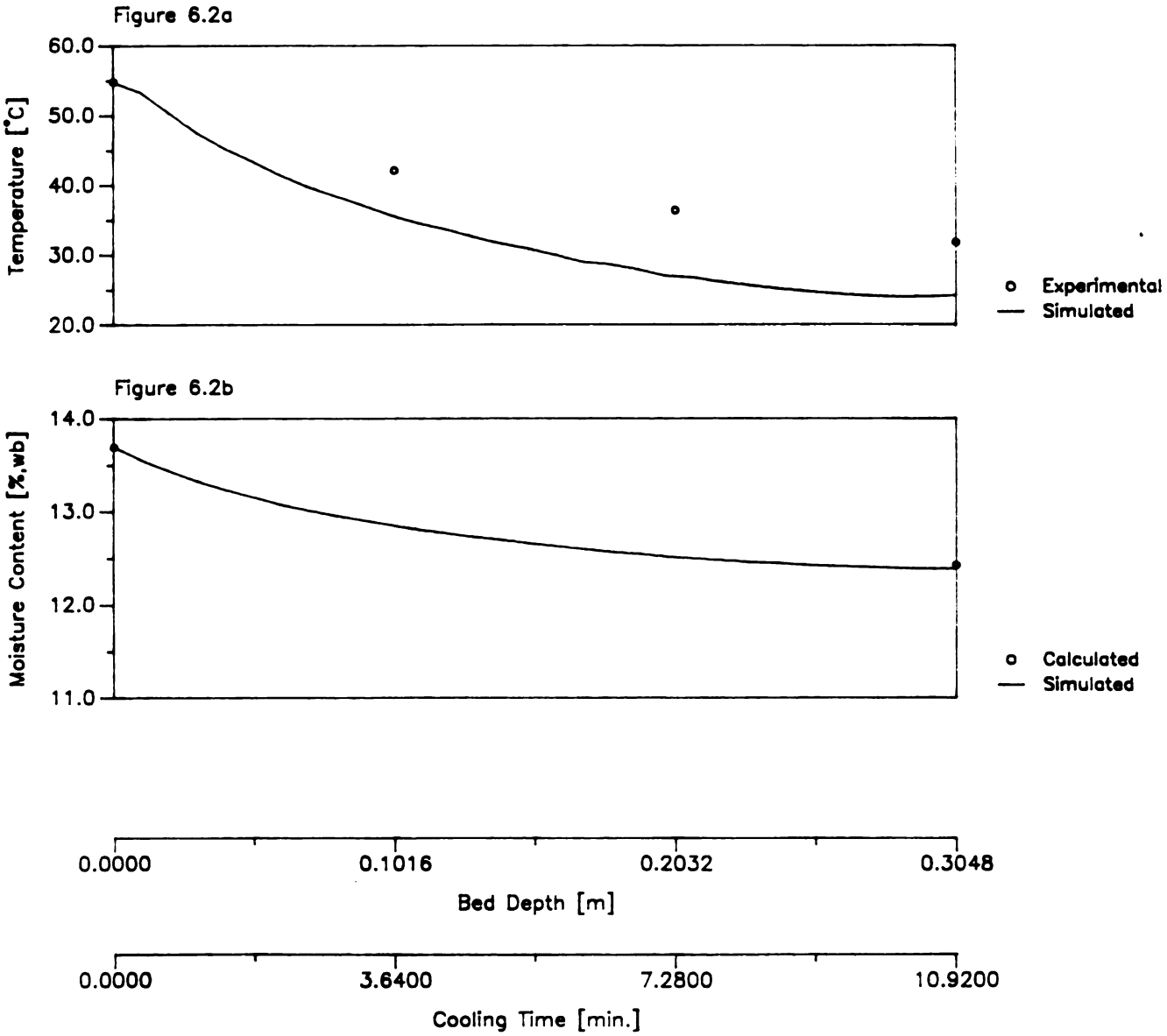


**Figure 6.2 Simulated versus experimental cooling bed temperatures and moistures for Test 3.**

cooling bed is nearly equal to the calculated value of 1.27%. The pellets remain in the cooling bed for about 11 minutes.

Figure 6.3a compares the simulated cooling temperatures versus the actual bed temperatures of Test 5. The shape of the curves is similar with a difference 3°C between the simulated ($\theta_{sim}$ = 27.6°C) and experimental ($\theta_{exp}$ = 30.6°C) outlet temperature.

Figure 6.3b shows the simulated moisture loss to be 0.31% in the cooling bed, compared to a calculated loss of 0.73%. The pellets remain in the cooling bed for about 6.6 minutes.

The cooling rate and moisture loss of Test 8 are compared in Figure 6.4. The simulated temperatures are lower in the top 30.48 cm of the cooler than the experimental temperatures (see Figure 6.4a). In the remainder of the cooling bed the simulated temperatures of the pellets increase slowly, approaching the inlet cooling air temperature. At the outlet the difference in the experimental ($\theta_{exp}$ = 26.09°C) and simulated ($\theta_{sim}$ = 25.06°C) temperature is less than 1.5°C. The bend in the cooling air temperature curve after about 10 minutes implies that the cooling model has not fully converged for the interior temperature values.

Figure 6.4b shows the moisture loss in the 91.44 cm cooling bed. The lowest moisture content is already reached after 6.7 minutes residence time. The simulated outlet moisture content of 0.49% is 0.41% lower than the calculated moisture content of 0.90%. The residence time for Test 8 in the cooling bed is 20.2 minutes.

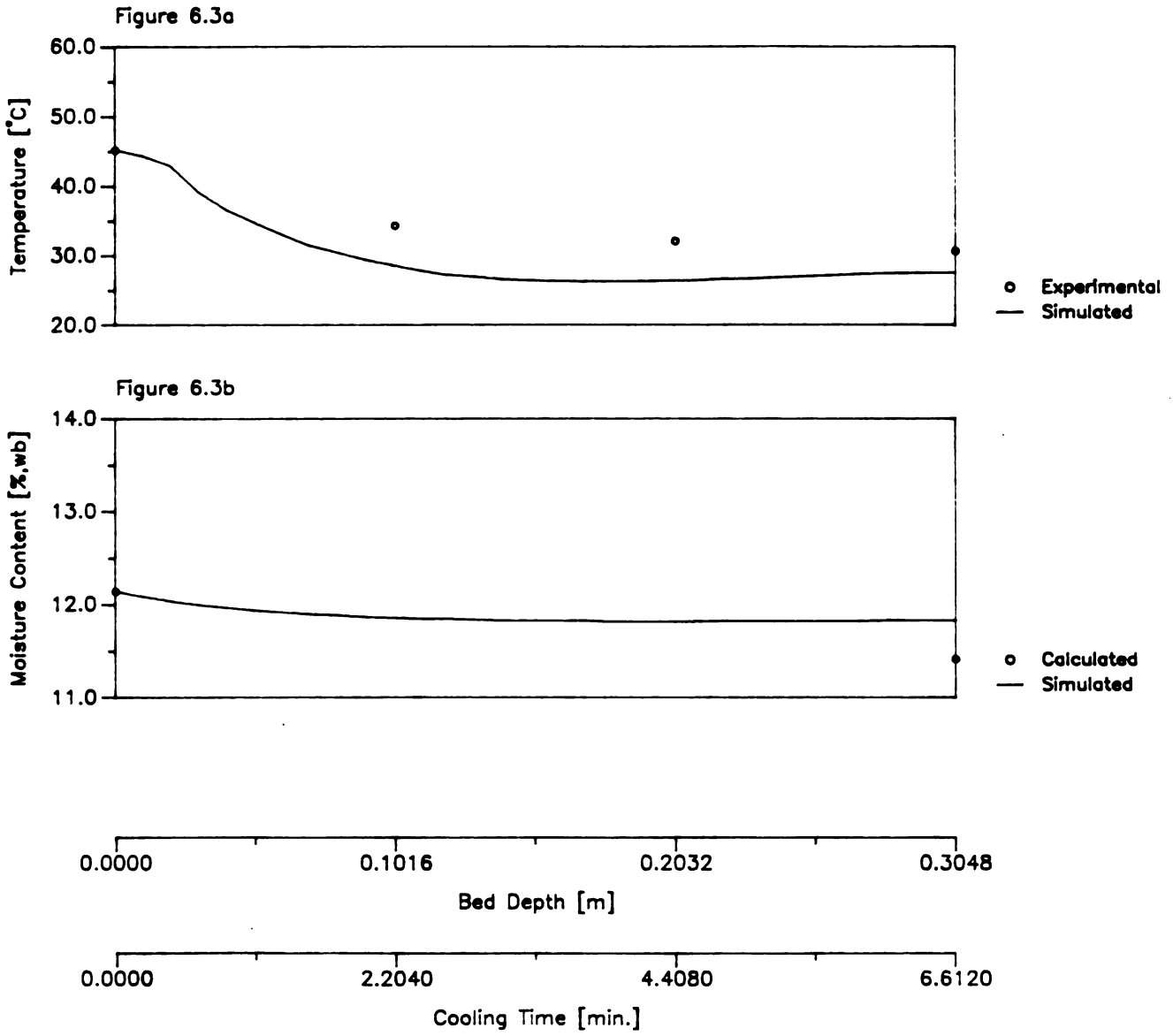


**Figure 6.3** Simulated versus experimental cooling bed temperatures and moistures for Test 5.

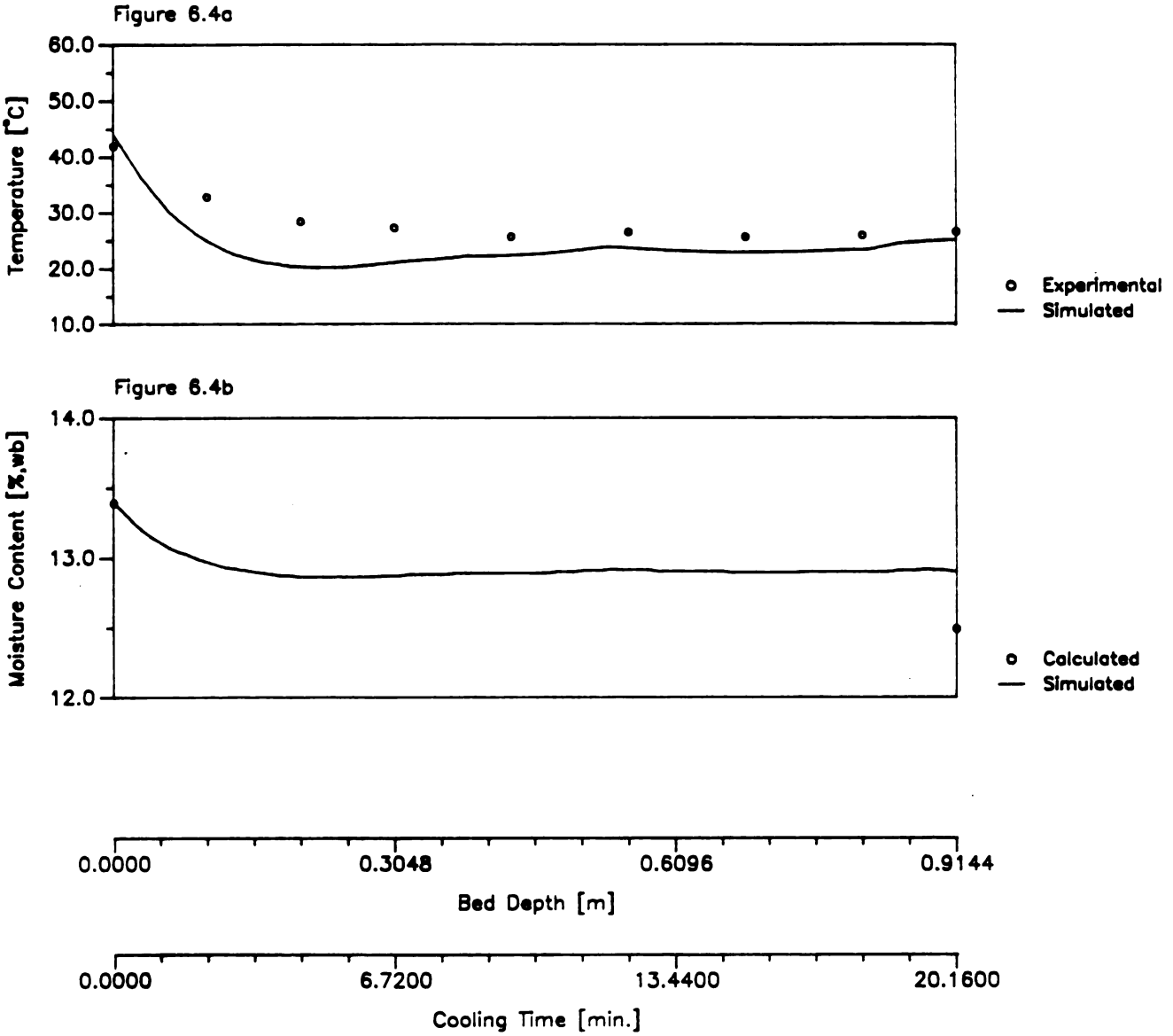


**Figure 6.4** Simulated versus experimental cooling bed temperatures and moistures for Test 8.

The simulated pellet and air temperatures of tests 1, 4, and 6 are compared to the experimental temperatures in Appendix C. The counterflow cooling model was unstable for these tests. It is suspected that the temperature differences of Tests 1 and 4 for the shallow bed are excessively small, and cause instability in the counterflow equations; in the deep bed of Test 6 the initial cooling effect is apparently too large and causes the temperatures to drop excessively. The residence times in the cooling bed for tests 1, 4, and 6, are 14.6, 10.9, and 54.5 minutes, respectively.

The parameters of Test 7 caused instability in the algorithm due to the pellet-to-airflow ratio of less than 0.5, and the very deep cooling bed. The simulation could not be used to verify the model.

The comparisons between the simulated and experimental temperatures of tests 2, 3, 5, and 8 indicate that the counterflow pellet cooling model predicts the temperatures in the cooling bed well. The temperature values of tests 2, 3, and 5 are underpredicted only by an average of 11.4%, 27.9%, and 17.4%, respectively. The temperatures of Test 8 are underpredicted by an average of 15.1%.

A comparison of the simulated and actual moisture loss indicates that the counterflow cooling model underpredicted the moisture loss of tests 2, 3, 5, and 8 by 43.1%, 3.15%, 57.5%, and 45.6%, respectively. The high values, with the exception of Test 3, imply that the moisture loss calculation in the cooling bed as assumed in the model is not accurate. A series of thin-layer

cooling/drying tests is needed to model the moisture loss more accurately from individual pellets (equation 4.9). [Just increasing the diffusion coefficient multiplier in equation 4.13 is not sufficient, however.]

The cooling rate of the feed pellets in the counterflow cooler is overpredicted by the cooling model for tests 2, 3, 5, and 8 by 20.2%, 32.1%, 20.6%, and 5.77%, respectively. In each of the four tests the pellets were cooled to within 5°C above the ambient cooling air. The pellet temperatures were 2.15° and 0.25°C above the cooling air temperatures in tests 2 and 5, respectively; while the pellet temperatures in tests 3 and 8 were 1.04° and 0.54°C below the cooling air temperatures, respectively. In the experimental tests the outlet pellet temperatures were 6.6°, 6.4°, 3.1°, and 0.5° C above the cooling air for tests 2, 3, 5, and 8, respectively. The overprediction of the cooling rate is reflected in the reduction of the difference between the pellet outlet temperature and the cooling air inlet temperature.

The current version of the counterflow pellet cooling model is valid within a certain range of conditions. The simulation equations are not sufficiently accurate to model the counterflow cooling process of feed pellets over the entire range of cooling parameters. Improved phenomenological equations must be developed for the heat transfer coefficient, the equilibrium moisture content and the diffusion coefficient; all three greatly affect the shape of the temperature and moisture curves.

It is assumed in this study that the counterflow cooling

model of feed pellets is valid within the ranges represented by Tests 2, 3, 5, and 8. In the following sections the influence of various design parameters on the counterflow cooling process is determined within these limits. It is noted that extrapolation of the results is not necessarily valid.

## 6.2 INFLUENCE OF VARIOUS DESIGN PARAMETERS

The influence of various design parameters on the performance of a counterflow cooler is determined using the parameters of Test 2 as the standard test parameters.

The standard input conditions of Test 2 are:

$\theta_{in}$ = 51.07°C $\quad$ $M_{win}$ = 13.57%

$T_{in}$ = 22.6°C $\quad$ $RH_{in}$ = 73.7%

$G_p$ = 2241.03 kg/h/m$^2$ $\quad$ $G_a$ = 2039.49 kg/h/m$^2$

H = 0.3048 m $\quad$ d = 0.004366 m

$G_p/G_a$ = 1.09

The pellet initial temperature and moisture content, the air inlet temperature and relative humidity, the pellet and airflow rates, the pellet-to-airflow ratio, the bed depth and pellet diameter are varied and the resulting change in the pellet temperature and moisture content analyzed.

A summary of the simulation parameter values and the outlet pellet and air temperatures, moisture contents and relative humidities are listed in Table D.1 of the Appendix.

A listing of the standard input and output of Test 2 from the computer model is found in Appendix E.

### 6.2.1 Initial Pellet Temperature

Figure 6.5a shows the effect of the initial pellet temperature, $\theta_{in}$, on the cooling rate in a 30.48 cm counterflow bed. The lowest initial pellet temperature reaches the lowest final temperature at the outlet, while the highest initial pellet temperature has the highest temperature at the outlet.

An initial difference of 11.4°C between the highest and lowest inlet pellet temperature decreases to less than 1°C at the outlet. Apparently, as the cooling time increases the effect of the initial pellet temperature on the cooling rate decreases.

The initial pellet temperature has a significant effect on the moisture loss (see Figure 6.5b). The highest initial pellet temperature causes the largest moisture loss; while the lowest initial pellet temperature causes the smallest moisture loss. The difference between the moisture loss of a higher and lower inlet pellet temperature increases as the cooling time increases. At the outlet of the 30.48 cm bed the largest difference in the moisture content is 0.30%.

The drying rate of the pellets is larger at higher pellet temperatures; thus more moisture is forced from the pellets into the air at the higher temperatures.

### 6.2.2 Initial Pellet Moisture Content

The effect of the initial moisture content of the pellets on the cooling rate is displayed in Figure 6.6a. The higher the initial moisture content, the lower the pellet temperatures in the cooling bed. The effect is most significant in the mid-

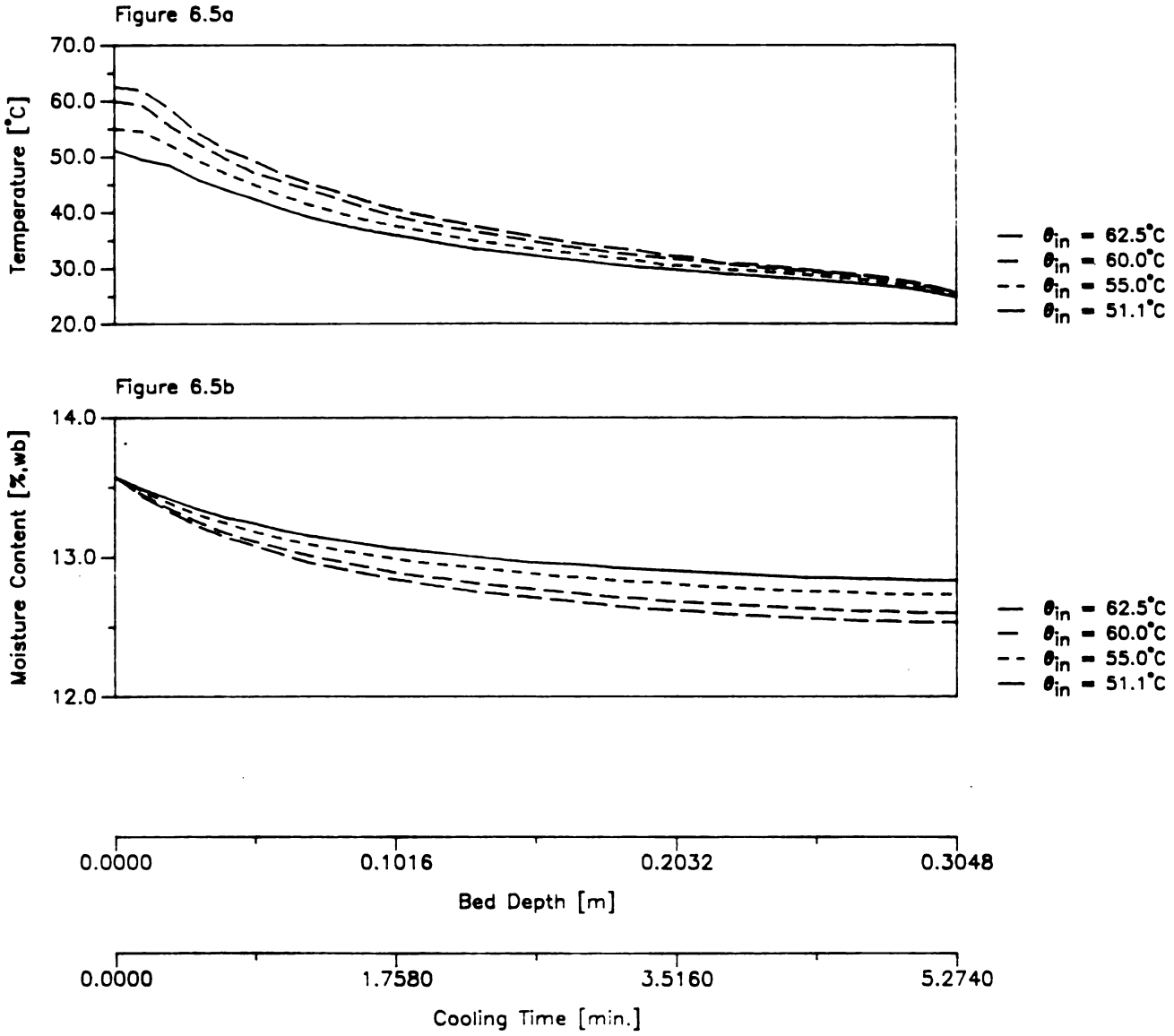


**Figure 6.5 Effect of the initial pellet temperature on the simulated cooling rate and moisture loss.**

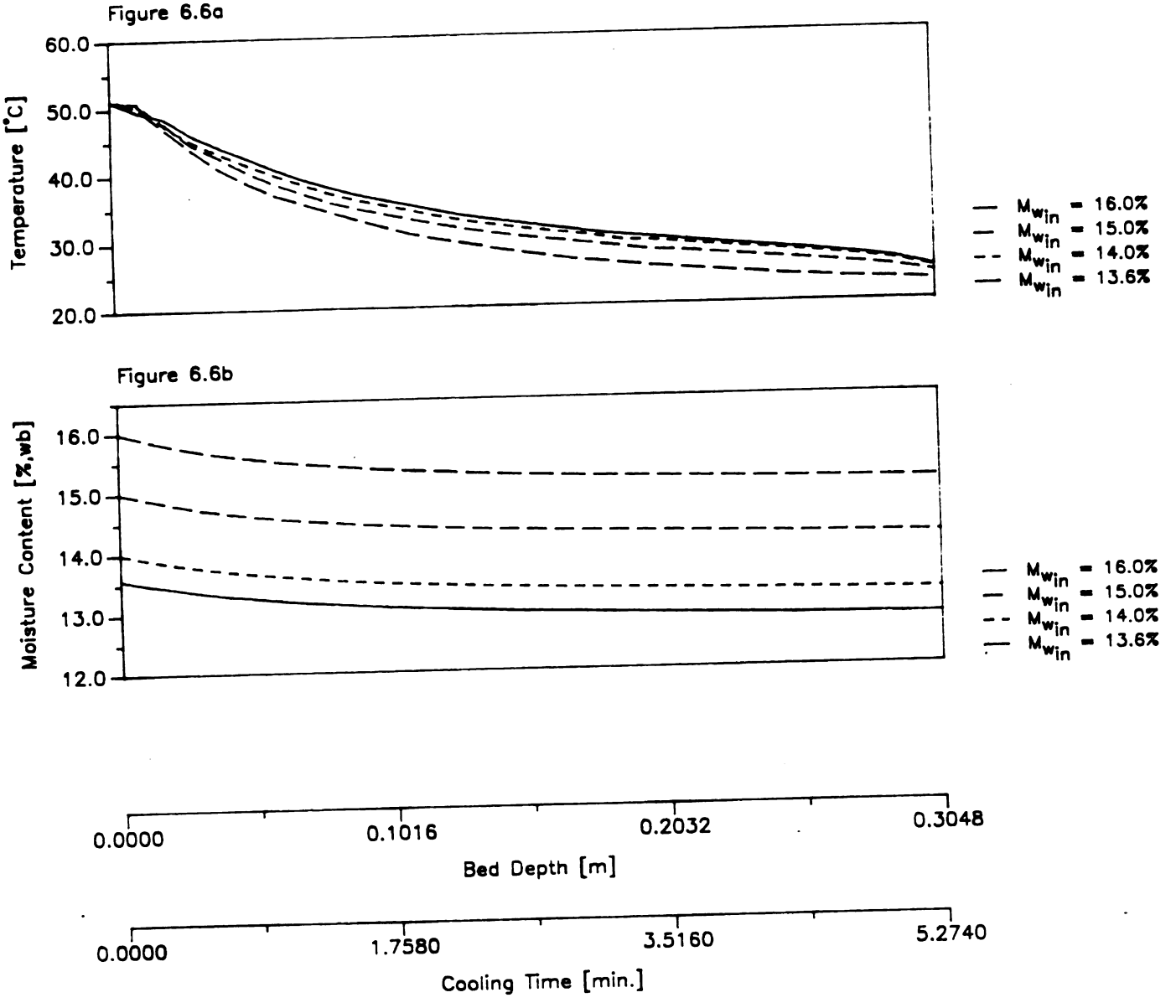


**Figure 6.6** Effect of the initial moisture content on the simulated cooling rate and moisture loss.

section of the bed. At the cooler outlet, however, the pellet temperatures are within a 2°C range.

Figure 6.6b shows the effect of the initial pellet moisture on the moisture loss in the 30.48 cm cooling bed. The initial difference in the moisture contents remains about the same for the moisture curves during the entire cooling period. The pellets with the highest inlet moisture content have the highest outlet moisture content, and vice versa. An initial difference in moisture of 2.4% between the lowest and highest moisture contents decreases to 2.3% at the outlet.

The initial pellet moisture content has no significant influence on the cooling rate and moisture loss of feed pellets in a 30.48 cm counterflow cooling bed.

### 6.2.3 Inlet Air Temperature

The effect of the temperature of the inlet cooling air on the cooling rate of pellets is evident from Figure 6.7a. The larger the temperature difference between the pellets at the top and the cooling air at the bottom of the cooler, the lower the pellet temperature at the cooler outlet.

The pellets cooled by the 12°C cooling air do not reside in the cooler long enough. The effect of the initial pellet temperature is not compensated by the cooling air within the 5.3 minute cooling period. The 17°, 22.6°, and 30°C cooling curves show a pellet temperature profile in the cooling bed which indicates gradual cooling of the pellets. At the outlet a maximum difference of 15.7°C exists between the pellet temperatures.

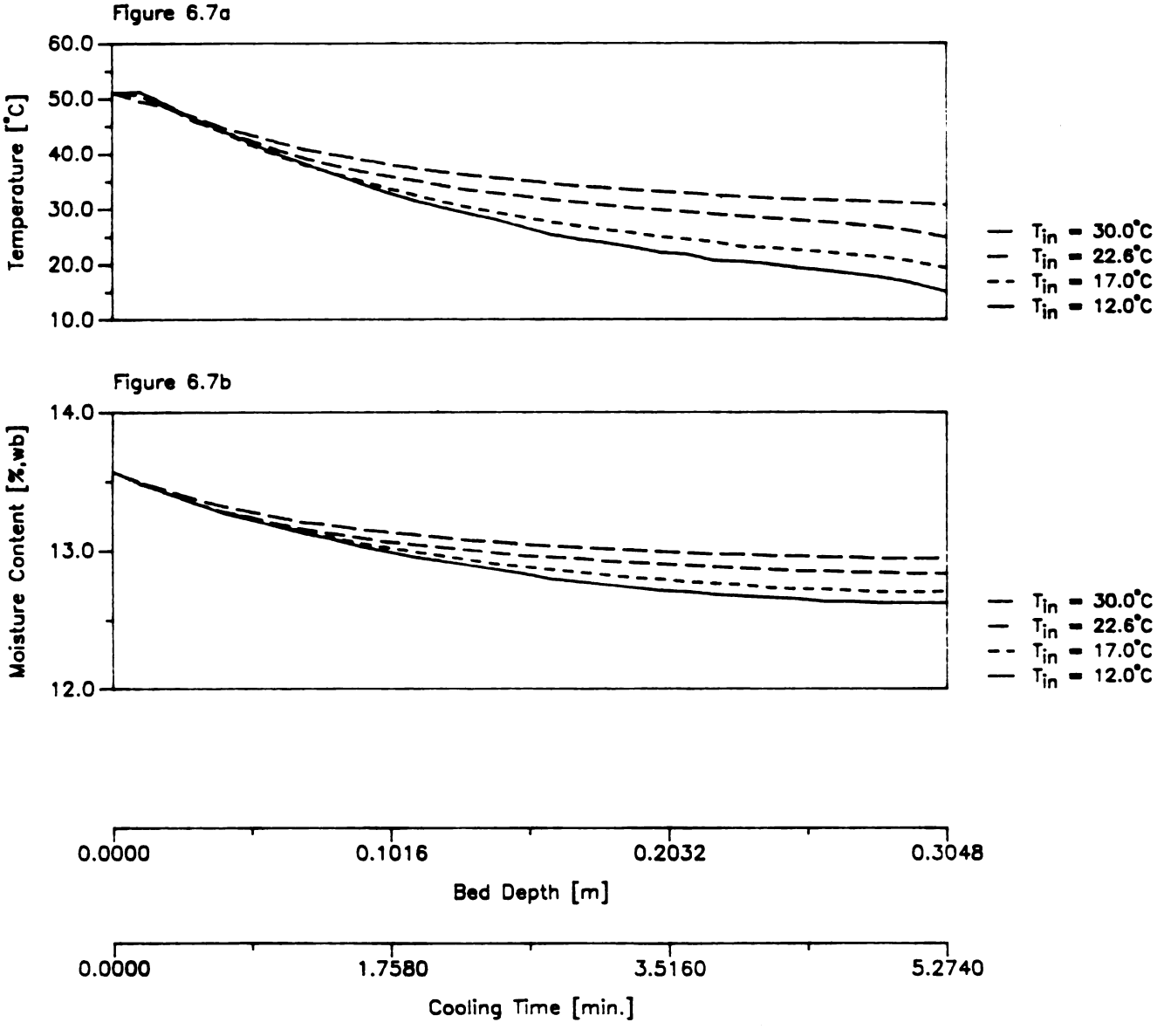


**Figure 6.7 Effect of the inlet air temperature on the simulated cooling rate and moisture loss.**

The moisture loss is highest for the lowest cooling air temperature (see Figure 6.7b). The difference in the moisture loss between the cooling air temperatures continues to increase over the entire cooling period. The outlet moisture contents of the pellets lie within a 0.32% range.

The effect of the inlet cooling air temperature is significant both on the cooling rate and the moisture loss of the pellets.

### 6.2.4 Inlet Air Relative Humidity

The relative humidity of the cooling air has little effect on the cooling rate and moisture loss of the pellets in the top third of the 30.48 cm cooling bed (see Figures 6.8a and 6.8b, respectively). Divergences of the pellet temperature and moisture content profiles are observed after the first 1.5 minutes in the cooler. The pellet temperatures and moisture contents caused by the relative humidities follow two distinct patterns; the differences of the pellet temperatures and the moisture contents of each pattern are negligible.

[The two distinct patterns are caused by the convergence criterion set at ±0.5°C (see section 4.11.4). Below 68% relative humidity the algorithm converges within only 3 iterations, while above 68% relative humidity the algorithm requires at least 5 iterations to converge (see section 4.11.5). It would require a convergence criterion of at least ±0.1°C to force the algorithm to more than 3 iterations for the relative humidities below 68%.]

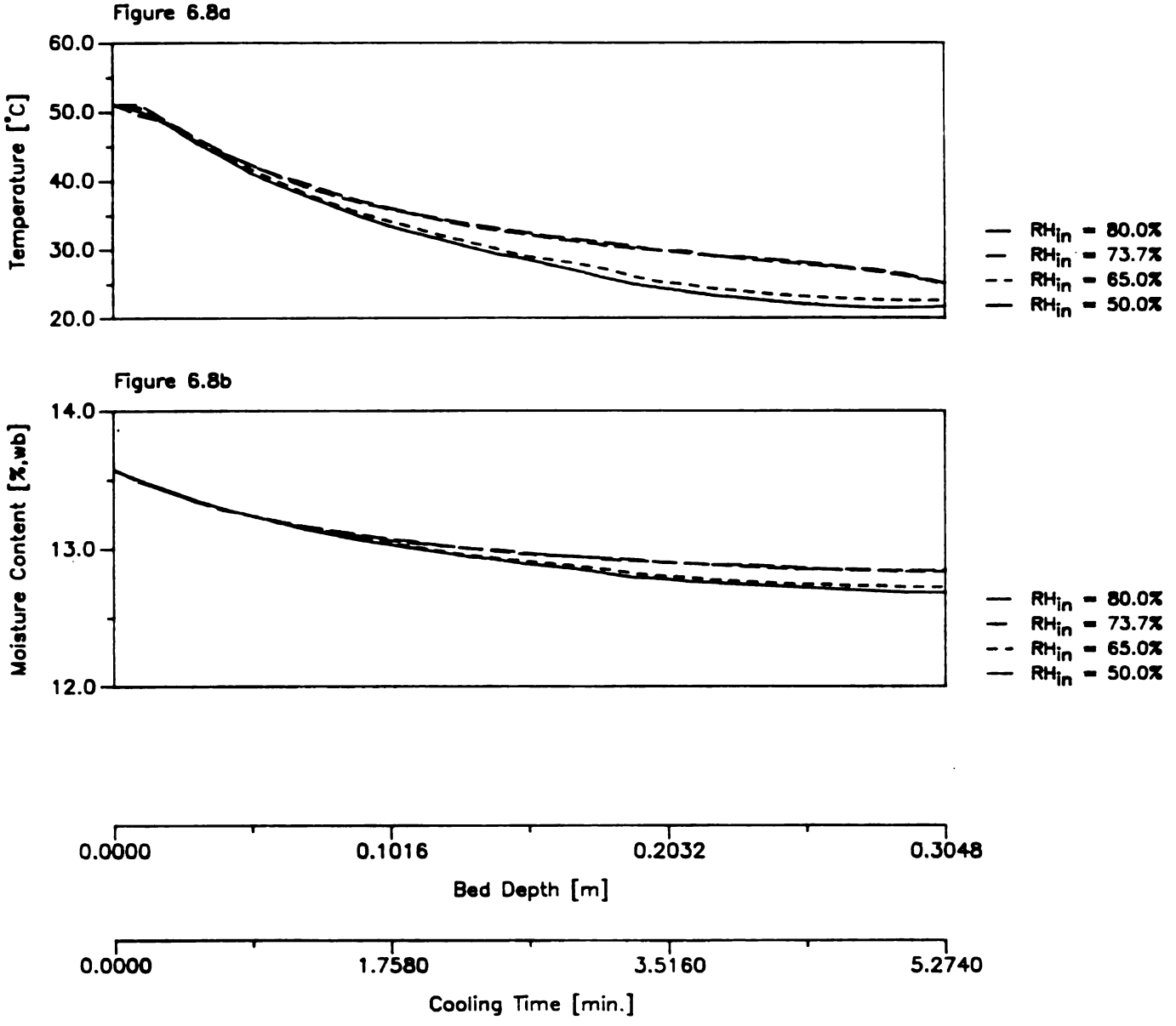


**Figure 6.8** Effect of the inlet relative humidity on the simulated cooling rate and moisture loss.

### 6.2.5 Pellet Flowrate

The pellet flowrate has a significant effect on the cooling behavior of the pellets in the 30.48 cm counterflow cooling bed. The lower the pellet flowrate, the lower the pellet temperatures (see Figure 6.9a) in the cooling bed.

The higher the pellet flowrate, the shorter the cooling time in the bed, causing a higher pellet temperature profile. The difference of the pellet temperatures at the outlet of the cooler, however, is only 1.3°C. At the lower pellet flowrate the cooling effect is almost completed half-way through the cooling bed. At higher capacities sufficient cooling of the pellets is still provided in the 30.48 cm bed.

The moisture contents of the pellets in the cooling bed indicate a reversal effect (see Figure 6.9b). Although the moisture loss at the lower pellet flowrates is initially high, the final moisture contents lie above the higher pellet flowrate curves. At the outlet the largest difference in moisture content is 0.18%.

As the pellet flowrate increases, the reversal phenomenon occurs deeper in the cooling bed. The final moisture content of the pellets cooled at the highest flowrate is the lowest.

The result of Figure 6.9 indicate, that there exists an optimum residence time for a given bed depth that allows control over the cooling rate and the moisture loss in a counterflow cooler.

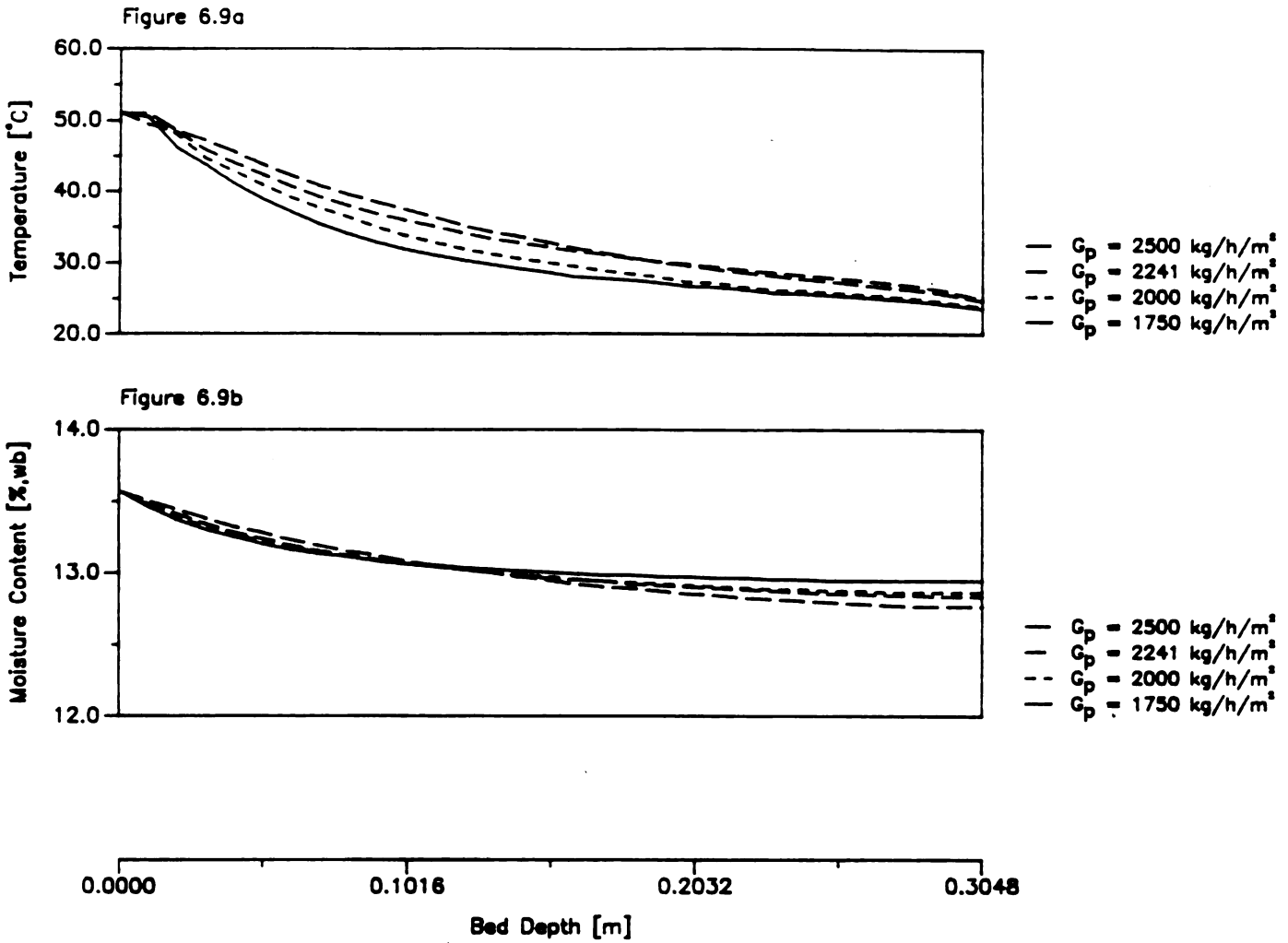


**Figure 6.9 Effect of the pellet flowrate on the simulated cooling rate and moisture loss.**

### 6.2.6 Airflow Rate

In Figure 6.10 the air flowrate through the cooling bed is varied. Figure 6.10a depicts the influence on the cooling rate of the feed pellets. The lower the airflow rate, the higher the pellet temperatures. A significant difference of 5.2°C in the pellet temperatures at the outlet of the cooler exists.

The moisture profiles indicate a reversal effect (see Figure 6.10b). The higher airflow rates cause initially a higher moisture loss; this effect later is off-set in the cooling bed. The low airflow rates result in a gradual moisture loss with lower outlet moisture contents.

Apparently, an optimum residence time to control the moisture loss for a given airflow rate exists. The lowest airflow rate causes the lowest pellet moisture content at the cooler outlet. The largest difference in the outlet moisture contents of the different airflow rates is 0.31%.

### 6.2.7 Pellet-to-Airflow Ratio

In order to determine the relationship between the pellet and airflow rates and the cooling rate and moisture loss, various pellet-to-airflow ratios are compared in Figure 6.11.

The lower the pellet-to-airflow ratio, the higher the cooling rate (see Figure 6.11a). A ratio above 2 is not sufficient to cool the pellets adequately in the 30.48 cm cooling bed because the outlet pellet temperature remains 6.6°C above the inlet cooling air. At the lower pellet-to-airflow ratio, the

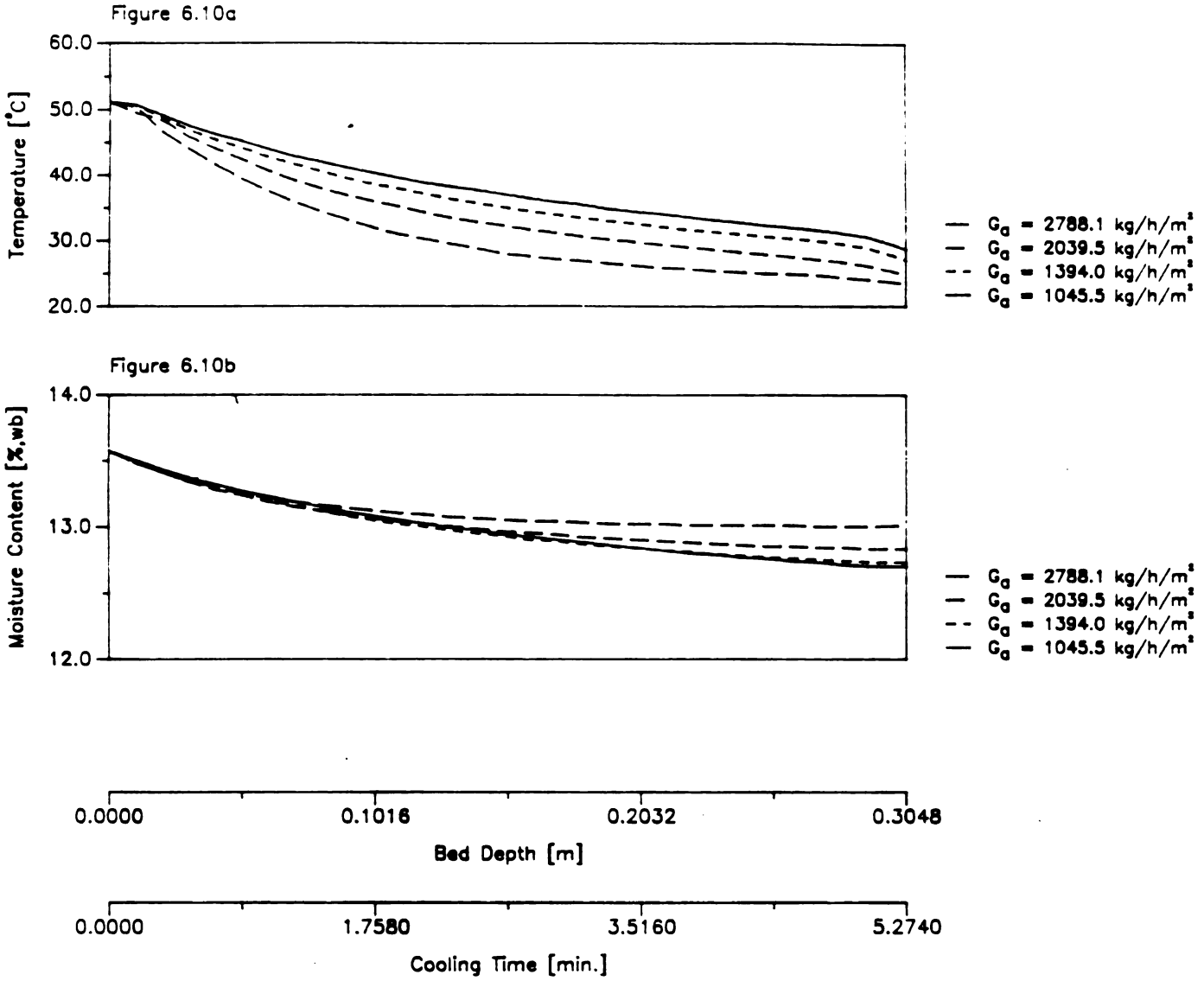


**Figure 6.10 Effect of the airflow rate on the simulated cooling rate and moisture loss .**

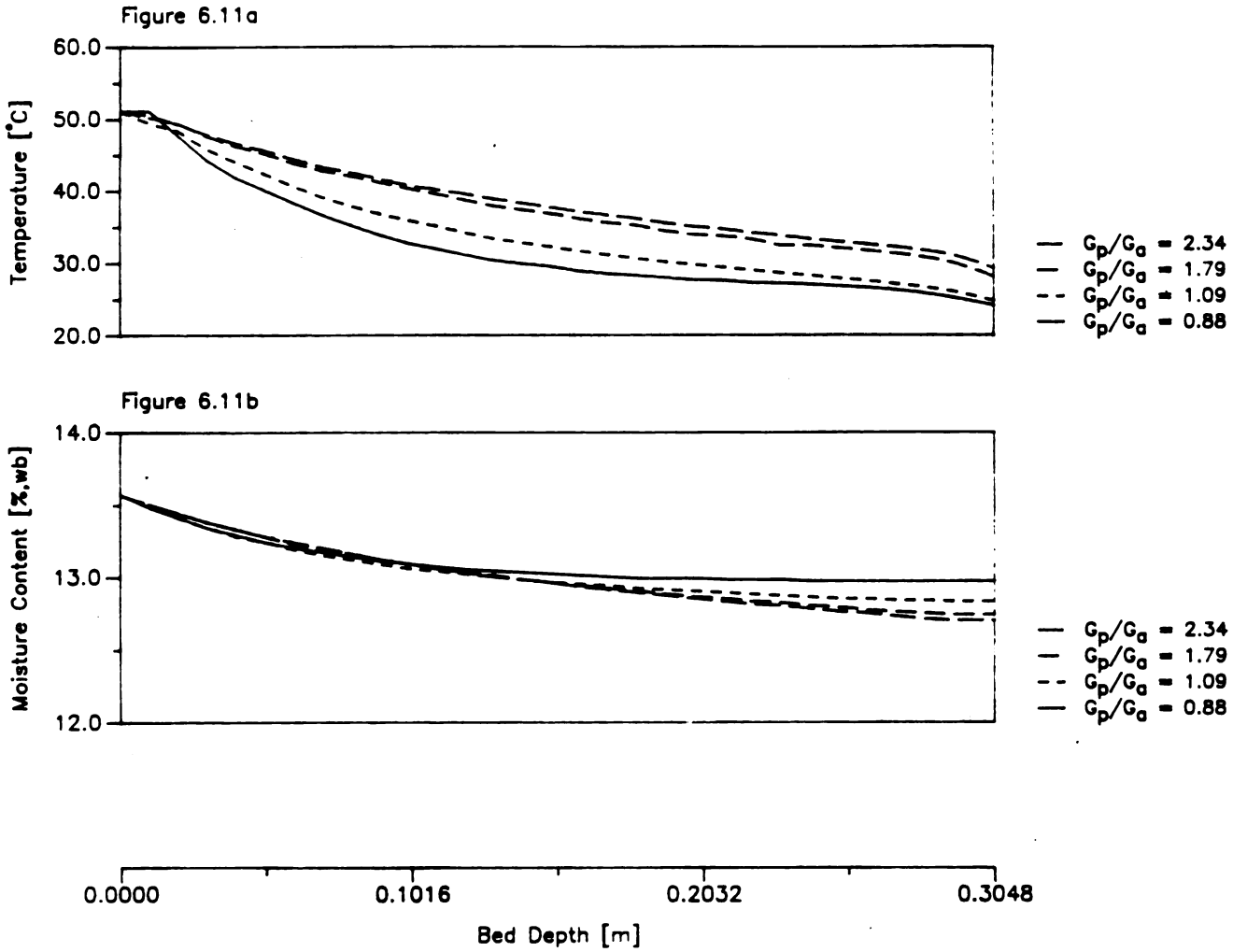


**Figure 6.11 Effect of the pellet-to-airflow ratio on the simulated cooling rate and moisture loss.**

cooling of the feed pellets is completed at a bed depth of 15.24 cm. At the outlet of the cooler the temperature difference of the pellets is within a 5.1°C range.

The moisture loss of the pellets show a reversal effect similar to that observed for the pellet flowrate (see Figure 6.11b). The lower the ratio, the higher the initial moisture loss, but the higher the final moisture content. At the outlet the moisture content of the pellets differs by a maximum of 0.27%.

The pellet-to-airflow ratios chosen have different residence times in the 30.48 cm bed. Apparently, the ratio can be used to chose an optimum bed depth to control the cooling rate and the moisture loss for given air and pellet conditions.

### 6.2.8 Bed Depth

The influence of the bed depth on the cooling rate and the moisture loss is evident from Figure 6.12.

Cooling under the conditions of Test 2 can be completed in a 15.24 cm cooling bed with a residence time of 2.6 minutes; the final pellet temperature had reached 27.7°C, or 4.5°C above the ambient cooling air (see Figure 6.12a). At a bed depth of 30.48 cm an additional cooling effect of 2.2°C above the inlet air is achieved. An additional 1.5°C is achieved by increasing the bed depth to 45.72 cm. The cooling air conditions of Test 2 show that the deeper cooling bed of 60.96 cm actually increases the final pellet temperature to 2.0°C above the inlet cooling air. At the outlet the difference in the pellet temperatures are within a

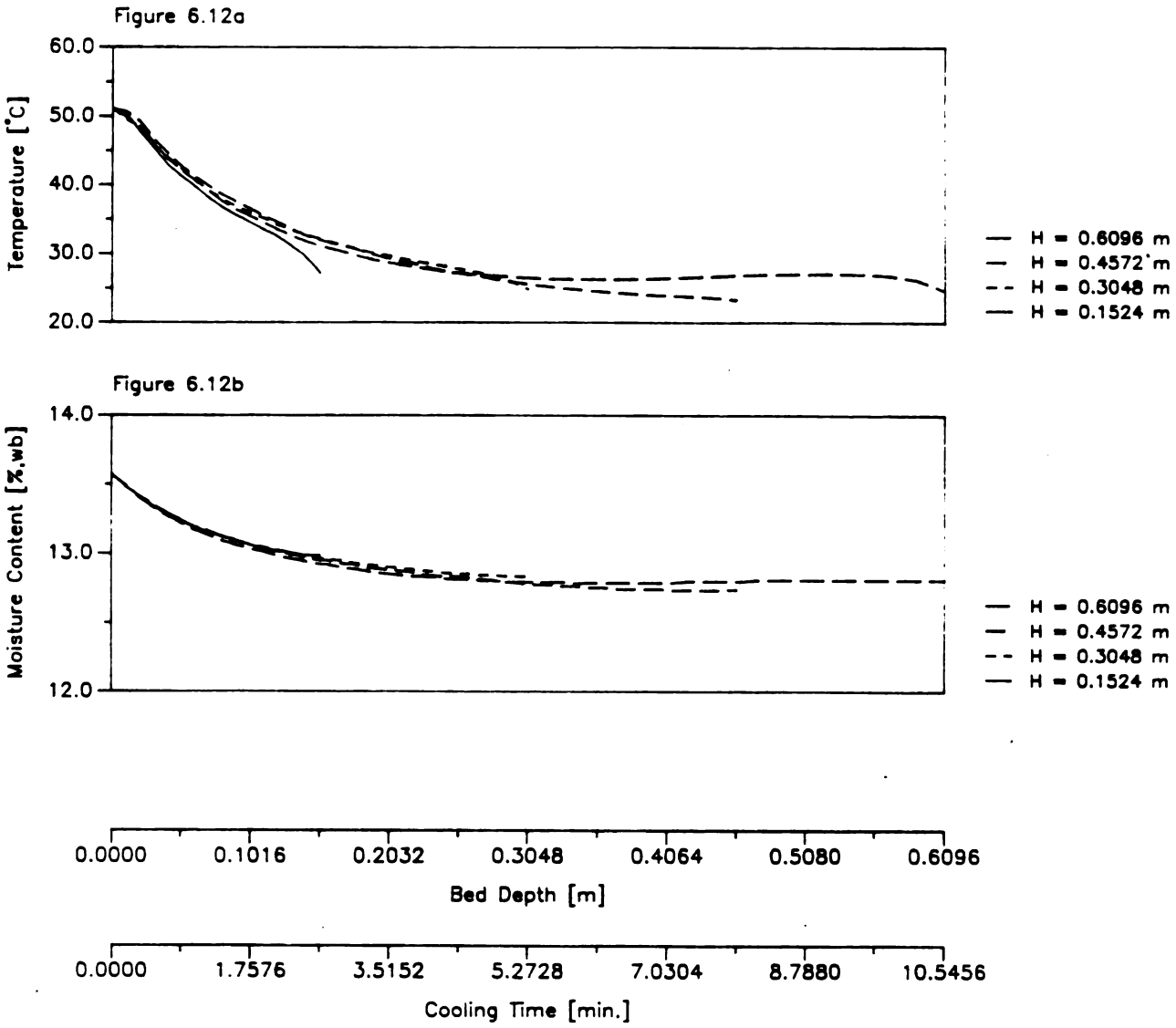


**Figure 6.12 Effect of the cooling bed depth on the simulated cooling rate and moisture loss.**

3.8°C range.

The short residence time effects the moisture loss; it is only 0.59% (see Figure 6.12b). By increasing the bed depth to 30.48 cm and 45.72 cm the moisture loss increases to 0.74% and 0.83%, respectively. The cooling air conditions of Test 2 show that at a residence time of 12.3 minutes in the 60.96 cm cooling bed the moisture content of the feed pellets increases after a maximum moisture loss of 0.78% during the first 6 minutes in the cooling bed. At the outlet the largest difference in pellet moisture content is 0.24%.

6.2.9 Pellet Diameter

The influence of the pellet diameter on the cooling rate and the moisture loss in the counterflow cooling bed is very significant (see Figure 6.13).

The smaller the pellet diameter, the higher the cooling rate. The larger pellet diameters of 6.35 mm and 9.53 mm have outlet temperatures of 4.4° and 7.8° C, respectively, above that of the inlet cooling air (see Figure 6.13a). The smaller diameter pellets reach outlet temperatures of less than 0.2°C above the inlet cooling air. At the outlet the maximum pellet temperature difference is 7.7°C.

The moisture loss of a small diameter pellet is much higher than of a larger sized pellet (see Figure 6.13b). The 3.18 mm pellets only require a bed depth of 21 cm to reach the final moisture content. The moisture content of the largest diameter pellet is 0.52% above that of the smallest diameter pellet.

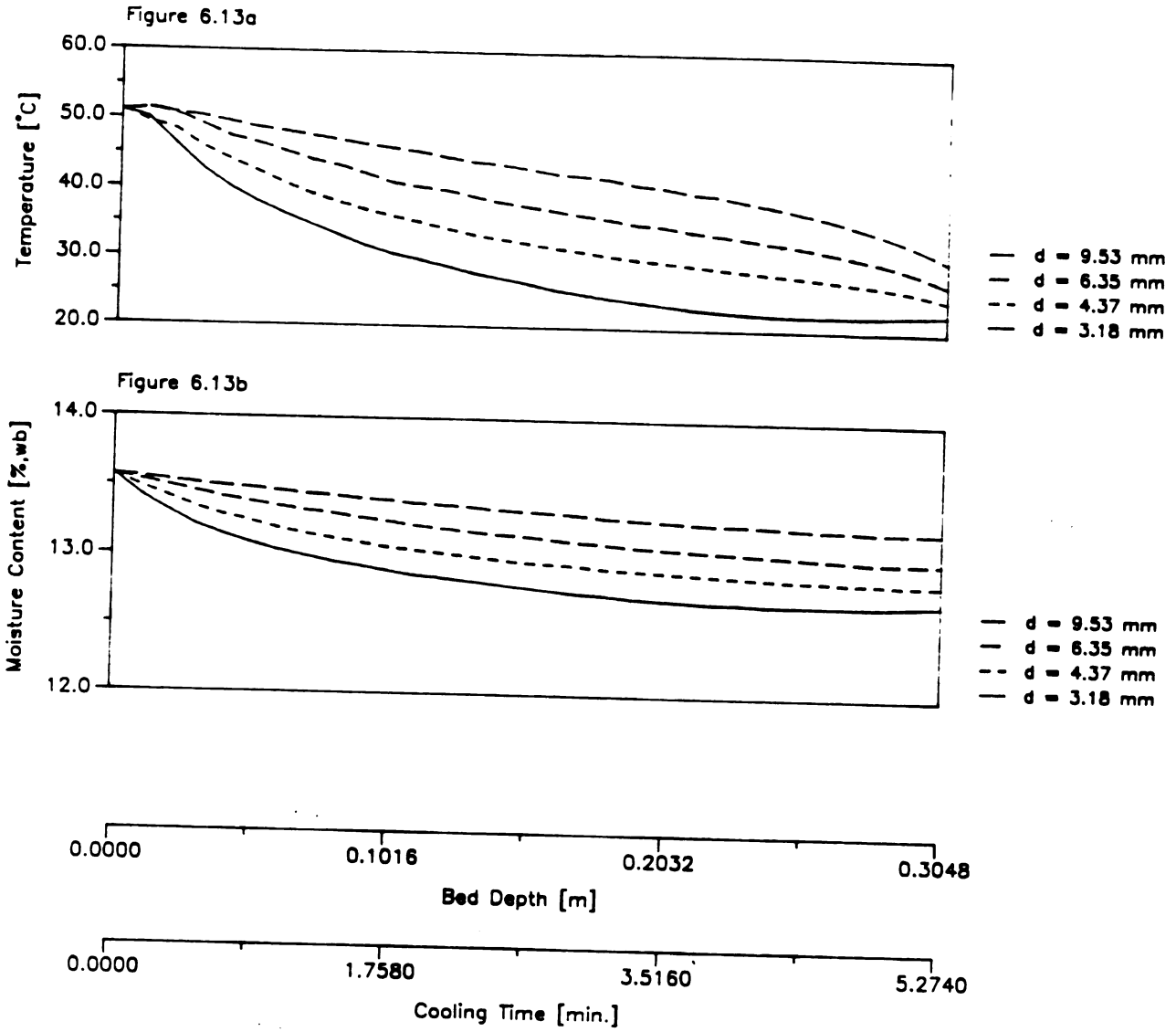


**Figure 6.13 Effect of the pellet diameter on the simulated cooling rate and moisture loss.**

6.2.10 Internal Moisture Gradient

The design of a feed pellet cooler must consider the internal moisture gradient in the pellets in order to preserve the pellet quality. A larger internal moisture gradient in the pellets after the cooling process results in a high accumulation of fines during the handling and storage of the pellets (Friedrich, 1980).

Table 6.1 is a summary of the effect of the various design parameters on the internal moisture gradient of the pellets at the outlet of the cooling bed.

The values of $M_1'$ , $M_2'$, $M_3'$, and $M_s'$ represent the internal moisture contents of the subregions 1, 2, 3, and the surface of the pellet. The subregions are of equal volume as described in Chapter 4. The internal moisture contents are listed together with the average outlet moisture content and the average equilibrium moisture content at the outlet of the cooler.

The largest internal moisture gradient of 3.14% is observed for an initial pellet temperature of 62.5°C; the moisture content in the first subregion is 13.56% and at the pellet surface 10.42% with an equilibrium moisture content of 12.83% at the outlet. The smallest internal moisture gradient is observed for the pellets with a diameter of 9.53 mm; the moisture content in the first subregion is 13.57% and at the pellet surface 12.20% with an equilibrium moisture content of 12.35%. The smallest internal moisture gradient for the 4.37 mm pellets is observed at an aiflow rate of 2788.1 kg/h/$m^2$. The moisture gradient is 1.75% with a moisture content of 13.56% in the first subregion and

Table 6.1 Summary of the effects of the simulation parameters on the moisture gradient [%,wb].

| Parameter | Value | $M_{out}$ | $M_1'$ | $M_2'$ | $M_3'$ | $M_s'$ | $M_{eq}$ |
|---|---|---|---|---|---|---|---|
| $\theta_{in}$ [°C] | 51.1* | 12.83 | 13.57 | 13.49 | 12.95 | 11.26 | 12.91 |
| | 55.0 | 12.73 | 13.57 | 13.47 | 12.85 | 10.94 | 12.88 |
| | 60.0 | 12.60 | 13.56 | 13.45 | 12.72 | 10.64 | 12.85 |
| | 62.5 | 12.53 | 13.56 | 13.44 | 12.64 | 10.42 | 12.83 |
| $M_{win}$ [%,wb] | 13.6* | 12.83 | 13.57 | 13.49 | 12.95 | 11.26 | 12.91 |
| | 14.0 | 13.24 | 14.00 | 13.91 | 13.36 | 11.64 | 12.93 |
| | 15.0 | 14.17 | 14.99 | 14.89 | 14.26 | 12.46 | 12.99 |
| | 16.0 | 15.08 | 15.99 | 15.86 | 15.12 | 13.25 | 13.11 |
| $T_{in}$ [°C] | 12.0 | 12.62 | 13.57 | 13.48 | 12.81 | 10.45 | 14.03 |
| | 17.0* | 12.71 | 13.57 | 13.48 | 12.87 | 10.85 | 13.51 |
| | 22.6* | 12.80 | 13.57 | 13.49 | 12.94 | 11.32 | 12.95 |
| | 30.0 | 12.94 | 13.57 | 13.48 | 12.99 | 11.68 | 12.34 |
| $RH_{in}$ [%] | 50.0 | 12.68 | 13.57 | 13.48 | 12.86 | 10.72 | 8.89 |
| | 65.0* | 12.72 | 13.57 | 13.48 | 12.85 | 10.90 | 11.37 |
| | 73.7* | 12.83 | 13.57 | 13.49 | 12.95 | 11.26 | 12.91 |
| | 80.0 | 12.85 | 13.57 | 13.49 | 12.95 | 11.32 | 14.45 |
| $G_p$ [kg/h/m$^2$] | 1750 | 12.94 | 13.56 | 13.47 | 12.96 | 11.74 | 13.04 |
| | 2000* | 12.86 | 13.57 | 13.48 | 12.93 | 11.40 | 13.02 |
| | 2241* | 12.83 | 13.57 | 13.49 | 12.95 | 11.26 | 12.91 |
| | 2500 | 12.76 | 13.57 | 13.49 | 12.91 | 10.98 | 12.93 |
| $G_a$ [kg/h/m$^2$] | 1045.5 | 12.70 | 13.56 | 13.47 | 12.86 | 10.87 | 12.53 |
| | 1394.0* | 12.73 | 13.57 | 13.48 | 12.88 | 10.98 | 12.69 |
| | 2039.5* | 12.83 | 13.57 | 13.49 | 12.95 | 11.26 | 12.91 |
| | 2788.1 | 13.01 | 13.57 | 13.51 | 13.09 | 11.82 | 13.06 |
| $G_p/G_a$ | 0.88* | 12.97 | 13.57 | 13.51 | 13.07 | 11.75 | 12.98 |
| | 1.09* | 12.83 | 13.57 | 13.49 | 12.95 | 11.26 | 12.91 |
| | 1.79 | 12.74 | 13.57 | 13.49 | 12.93 | 10.92 | 12.58 |
| | 2.34 | 12.70 | 13.56 | 13.47 | 12.86 | 10.87 | 12.47 |
| H [m] | 0.1524* | 12.98 | 13.57 | 13.55 | 13.26 | 11.54 | 12.68 |
| | 0.3048* | 12.83 | 13.57 | 13.49 | 12.95 | 11.26 | 12.91 |
| | 0.4572 | 12.74 | 13.56 | 13.41 | 12.68 | 11.26 | 13.07 |
| | 0.6096 | 12.81 | 13.55 | 13.34 | 12.66 | 11.74 | 12.92 |
| d [mm] | 3.18* | 12.69 | 13.55 | 13.33 | 12.51 | 11.36 | 13.12 |
| | 4.37* | 12.83 | 13.57 | 13.49 | 12.95 | 11.26 | 12.91 |
| | 6.35 | 12.99 | 13.57 | 13.55 | 13.28 | 11.55 | 12.69 |
| | 9.53 | 13.21 | 13.57 | 13.57 | 13.47 | 12.20 | 12.35 |

* standard test parameters

11.82% at the pellet surface.

The moisture content in the first subregion of the pellet for all simulation parameters is essentially the same as the initial moisture content of the pellets at the cooler inlet. In the second subregion, the moisture content ranges from 0.0 to 0.22% below the moisture content of the first subregion. No change occurred for the 9.53 mm pellet and the largest change occurred for the 3.18 mm pellet. The moisture content in the third subregion ranged from 0.10 to 0.82% below the moisture content in the second subregion. The smallest change occurred in the 9.53 mm pellet, while the largest change occurred in the 3.18 mm pellet. The moisture content at the surface of the pellets ranged from 0.92 to 2.33% below the moisture content in the third subregion. The smallest difference occurred for the 60.96 cm bed and the largest difference for an air temperature of 12°C.

The results of the simulation model indicate that adequate cooling with the smallest internal moisture gradient can only be achieved if the airflow rate and the residence time in the cooler are adjusted properly. Internal moisture gradients of the order of 3.14% at the outlet of the counterflow cooler are suspected to contribute significantly to the accumulation of fines during the handling and storage operations in a feed mill. The maximum allowable internal moisture gradient for feed pellets after the cooling process is not specified in the literature.

### 6.2.11 Usefulness of the Simulation Model

The results of the simulation study on the influence of various design parameters on the cooling rate, the moisture loss, and the internal moisture gradient of feed pellets in a counterflow cooler indicate that the following are the most significant design parameters:

1) the cooling bed depth, and

2) the residence time.

The cooling rate and the moisture loss of the pellets in the counterflow cooler can be optimized if the proper combination of bed depth and residence time is determined for given ambient and pellet conditions. The pellets can generally be cooled with a short residence time and in a shallow cooling bed.

The control of the residence time is achieved by adjusting the pellet flowrate. In a commercial operation, a maximum pellet flowrate through the cooler means a maximum capacity at the pellet mill. In order to obtain the desired cooling rate, the moisture loss and the allowable internal moisture gradient at a particular air and pellet flowrate have to be considered. Thus, the proper residence time in a counterflow cooler is best determined as a function of the pellet-to-airflow ratio.

Current designs of commercial counterflow coolers do not allow for the adjustment of the bed depth. The simulation study, however, has shown that the proper bed depth is crucial in achieving the desired cooling rate, moisture loss, and internal moisture gradient.

Furthermore, the simulation results have shown that the

counterflow cooling process is dominated more by the temperature of the pellets and the cooling air than by the moisture content of the pellets and the relative humidity of the cooling air. Since a feed mill operation has generally no control over the condition of the cooling air , and since the temperature of the pellets reaching the counterflow cooler depends on the optimum pellet mill operation, it is important to understand how the counterflow pellet cooler is best adjusted using a combination of the pellet-to-airflow ratio and the bed depth.

In the simulation study, the experimental results of Chapter 5 were confirmed; i.e. the bed depth and pellet-to-airflow ratio have a significant effect on the cooling rate and the moisture loss of the feed pellets in a counterflow cooler. The simulation model was used to evaluate further the parameters of the experimental tests. The trends of the simulation model allow its use for the evaluation of the cooling rate of pellets in a counterflow cooler under conditions falling within the stability range of the model. It appears that the simulation model somewhat underestimates the moisture loss in the cooling bed.

The growing popularity of counterflow coolers (Westlaken, 1988) in Europe, in part due to the advertised advantages of the counterflow design such as reduced moisture loss and smaller dimensions, have been verified and are supported by the results of this simulation study. U.S. feed equipment manufacturers should begin building counterflow pellet coolers to secure a market share as the popularity of these coolers in the feed industry will continue to rise.

# 7 SUMMARY AND CONCLUSIONS

In this study the following objectives were achieved:

1) Experimental data on the counterflow cooling of feed pellets in a laboratory-size cooler was collected for various design and operating parameters.

2) A computer simulation was developed to model the counterflow cooling of feed pellets and was validated with the experimental data.

3) The experimental cooler and the simulation model were used to determine the influence of various design parameters on the cooling rate and moisture loss of feed pellets in a counterflow cooler.

The following conclusions can be drawn from this study:

1) The counterflow cooler is an excellent design for the cooling of feed pellets.

2) The simulation model has been validated within a certain range of design parameters (see Appendix D). Extrapolation beyond the limits may not be valid.

3) The importance of the pellet flowrate and the air flowrate on the counterflow cooler design are best evaluated in the form of the pellet-to-airflow ratio.

4) The experimental results suggest that the bed depth has the most significant influence on the cooling rate and the moisture loss of the feed pellets. The simulation model confirms this observation and, in addition, shows that the residence time has an equally significant influence on the control of the cooling rate, the moisture loss, and the internal moisture gradient of feed pellets in a counterflow cooler.

5) The simulation model further indicates that the pellet-to-airflow ratio, the initial pellet temperature, and the inlet cooling air temperature have a significant influence on the pellet temperature, the moisture content, and the internal moisture gradient at the cooler outlet; while the initial moisture content, and the relative humidity of the cooling air are of minor importance in the design of a counterflow pellet cooler.

6) According to the simulation results the bed depth and residence time must be adjusted, if feed pellets of varying sizes are to be used in a single counterflow cooler .

7) The maximum capacity of the experimental counterflow cooler was 1758 kg/h/m$^2$ at a bed depth of 30.48 cm and an air velocity of 0.61 m/s. The simulation model predicts that a capacity of 2500 kg/h/m$^2$ can be obtained at this bed depth with an air velocity of 0.49 m/s.

# 8 RECOMMENDATIONS

The following recommendations for further study are proposed:

1) Perform a thorough analysis of the sensitivity of the model to the heat transfer coefficient, equilibrium moisture content equation, and diffusion coefficient to determine whether the development of pellet-specific phenomenological equations would increase the accuracy of the simulation model significantly.

2) Determine the influence of the counterflow cooling process on the quality of the feed pellets.

3) Perform a comparative engineering and economic study of the counterflow cooler versus the traditional double-deck horizontal cooler.

# LIST OF REFERENCES

# 9 LIST OF REFERENCES


Atkinson, E. 1981. Cool It! Agritrade. (9):14-15.

Apelt, J. 1987a. Die physikalische Qualität des Mischfutters. Die Mühle + Mischfuttertechnik. 124(15):191.

Apelt, J. 1987b. Personal Communication. Forschungsinstitut Futtermitteltechnik der IFF. Braunschweig-Thune. Federal Republic of Germany.

Bakker-Arkema, F.W., W.G. Bickert, and R.J. Patterson. 1967. Simultaneous Heat and Mass Transfer during the Cooling of a Deep Bed of Biological Products under Varying Inlet Air Conditions. Journal of Agricultural Engineering Research. 12(4):297-307.

Bakker-Arkema, F.W. and I.P. Schisler. 1984. Counterflow Cooling of Grain. ASAE Paper No 84-3523. American Society of Agricultural Engineers, St Joseph, MI.

Bakker-Arkema, F.W., D.E. Maier and H. Pierik. 1988. Pellet Cooling in a Single-deck Horizontal Cooler. Submitted to Die Mühle + Mischfuttertechnik.

Beck, J.V. 1988. Personal Communication. Department of Mechanical Engineering. Michigan State University. East Lansing, MI.

Biagi, J.D. 1986. Modeling of the Feed-Pellet Cooling Process. Ph.D. Thesis. Michigan State University. East Lansing, MI.

Brook, R.C. and G.H. Foster. 1981. Drying, Cleaning and Conditioning. In Handbook of Transportation and Marketing in Agriculture. Volume II. Field Crops. 63-110. Finney, E.E. Ed. CRC Press Inc. Boca Raton, FL.

Brooker, D.B., F.W. Bakker-Arkema and C.W. Hall. 1982. Drying Cereal Grains. 5th Printing. AVI Publishing Company. Westport, CT.

Bühler-Miag. 1987. Bühler-Miag brochure. Uzwil, Switzerland.

Chu, S.T. and A. Hustrulid. 1968. Numerical Solution of Diffusion Equations. Transactions of the ASAE. (11):705-709.

CPM. 1987. California Pellet Mill brochure. San Francisco, CA.

Die Mühle + Mischfuttertechnik. 1986. Karussell-Kühler, Bauart Klöckner. 123(30):412.

Evans, T.W. 1970. Simulation of Counter-flow Drying. M.S. Thesis. Michigan State University, East Lansing, MI.

Falk, D. 1985. Pelleting Cost Center. In Feed Manufacturing Technology III. 167-190. McEllhiney, R.R. Ed. American Feed Industry Association, Inc. Arlington, VA.

Feed & Grain Times. 1988. Beta Raven advertisement. 27(4):18-20.

Föller-Friedrich, I. 1984. Today's Research Work - Tomorrow's Technology and Success. IFF - Schrift. Forschungsinstitut Futtermitteltechnik der IFF. Braunschweig-Thune. Federal Republic of Germany.

Fortes, M. and M.R. Okos. 1982. Heat and Mass Transfer in Hygroscopic Capillary Extruded Products. AIChE Journal. 27(2):255-262.

Friedrich, W. 1980. Der Kühlvorgang von Mischfutterpellets und sein Einfluß auf die Pelletfestigkeit. Die Mühle und Mischfuttertechnik. 117(20):268-281.

Haggas, D. 1987. Possible Methods of Reducing Production Energy Costs. Holmen Symposium 87. Hounslow, Middlesex, U.K. F(1)-F(8).

Heinemans, H. 1986. Cooling by Counterflow. Feed International. 7(9):64.

Holman, J.P. 1981. Heat Transfer. 5th Edition. McGraw-Hill Book Company. New York, NY.

IFF Report Nr.1. 1984. Das Pelletieren von Mischfutter. Forschungsinstitut Futtermitteltechnik der IFF. Braunschweig-Thune. Federal Republic of Germany.

Koch, V. 1987. 97 Mill. Tonnen Mischfutter in der EG. Kraftfutter. 70(9):308.

Kraftfutter. 1985. Geelen Techniek advertisement. 68(4):137.

Lastman, G.J. 1963. Solution of First-order Differential Equations by Runge-Kutta or Adams-Moulton Method. Computer Laboratory Library. Michigan State University, East Lansing, MI.

Lin, W. and M. Ash. 1988. Characteristics of the Feed Manufacturing Industry. Grain & Feed Marketing. 7(1):11-12,65-74.

McEllhiney, R.R. 1985. Feed Manufacturing Technology III. American Feed Industry Association, Inc. Arlington, VA.

McEllhiney, R.R. 1986. What's New in Pelleting. Feed Management. 38(2):22-34.

Parry, J.L. 1985. Mathematical Modeling and Computer Simulation of Heat and Mass Transfer in Agricultural Grain Drying: A Review. Journal of Agricultural Engineering Research. 32(1):1-29.

Perry, T.W. 1984. Animal Life-Cycle Feeding and Nutrition. Academic Press Inc. Harcourt Brace Jovanovich, Publishers.

Redus, R. 1987. The APC System - An Alternative Steam Conditioning System. Holmen Symposium 87. Hounslow, Middlesex, U.K. G(1)-G(10).

Robinson, R.A. 1970. Pelleting - Introduction and General Definitions. In Feed Manufacturing Technology. 96-104. Pfost, H.B. Ed. American Feed Manufacturers Association, Inc. Chicago, IL.

Robinson, R.A. 1971. The Pelleting of Animal Feeds. 12th Biannual Conference of the Institute For Briquetting and Agglomeration. 12(8):97-112.

Robinson, R.A. 1983. Pellet Cooling. Feed Compounding. Milling. (12):26-27.

Rohbohm, K.F. 1987a. Personal Communication. Forschungsinstitut Futtermitteltechnik der IFF. Braunschweig-Thune. Federal Republic of Germany.

Rohbohm, K.F. 1987b. Qualitätssicherung von Mischfutterpellets durch Bestimmung physikalischer Stoffeigenschaften. Die Mühle + Mischfuttertechnik. 124(15):191-197.

Schisler, I.P. 1987, 1988. Personal Communication. Schisler Consulting, Inc. Durand, MI.

Scott, M.R. 1973. Invariant Imbedding and its Application to Ordinary Differential Equations - An Introduction. Addison-Wesley Publishing Company, Inc. Reading, MA.

Walter, U. 1986. Pellet Quality - a Matter of Cooling. Feed International. 7(9):60-63.

Westlaken, C. 1988. Personal Communication. Westlaken Agricultural Engineering and Consulting, Inc. St. Marys, Ontario, Canada.

Winowiski, T. 1985. Testing Pellet Quality. Feed Management. 36(8):254-28.

## DISCLAIMER

Trade names are used in this study solely to provide specific information. Mention of a trade name does not constitute a warranty of the product by the author nor by Michigan State University nor an endorsement of the product to the exclusion of other products not mentioned.

# APPENDICES

**APPENDIX A** Experimental cooling results

**APPENDIX B** Steady-state cooling bed temperatures

**APPENDIX C** Unstable simulation results

**APPENDIX D** Summary of simulation parameters

**APPENDIX E** Input and output of the computer model

# APPENDIX A

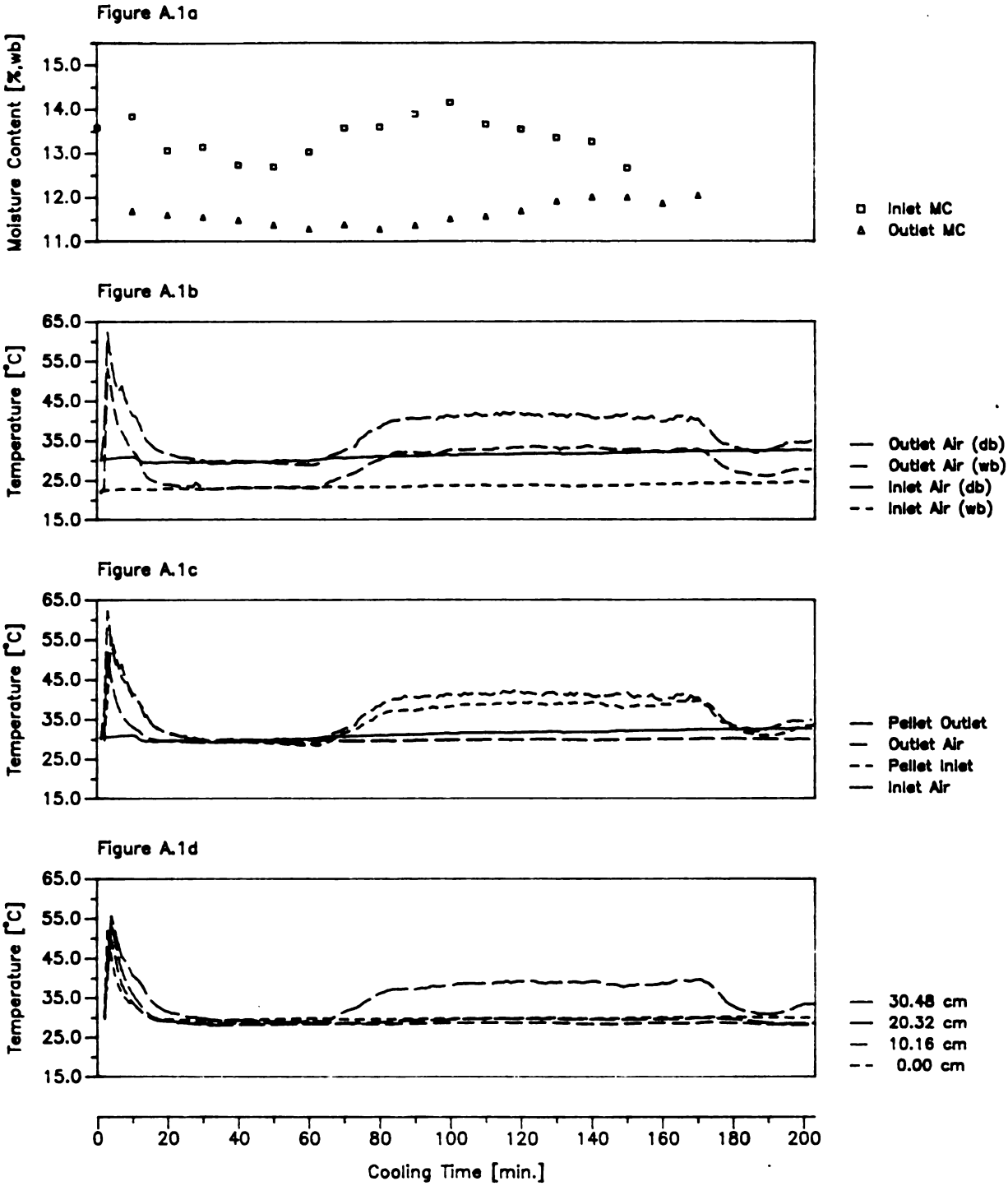


**Figure A.1 Experimental cooling results for Test 1.**

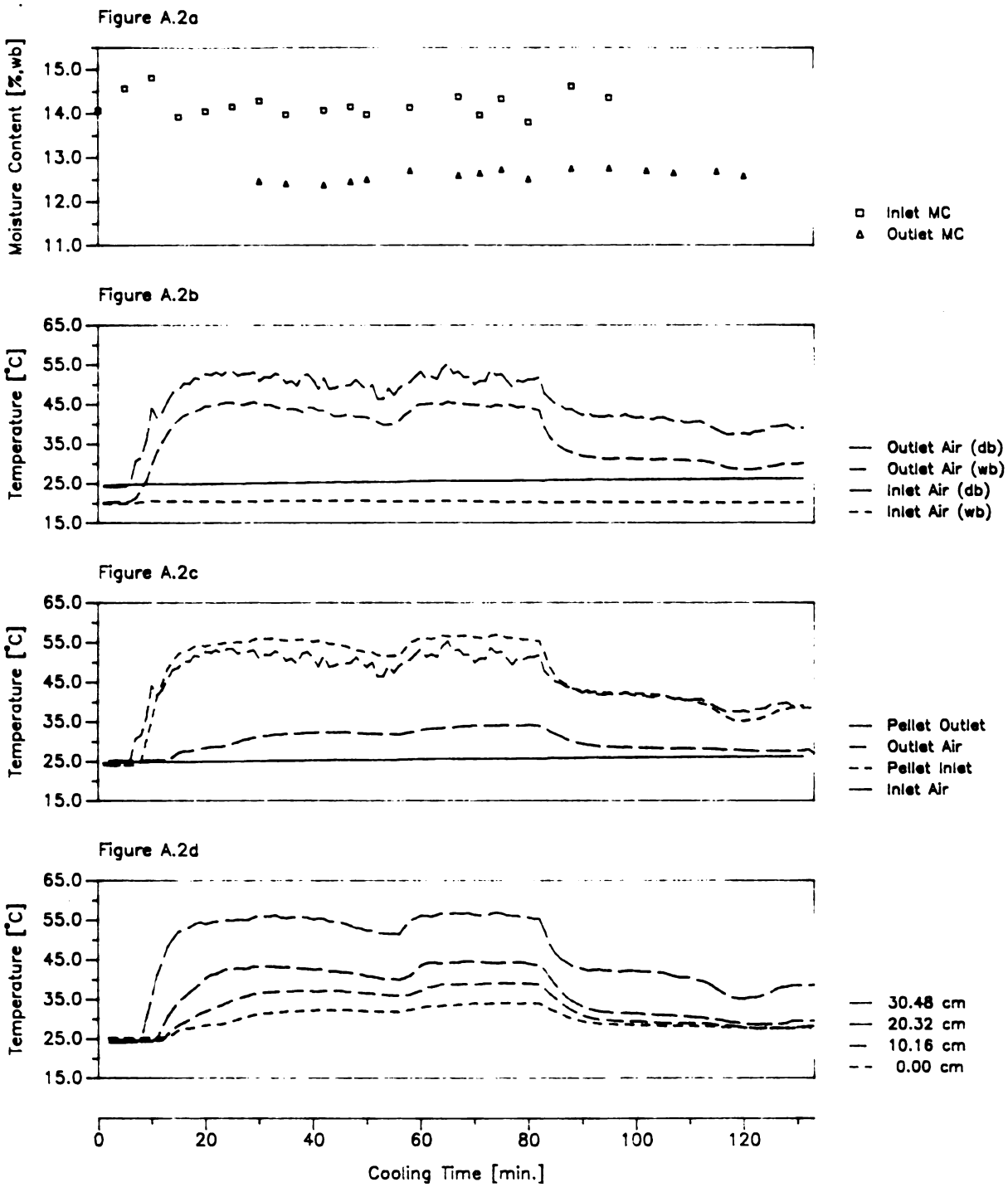


**Figure A.2 Experimental cooling results for Test 3 and Test 4. (NOTE: The air flowrate was changed after 75 minutes)**

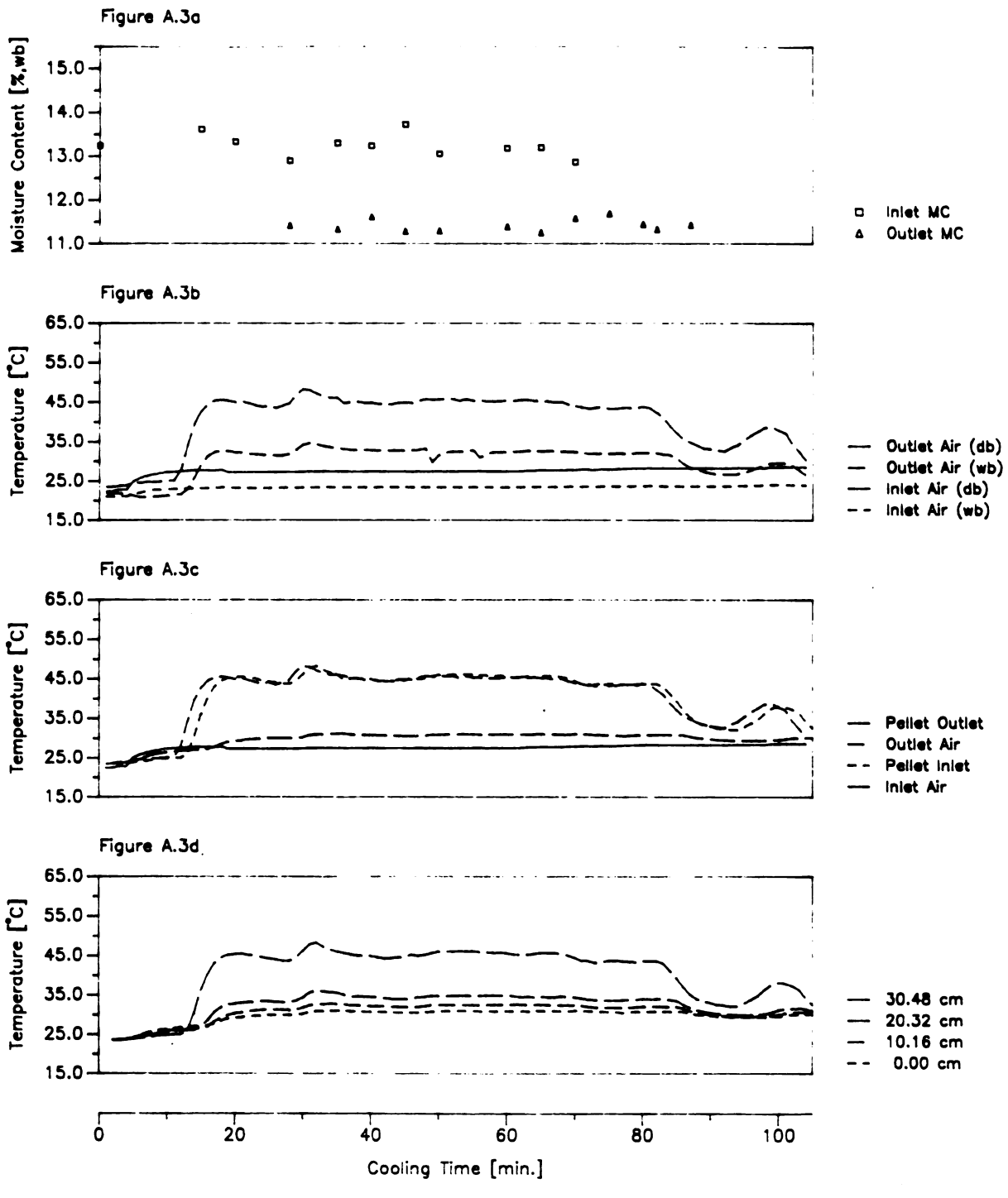


**Figure A.3 Experimental cooling results for Test 5.**

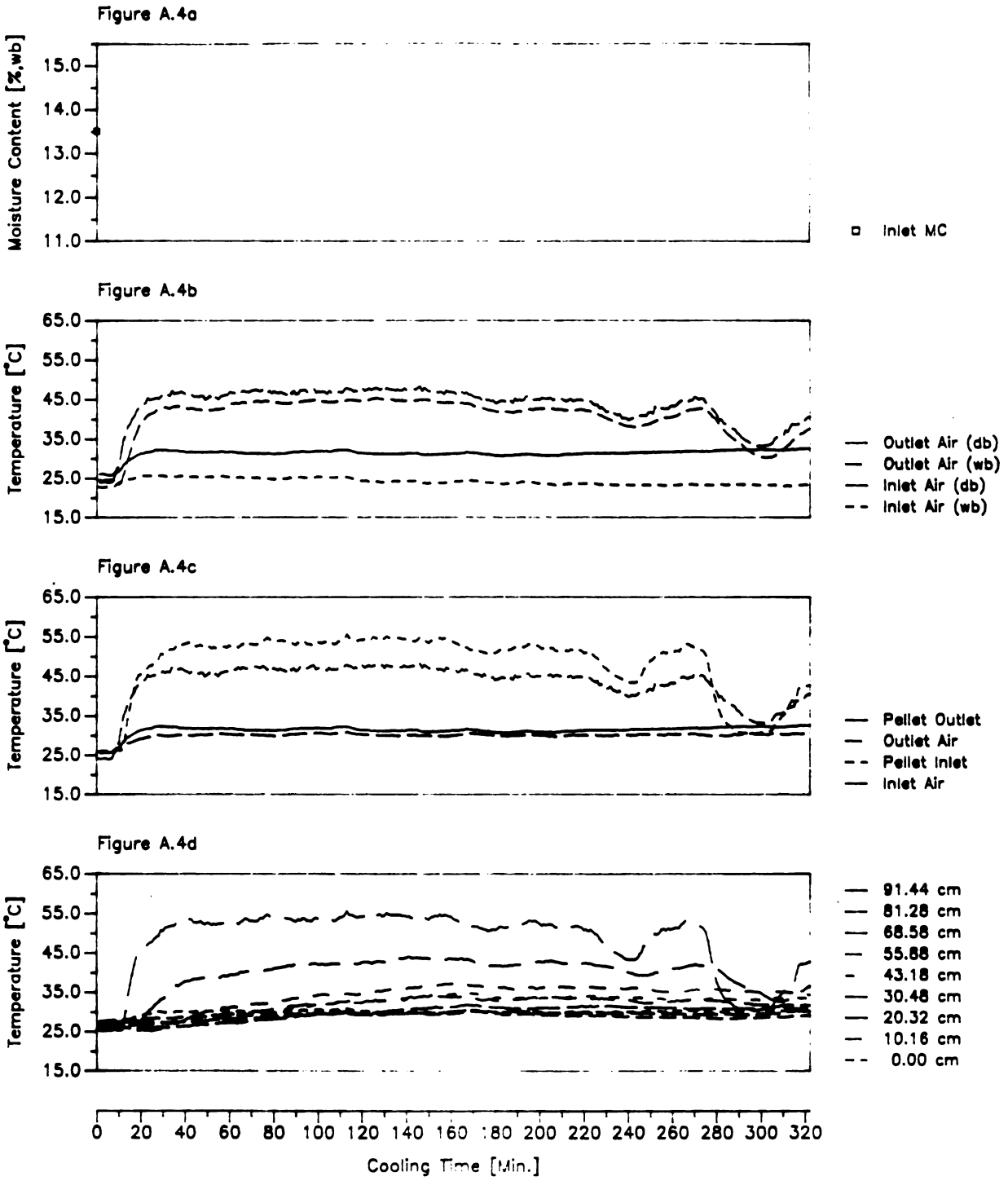


**Figure A.4 Experimental** cooling results for Test 6.

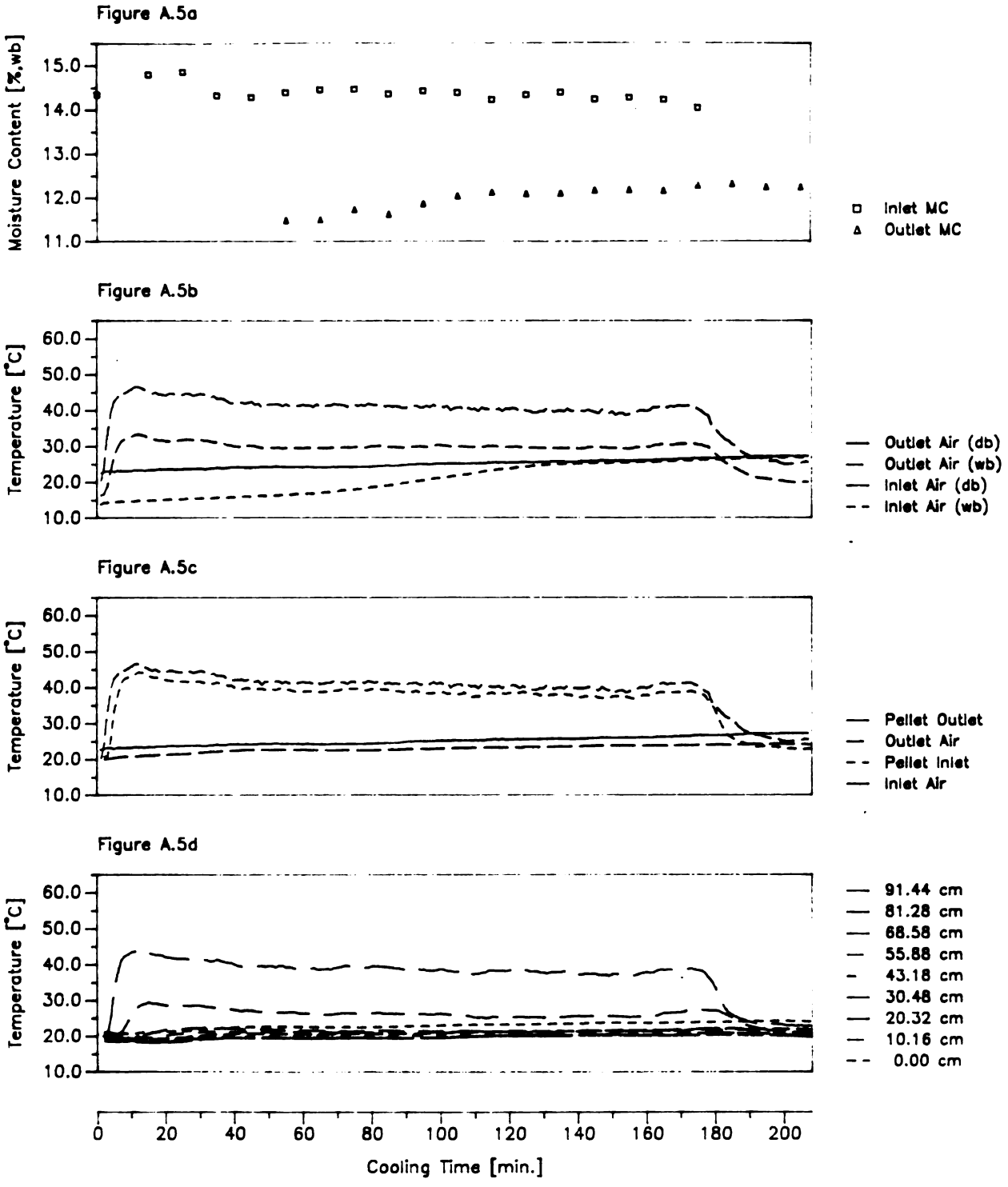


**Figure A.5 Experimental cooling results for Test 7.**

# APPENDIX B

Table B.1 Average pellet temperatures [°C] of Test 1.

| | Thermocouple Position/Layer | | | | | |
|---|---|---|---|---|---|---|
| Time [min] | Cooler Outlet | 0.00 cm | 10.16 cm | 20.32 cm | 30.48 cm | Cooler Inlet |
| 10 | 29.04 | 29.48 | 28.30 | 28.69 | 33.81 | 70.44 |
| 20 | 28.07 | 29.56 | 28.29 | 29.12 | 37.07 | 68.68 |
| 30 | 28.80 | 29.76 | 28.57 | 29.44 | 37.86 | 66.91 |
| 40 | 29.04 | 29.81 | 28.67 | 29.69 | 38.67 | 66.35 |
| 50 | 29.24 | 29.83 | 28.67 | 29.78 | 39.01 | 61.39 |
| 60 | 28.81 | 29.92 | 28.64 | 29.77 | 38.96 | 62.00 |
| 70 | 29.04 | 29.75 | 28.37 | 29.52 | 38.99 | 57.80 |
| 80 | 29.05 | 29.76 | 28.25 | 29.48 | 38.41 | 32.58 |
| 100 | 28.86 | 29.96 | 28.53 | 29.58 | 38.37 | 34.40 |
| 120 | 28.80 | 29.99 | 28.53 | 29.74 | 39.31 | 37.99 |
| 140 | 29.21 | 30.12 | 28.69 | 29.79 | 36.29 | 39.78 |
| Average | 28.91 | 29.81 | 28.50 | 29.51 | 37.88 | 54.39 |

Table B.2 Average pellet temperatures [°C] of Test 3.

| | Thermocouple Position/Layer | | | | | |
|---|---|---|---|---|---|---|
| Time [min] | Cooler Outlet | 0.00 cm | 10.16 cm | 20.32 cm | 30.48 cm | Cooler Inlet |
| 10 | 25.69 | 27.54 | 30.04 | 37.00 | 52.86 | 70.79 |
| 20 | 28.48 | 30.33 | 35.61 | 42.97 | 55.38 | 65.09 |
| 30 | 29.94 | 32.06 | 37.13 | 42.84 | 55.58 | 67.08 |
| 40 | 31.97 | 32.08 | 36.78 | 41.39 | 53.30 | 66.89 |
| 50 | 33.57 | 32.33 | 36.64 | 41.59 | 53.78 | 63.86 |
| 60 | 34.33 | 33.70 | 38.82 | 44.39 | 56.48 | 55.38 |
| 70 | 36.41 | 34.03 | 39.04 | 44.17 | 56.02 | 57.42 |
| Average | 31.48 | 31.72 | 36.29 | 42.05 | 54.77 | 63.78 |

Table B.3 Average pellet temperatures [°C] of Test 4.

| | Thermocouple Position/Layer | | | | | |
|---|---|---|---|---|---|---|
| Time [min] | Cooler Outlet | 0.00 cm | 10.16 cm | 20.32 cm | 30.48 cm | Cooler Inlet |
| 10 | 35.02 | 30.66 | 33.13 | 36.01 | 45.04 | 61.82 |
| 20 | 31.25 | 28.52 | 29.41 | 31.44 | 42.11 | 58.47 |
| 30 | 29.19 | 28.19 | 28.86 | 30.67 | 40.75 | 46.21 |
| 40 | 28.92 | 27.85 | 28.15 | 29.25 | 36.41 | 47.15 |
| 50 | 28.58 | 27.65 | 27.78 | 29.01 | 37.65 | 48.52 |
| Average | 30.59 | 28.57 | 29.47 | 31.28 | 40.39 | 52.43 |

Table B.4 Average pellet temperatures [°C] of Test 5.

| | Thermocouple Position/Layer | | | | | |
|---|---|---|---|---|---|---|
| Time [min] | Cooler Outlet | 0.00 cm | 10.16 cm | 20.32 cm | 30.48 cm | Cooler Inlet |
| 10 | 27.92 | 29.52 | 30.72 | 33.02 | 44.75 | 73.39 |
| 20 | 31.45 | 30.68 | 32.24 | 34.93 | 46.11 | 66.69 |
| 30 | 33.42 | 30.61 | 32.03 | 34.21 | 44.71 | 68.44 |
| 40 | 32.70 | 30.90 | 32.44 | 34.78 | 45.92 | 73.45 |
| 50 | 33.21 | 30.91 | 32.49 | 34.57 | 45.51 | 64.96 |
| 60 | 33.15 | 30.77 | 31.98 | 33.93 | 43.94 | 64.22 |
| Average | 31.98 | 30.57 | 31.98 | 34.24 | 45.16 | 68.53 |

Table B.5 Average pellet temperatures [°C] of Test 6.

| | | Thermocouple Position/Layer | | | |
|---|---|---|---|---|---|
| Time [min] | Cooler Outlet | 0.00 cm | 10.16 cm | 20.32 cm | 30.48 cm |
| 10 | 28.54 | 29.21 | 28.85 | 28.87 | 28.45 |
| 20 | 27.57 | 29.54 | 29.22 | 29.28 | 29.07 |
| 30 | 28.71 | 29.66 | 29.44 | 29.66 | 29.46 |
| 40 | 28.91 | 29.73 | 29.55 | 29.64 | 29.60 |
| 50 | 27.72 | 29.41 | 29.33 | 29.51 | 29.59 |
| 60 | 28.67 | 29.45 | 29.52 | 29.81 | 30.11 |
| 70 | 28.95 | 29.66 | 29.80 | 30.09 | 30.60 |
| 80 | 28.23 | 29.51 | 29.68 | 30.20 | 30.88 |
| 100 | 29.30 | 29.92 | 30.19 | 30.75 | 31.36 |
| 120 | 29.35 | 30.00 | 30.37 | 30.70 | 31.35 |
| 140 | 29.00 | 29.62 | 29.95 | 30.40 | 31.10 |
| 150 | 29.30 | 29.79 | 30.02 | 30.55 | 31.02 |
| 160 | 29.25 | 29.48 | 29.79 | 30.28 | 31.16 |
| 170 | 28.91 | 29.51 | 29.75 | 30.33 | 31.37 |
| 180 | 27.86 | 29.68 | 29.84 | 30.43 | 31.37 |
| 190 | 28.80 | 29.56 | 29.73 | 30.33 | 31.32 |
| 200 | 28.76 | 29.69 | 29.65 | 30.25 | 31.23 |
| 210 | 27.98 | 29.72 | 29.68 | 30.20 | 31.17 |
| 220 | 28.80 | 29.72 | 29.62 | 30.10 | 31.07 |
| 230 | 29.17 | 29.59 | 29.52 | 29.99 | 31.16 |
| Average | 28.68 | 29.62 | 29.68 | 30.07 | 30.61 |

Table B.5 (cont'd.)

| Time [min] | Thermocouple Position/Layer | | | | | |
|---|---|---|---|---|---|---|
| | 43.18 cm | 55.88 cm | 68.58 cm | 81.28 cm | 91.44 cm | Cooler Inlet |
| 10 | 29.65 | 31.95 | 33.75 | 39.84 | 50.17 | 68.82 |
| 20 | 30.51 | 32.76 | 34.52 | 40.30 | 50.22 | 69.00 |
| 30 | 31.17 | 33.34 | 34.75 | 40.40 | 50.35 | 70.18 |
| 40 | 31.70 | 33.45 | 34.98 | 40.54 | 51.08 | 69.78 |
| 50 | 31.50 | 33.70 | 35.35 | 40.71 | 51.07 | 67.69 |
| 60 | 32.08 | 34.29 | 35.72 | 41.22 | 51.20 | 67.56 |
| 70 | 32.65 | 34.91 | 36.46 | 41.65 | 50.93 | 66.80 |
| 80 | 33.19 | 35.45 | 36.64 | 41.44 | 50.95 | 65.12 |
| 100 | 33.59 | 35.65 | 36.64 | 41.29 | 49.73 | 63.68 |
| 120 | 33.10 | 35.22 | 36.13 | 40.22 | 48.23 | 62.65 |
| 140 | 32.49 | 34.70 | 35.72 | 39.87 | 48.18 | 62.00 |
| 150 | 32.52 | 34.84 | 35.84 | 40.37 | 49.27 | 61.55 |
| 160 | 32.71 | 34.97 | 36.10 | 40.75 | 48.68 | 59.77 |
| 170 | 32.83 | 34.94 | 36.01 | 40.39 | 48.35 | 56.77 |
| 180 | 32.98 | 34.93 | 35.93 | 40.22 | 46.85 | 50.82 |
| 190 | 32.80 | 34.79 | 35.79 | 39.35 | 43.09 | 51.58 |
| 200 | 32.76 | 34.75 | 35.26 | 38.21 | 42.80 | 56.09 |
| 210 | 32.64 | 34.27 | 34.85 | 38.68 | 47.12 | 59.08 |
| 220 | 32.29 | 34.24 | 35.43 | 39.74 | 49.04 | 58.03 |
| 230 | 32.49 | 34.76 | 35.87 | 40.34 | 48.08 | 48.19 |
| Average | 32.26 | 34.39 | 35.58 | 40.28 | 48.78 | 61.96 |

Table B.6 Average pellet temperatures [°C] of Test 7.

| | Thermocouple Position/Layer | | | | |
|---|---|---|---|---|---|
| Time [min] | Cooler Outlet | 0.00 cm | 10.16 cm | 20.32 cm | 30.48 cm |
| 10 | 19.86 | 22.25 | 20.55 | 19.44 | 19.57 |
| 20 | 20.62 | 22.64 | 20.77 | 19.53 | 19.59 |
| 30 | 21.07 | 22.66 | 20.65 | 19.47 | 19.57 |
| 40 | 20.91 | 22.54 | 20.65 | 19.48 | 19.55 |
| 50 | 20.90 | 22.55 | 20.74 | 19.58 | 19.55 |
| 60 | 21.02 | 22.70 | 20.68 | 19.51 | 19.42 |
| 70 | 21.15 | 22.93 | 20.84 | 19.60 | 19.55 |
| 80 | 21.30 | 23.14 | 21.10 | 19.87 | 19.85 |
| 100 | 21.41 | 23.29 | 21.36 | 20.16 | 20.08 |
| 120 | 21.50 | 23.38 | 21.46 | 20.23 | 20.10 |
| 140 | 21.67 | 23.54 | 21.55 | 20.30 | 20.23 |
| 150 | 21.68 | 23.77 | 21.66 | 20.44 | 20.31 |
| 160 | 21.74 | 23.79 | 21.77 | 20.42 | 20.26 |
| 170 | 22.03 | 23.85 | 21.66 | 20.31 | 20.27 |
| Average | 21.20 | 23.07 | 21.10 | 19.88 | 19.85 |

Table B.6 (cont'd.)

| | Thermocouple Position/Layer | | | | | |
|---|---|---|---|---|---|---|
| Time [min] | 43.18 cm | 55.88 cm | 68.58 cm | 81.28 cm | 91.44 cm | Cooler Inlet |
| 10 | 19.85 | 21.21 | 22.19 | 27.73 | 40.69 | 69.48 |
| 20 | 20.05 | 21.16 | 21.87 | 26.83 | 39.59 | 68.57 |
| 30 | 20.21 | 21.19 | 21.64 | 26.50 | 39.11 | 67.89 |
| 40 | 20.19 | 21.07 | 21.40 | 26.12 | 38.87 | 68.25 |
| 50 | 20.13 | 21.01 | 21.34 | 26.38 | 39.49 | 68.74 |
| 60 | 20.14 | 21.04 | 21.47 | 26.22 | 39.00 | 67.28 |
| 70 | 20.28 | 21.14 | 21.36 | 26.12 | 38.55 | 65.57 |
| 80 | 20.43 | 21.23 | 21.45 | 25.64 | 37.81 | 65.32 |
| 100 | 20.42 | 21.18 | 21.20 | 25.19 | 38.21 | 66.56 |
| 120 | 20.39 | 21.06 | 21.15 | 25.28 | 38.09 | 65.10 |
| 140 | 20.38 | 21.13 | 21.21 | 25.45 | 37.66 | 62.48 |
| 150 | 20.52 | 21.33 | 21.51 | 25.53 | 37.18 | 61.21 |
| 160 | 20.66 | 21.46 | 21.55 | 25.42 | 37.34 | 63.30 |
| 170 | 20.75 | 21.58 | 21.81 | 26.41 | 38.48 | 63.02 |
| Average | 20.31 | 21.20 | 21.51 | 26.06 | 38.58 | 65.91 |

# APPENDIX C

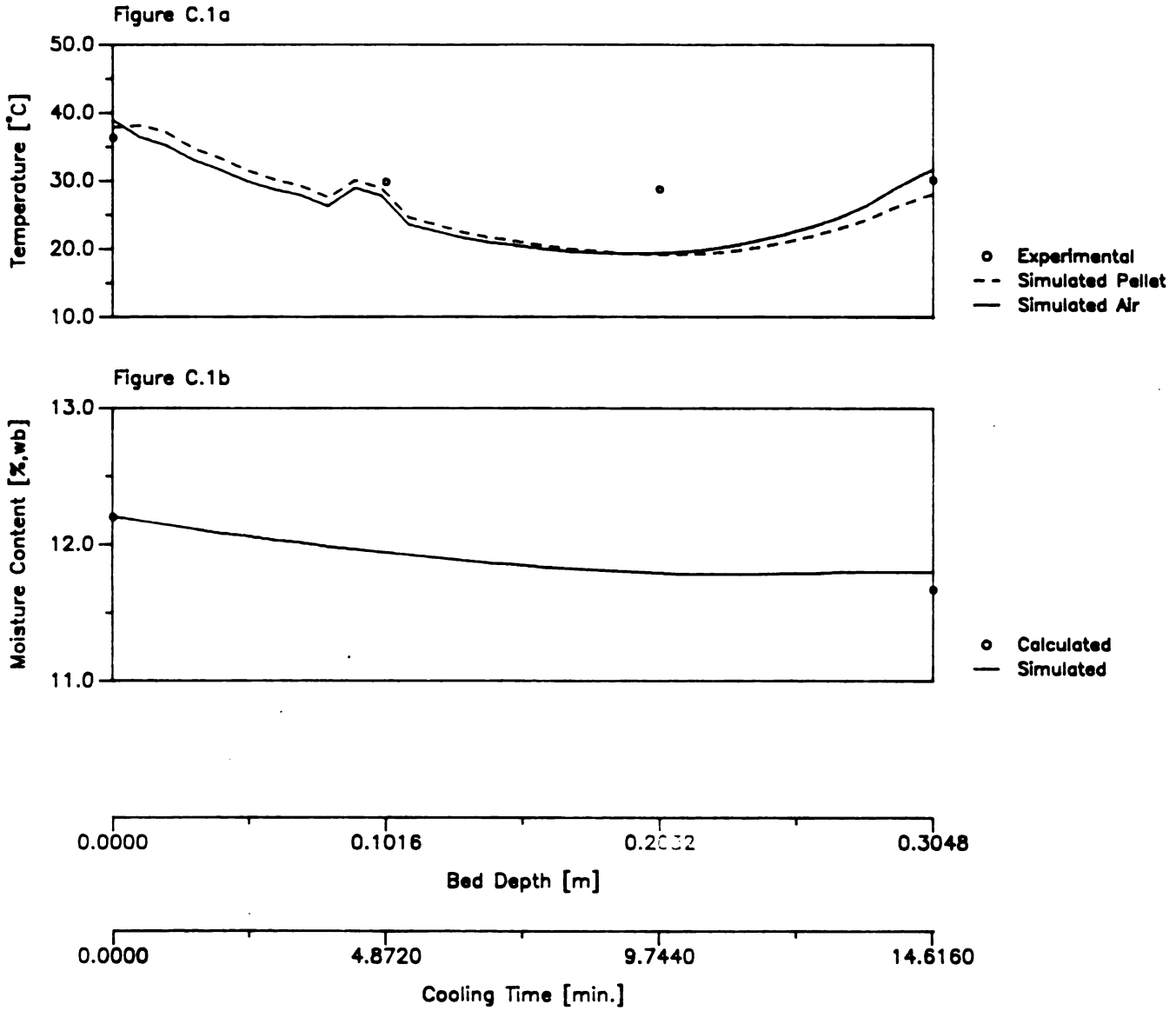


**Figure C.1 Simulated versus experimental cooling bed temperatures and moistures for Test 1.**

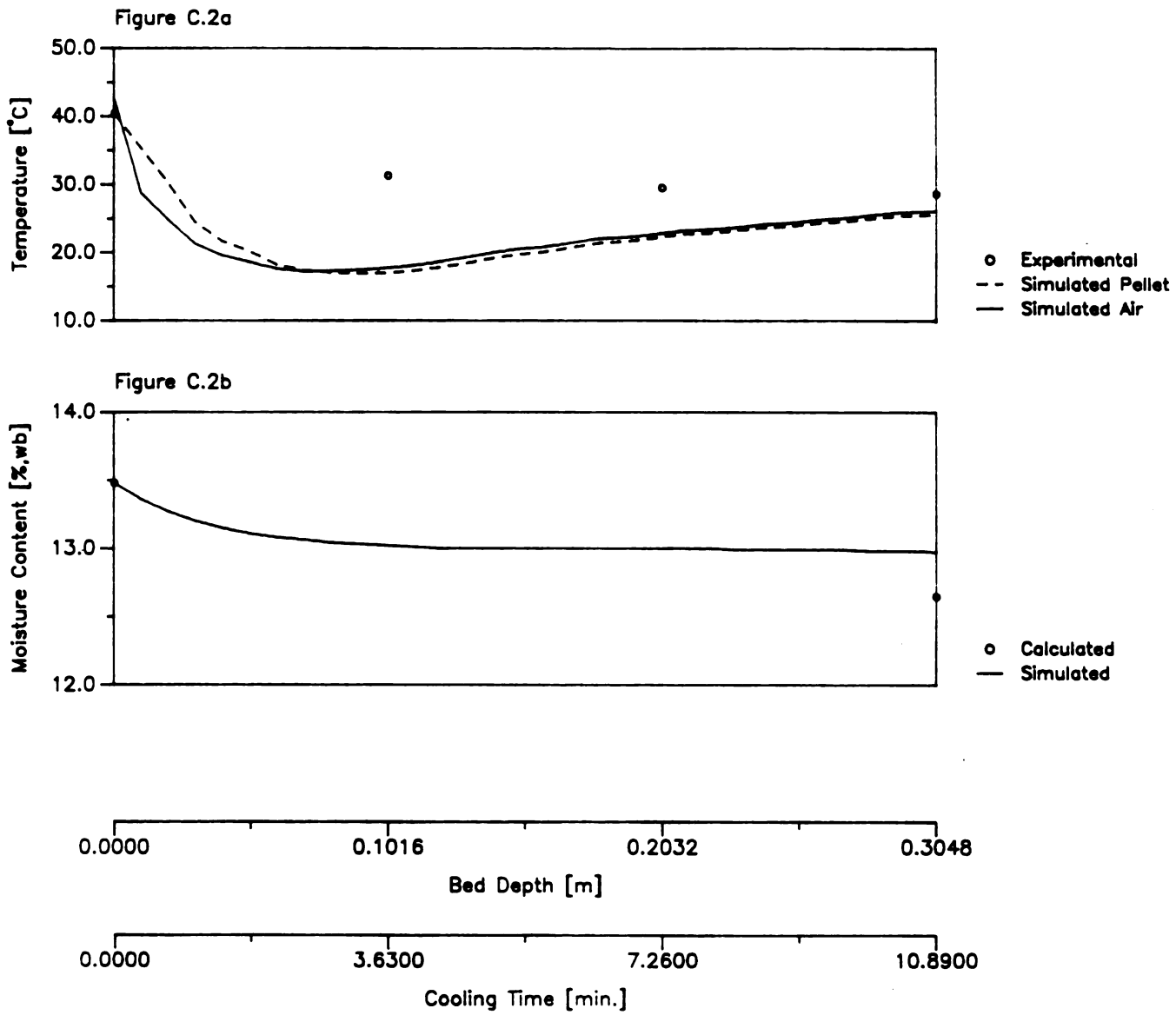


**Figure C.2 Simulated versus experimental cooling bed temperatures and moistures for Test 4.**

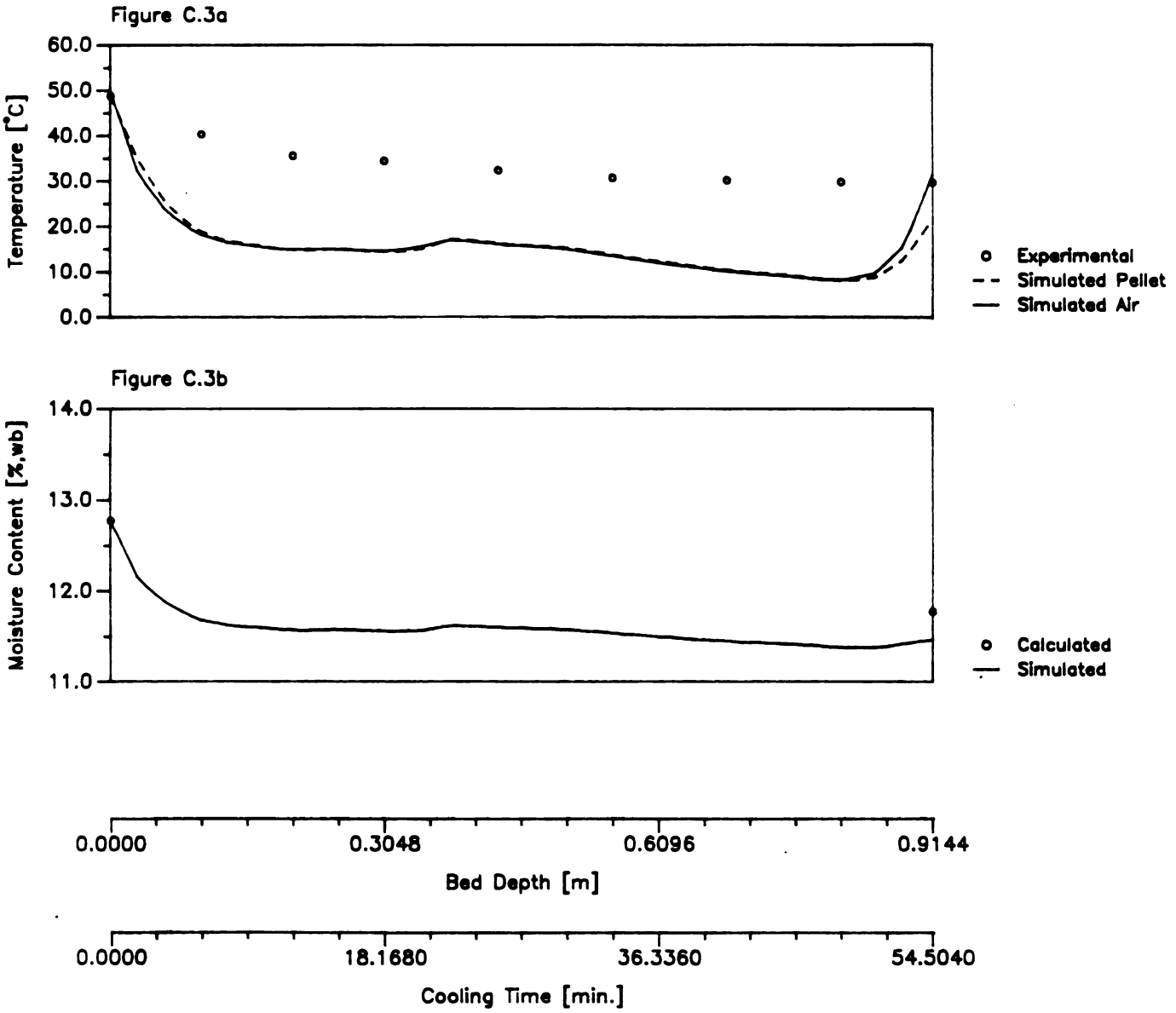


**Figure C.3** Simulated versus experimental cooling bed temperatures and moistures for Test 6.

# APPENDIX D

Table D.1 Summary of simulation parameters.

| Parameter | Value | $\theta_{out}$ [°C] | $T_{out}$ [°C] | $M_{out}$ [%,wb] | $RH_{out}$ [%] |
|---|---|---|---|---|---|
| $\theta_{in}$ [°C] | 51.1* | 24.75 | 52.45 | 12.83 | 24.54 |
| | 55.0 | 25.07 | 56.13 | 12.73 | 21.69 |
| | 60.0 | 25.40 | 61.12 | 12.60 | 18.28 |
| | 62.5 | 25.50 | 64.27 | 12.53 | 16.37 |
| $M_{win}$ [%,wb] | 13.6* | 24.75 | 52.45 | 12.83 | 24.54 |
| | 14.0 | 24.60 | 52.02 | 13.24 | 25.39 |
| | 15.0 | 23.97 | 51.74 | 14.17 | 26.84 |
| | 16.0 | 22.86 | 51.95 | 15.08 | 28.02 |
| $T_{in}$ [°C] | 12.0 | 14.91 | 53.20 | 12.62 | 19.36 |
| | 17.0* | 19.23 | 52.36 | 12.71 | 21.99 |
| | 22.6* | 24.75 | 52.45 | 12.83 | 24.54 |
| | 30.0 | 30.58 | 53.53 | 12.94 | 29.48 |
| $RH_{in}$ [%] | 50.0 | 21.77 | 52.03 | 12.68 | 22.58 |
| | 65.0* | 22.51 | 52.90 | 12.72 | 23.84 |
| | 73.7* | 24.75 | 52.45 | 12.83 | 24.54 |
| | 80.0 | 24.95 | 52.20 | 12.85 | 25.89 |
| $G_p$ [kg/h/m$^2$] | 1750 | 23.49 | 53.01 | 12.94 | 20.67 |
| | 2000* | 23.70 | 53.09 | 12.86 | 22.46 |
| | 2241* | 24.75 | 52.45 | 12.83 | 24.54 |
| | 2500 | 24.59 | 53.08 | 12.76 | 25.95 |
| $G_a$ [kg/h/m$^2$] | 1045.5 | 28.54 | 51.42 | 12.70 | 39.16 |
| | 1394.0* | 26.95 | 51.53 | 12.73 | 32.52 |
| | 2055.5* | 24.75 | 52.45 | 12.83 | 24.54 |
| | 2788.1 | 23.37 | 52.76 | 13.01 | 19.87 |
| $G_p/G_a$ | 0.88* | 24.09 | 53.44 | 12.98 | 20.05 |
| | 1.09* | 24.75 | 52.45 | 12.83 | 24.54 |
| | 1.79 | 28.04 | 52.83 | 12.74 | 32.19 |
| | 2.34 | 29.20 | 51.35 | 12.70 | 41.47 |
| H [m] | 0.1524* | 27.07 | 52.74 | 12.98 | 22.28 |
| | 0.3048* | 24.75 | 52.45 | 12.83 | 24.54 |
| | 0.4572 | 23.23 | 53.13 | 12.74 | 24.95 |
| | 0.6096 | 24.64 | 53.68 | 12.81 | 23.41 |
| d [mm] | 3.18* | 22.77 | 53.24 | 12.99 | 25.41 |
| | 4.37* | 24.75 | 52.45 | 12.83 | 24.54 |
| | 6.35 | 26.97 | 51.84 | 12.99 | 23.15 |
| | 9.53 | 30.44 | 50.98 | 13.21 | 20.96 |

* standard test parameters

# APPENDIX E

M I C H I G A N  S T A T E  U N I V E R S I T Y
AGRICULTURAL ENGINEERING DEPARTMENT

SIMULATION OF A CONCURRENT/COUNTER FLOW DRYER ON 08/24/1987

OUTPUT FOR STAGE 1

AMBIENT CONDITIONS:
AIR TEMP, C: 22.60
AIR R.H., %: 73.70 ; AIR ABS HUM, KG/KG: 0.0130

INLET CONDITIONS:
AIR TEMP, C: 22.60
AIR R.H., %: 73.70 ; AIR ABS HUM, KG/KG: 0.0130

AIR FLOW: 29.26 M3/M2/MIN , 2039.49 KG/HR/M2
29.87 M3/M2/MIN [AT TIN]

PRODUCT TEMP, C: 51.07
PRODUCT MC wb, %: 13.57 ; MC db, %: 15.70

PRODUCT FLOW: 2241.03 KG/HR/M2 , 3.47 M/HR ,
2.241 MTON/HR/M2

HEAT & MASS TRANSFER:
EQ MC wb, %: 10.69 ; EQ MC db, %: 11.97

CONV HT COEFF, KJ/HR/M2/C: 385.82
LATENT HEAT COEFF, KJ/KG : 2594.81

CA, KJ/KG/C : 1.0057 ; CP, KJ/KG/C : 2.0242
CV, KJ/KG/C : 2.0600 ; CW, KJ/KG/C : 0.0000

TOTAL LOOP CONVERGED IN 5 MAXIMUM 8
OUTLET THETAS AGREE -.2903E+00 CRITERION 0.5000E+00

BED SIMULATION:

| DEPTH | TIME | AIR TEMP | ABS HUM | REL HUM | GRAIN TEMP | MC WB | MC EQ WB |
|---|---|---|---|---|---|---|---|
| M | HR | C | KG/KG | DECIMAL | C | PERCENT | PERCENT |
| 0.0000 | 0.0000 | 52.45 | 0.02227 | 0.2454 | 51.07 | 13.57 | 1.74 |
| 0.0100 | 0.0029 | 47.64 | 0.02111 | 0.2958 | 49.39 | 13.48 | 2.79 |
| 0.0200 | 0.0058 | 46.51 | 0.02018 | 0.2999 | 48.32 | 13.41 | 2.95 |
| 0.0300 | 0.0087 | 44.29 | 0.01934 | 0.3225 | 45.81 | 13.34 | 3.56 |
| 0.0400 | 0.0115 | 42.65 | 0.01865 | 0.3390 | 44.00 | 13.28 | 4.00 |
| 0.0500 | 0.0144 | 41.12 | 0.01805 | 0.3559 | 42.36 | 13.24 | 4.43 |
| 0.0600 | 0.0173 | 39.58 | 0.01748 | 0.3745 | 40.65 | 13.19 | 4.90 |
| 0.0700 | 0.0202 | 38.20 | 0.01700 | 0.3926 | 39.14 | 13.15 | 5.33 |
| 0.0800 | 0.0231 | 37.05 | 0.01659 | 0.4079 | 37.91 | 13.12 | 5.70 |
| 0.0900 | 0.0260 | 36.05 | 0.01621 | 0.4212 | 36.81 | 13.09 | 6.02 |
| 0.1000 | 0.0288 | 35.24 | 0.01587 | 0.4315 | 35.92 | 13.06 | 6.27 |
| 0.1100 | 0.0317 | 34.48 | 0.01557 | 0.4417 | 35.12 | 13.04 | 6.52 |
| 0.1200 | 0.0346 | 33.63 | 0.01530 | 0.4552 | 34.21 | 13.02 | 6.82 |
| 0.1300 | 0.0375 | 32.85 | 0.01505 | 0.4679 | 33.36 | 13.00 | 7.11 |
| 0.1400 | 0.0404 | 32.28 | 0.01483 | 0.4765 | 32.76 | 12.98 | 7.31 |
| 0.1500 | 0.0433 | 31.76 | 0.01462 | 0.4839 | 32.21 | 12.96 | 7.49 |
| 0.1600 | 0.0461 | 31.19 | 0.01443 | 0.4932 | 31.59 | 12.95 | 7.70 |
| 0.1700 | 0.0490 | 30.73 | 0.01426 | 0.5005 | 31.11 | 12.94 | 7.87 |
| 0.1800 | 0.0519 | 30.17 | 0.01410 | 0.5115 | 30.53 | 12.92 | 8.11 |
| 0.1900 | 0.0548 | 29.74 | 0.01395 | 0.5183 | 30.07 | 12.91 | 8.27 |
| 0.2000 | 0.0577 | 29.42 | 0.01381 | 0.5231 | 29.73 | 12.90 | 8.38 |
| 0.2100 | 0.0606 | 29.03 | 0.01369 | 0.5304 | 29.33 | 12.89 | 8.55 |
| 0.2200 | 0.0634 | 28.66 | 0.01356 | 0.5369 | 28.94 | 12.88 | 8.70 |
| 0.2300 | 0.0663 | 28.30 | 0.01345 | 0.5439 | 28.57 | 12.87 | 8.85 |
| 0.2400 | 0.0692 | 27.93 | 0.01335 | 0.5515 | 28.22 | 12.86 | 9.02 |
| 0.2500 | 0.0721 | 27.56 | 0.01324 | 0.5593 | 27.86 | 12.85 | 9.18 |
| 0.2600 | 0.0750 | 27.16 | 0.01315 | 0.5688 | 27.51 | 12.85 | 9.38 |
| 0.2700 | 0.0779 | 26.61 | 0.01308 | 0.5838 | 27.09 | 12.84 | 9.69 |
| 0.2800 | 0.0807 | 26.01 | 0.01301 | 0.6017 | 26.66 | 12.84 | 10.04 |
| 0.2900 | 0.0836 | 25.09 | 0.01296 | 0.6334 | 26.09 | 12.83 | 10.68 |
| 0.3000 | 0.0865 | 23.52 | 0.01297 | 0.6963 | 25.23 | 12.83 | 11.99 |
| 0.3048 | 0.0879 | 22.60 | 0.01298 | 0.7370 | 24.75 | 12.83 | 12.91 |

INTERNAL MOISTURE AFTER COOLING FOR 0.8789E-01 HR

0.1357 0.1349 0.1295 0.1126

ENERGY CALCULATIONS:

STATIC PRESSURE, CM OF H2O: 5.5009

HORSEPOWER, HP/M2 : 0.3524 (EFF = 1.000)

WATER REMOVED, KG-H2O/M2: 1.6644 ; KG/KG PRODUCT: 0.0098

| | | | |
|---|---|---|---|
| THIS STAGE, KJ/M2 : | 157.72; | CUMULATIVE, KJ/M2 : | 157.72 |
| THIS STAGE, KJ/HR/M2/ : | 1794.60; | CUMULATIVE, KJ/HR/M2/ : | 1794.60 |
| THIS STAGE, KJ/KG H2O : | 94.76; | CUMULATIVE, KJ/KG H2O : | 94.76 |
| THIS STAGE, KJ/KG PROD: | 0.93; | CUMULATIVE, KJ/KG PROD: | 0.93 |